HIGHLY FLUORINATED, COINAGE METAL COMPLEXES OF TRIS(PYRAZOLYL)BORATES WITH ADDITIONAL ELECTRON WITHDRAWING GROUPS AND PYRAZOLATE π-STACKINGS WITH ARENES

by

NALEEN BANDUPRIYA JAYARATNA

Presented to the Faculty of the Graduate School of

The University of Texas at Arlington in Partial Fulfillment

of the Requirements

for the Degree of

DOCTOR OF PHILOSOPHY

THE UNIVERSITY OF TEXAS AT ARLINGTON

May 2016

Acknowledgements

I would like to express my sincere gratitude to my advisor Dr. Rasika Dias for the guidance and support throughout this study. His patience, advice and motivation have been invaluable to me to complete my graduate studies with success. I greatly admire and appreciate my dissertation committee members Dr. Frank W. Foss and Dr. Frederick MacDonnell for providing insightful suggestions.

I would like to thank past and present members of the Dias group, Dr. Jiang Wu, Dr. Yoshihiro Kobayashi, Dr. Xiaodi Kou, Dr. Nazhen Liu, Dr. Champika Hettiarachchi, Dr. Chandrakanta Dash, Dr. Sriparna Ray, Dr. Animesh Das, Dr. Venkata Adiraju, Dr. Suchismitha Acharya, Dr. Naveen Kulkarni, Dr. Guocang Wang, Shawn G. Ridlen, Abhijit Pramanik, Devaborniny Parasar, Jaspreet Singh and Tharun Ponduru for their friendship and valuable suggestions. I am also grateful to my undergraduate students Preston Rogers, Allison Conway and Skye Segovia forgiving me a chance to teach which I enjoy the most.

I would like to offer my thanks to all the faculty members and the staff of the chemistry and biochemistry department. Without the technical support of Dr. Muhammed Yousufuddin, Dr. Brian Edwards, and Dr. Chuck Savage my research work would not have been possible.

More importantly, I am grateful to my mother for her loving kindness and encouragement given to me and to my late farther for showed me the insight of the life. I would appreciate my brother and his family and finally I thank my wife for sharing the life with me.

April 06, 2016

Abstract

HIGHLY FLUORINATED, COINAGE METAL COMPLEXES OF TRIS(PYRAZOLYL)BORATES WITH ADDITIONAL ELECTRON WITHDRAWING GROUPS AND PYRAZOLATE π-STACKINGS WITH ARENES

Naleen Bandupriya Jayaratna, PhD

The University of Texas at Arlington, 2016

Supervising Professor: H.V. Rasika Dias

Tris(pyrazolyl)borates are very popular ligands in inorganic chemistry, bioinorganic chemistry, and organometallic chemistry due to their attractive properties. It is possible to extensively modify the steric and electronic properties of these ligands by changing the pyrazolyl substituent groups. Taking into account the importance and current interest of fluorinated tris(pyrazolyl)borates and weakly coordinating anions in general, three new tris(pyrazolyl)borates, $[HB(4\text{-}Cl\text{-}3,5\text{-}(CF_3)_2Pz)_3]^-$, $[HB(3,4,5\text{-}(CF_3)_3Pz)_3]$ and $[HB(4\text{-}(NO_2)\text{-}3,5\text{-}(CF_3)_2Pz)_3]^-$ have been developed (Pz = pyrazolyl). Silver alkene adducts of the ligands have been isolated to evaluate the electronic properties of the ligands and to study their catalytic properties. These adducts found to be the most electron deficient tris(polyazolyl)borates reported. The silver alkene adducts formed by these species are also important due to the scarcity of thermally stable isolable silver ethylene, *cis*-cyclooctene adducts.

Also some of these ligands were used to synthesize copper ethylene and silver carbonyl adducts. The CO stretching frequency of non-classical silver carbonyl adducts appear at a region less sensitive to the ligand electronic effects of tris(azolyl)borate Ag adducts. The alkene ^{13}C NMR chemical shift of silver alkene adducts is sensitive to ligand

electronic property changes according to the ^{13}C NMR. All the silver alkene adducts and a carbonyl adduct were structurally characterized by means of single crystal X-ray diffractions. All the compound reported were characterized by various NMR experiments and elemental analysis. Coinage metal ions supported by highly fluorinated ligands such as fluorinated tris(pyarazolyl)borates are excellent catalysts for carbene insertion into C-H bonds. The activity of silver adducts are particularly noteworthy. The activity and the selectivity of the catalyst can be fine-tuned using the substituents on the supporting ligand. The silver alkene adducts effectively catalyzed the insertion of the carbene moiety of ethyl diazoacetate into C-H bonds of 2,3-dimethylbutane. More electron deficient catalysts have shown higher selectivity towards primary C-H bonds.

Moreover our interest was directed towards the chemistry of the primary building block of tris(pyrazolyl)borate, the pyrazolate ligand. This simple ligand has been widely used in inorganic, bioinorganic, and organometallic chemistry. These ligands can strongly bind to the metal ions such as Cu(I), Ag(I) and Au(I). We are interested in the highly fluorinated pyrazolate coinage metal complexes due to the scarcity, their reversed π-stacking ability and the remarkable photophysical properties. The π-acid/ π-base adducts of $\{[3,5\text{-}(CF_3)_2Pz]Cu\}_3$ [Cu_3] and benzene [Bz], mesitylene [Mes] and naphthalene [Nap] have been isolated. They form columnar structures of the type $\{[Bz][Cu_3]_2\}_\infty$, $\{[Mes][Cu_3]\}_\infty$ and $\{[Nap][Cu_3]\}_\infty$ in the solid state, and are luminescent. The novel coinage metal complexes, $C_{60}\{[(3,5\text{-}(CF_3)_2Pz)Cu]_3\}_4$, $C_{60}\{[(3,5\text{-}(CF_3)_2Pz)Ag]_3\}_4$ and $C_{60}\{[(3,5\text{-}(CF_3)_2Pz)Au]_3\}_4$, represent the first coinage metal pyrazolate fullerene adducts to the best of our knowledge. Interestingly, these adducts possess same space group to that of "free" C_{60} and the crystals are formed in their pure form with no co-crystalized solvent molecules.

Table of Contents

List of Illustrations

List of Tables

Chapter 1

Coinage metal complexes of fluorinated weakly coordinating tris(pyrazolyl)borate

1.1 Introduction

1.1.1 Tris(pyrazolyl)borate ligand

Tris(pyrazolyl)borates (Tp) are known for almost five decades and are used extensively in inorganic, bioinorganic, and organometallic chemistry.[1] They have gained much attraction due to their tunability. The steric and electronic properties are quite easily tuned by changing the substituents on the boron atom or pyrazolyl moiety (9 possible sites)(Figure 1.1).

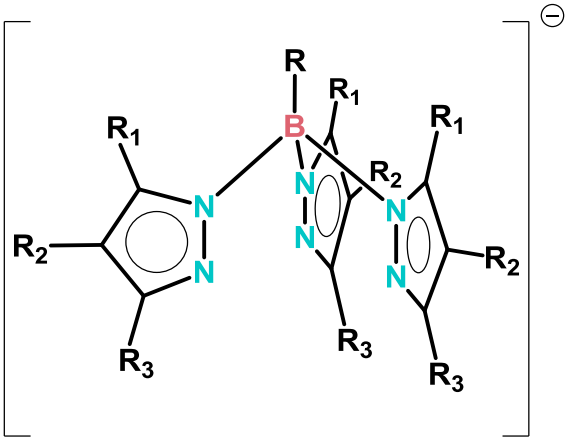

Figure 1.1 Tris(pyrazolyl)borate ligand

Tp belongs to the main family of poly(pyrazolyl)borates (Figure 1.2). In the main family R and/or R' can be H, alkyl, aryl or pyrazolyl groups. However in this research project we reflected on tris(pyrazolyl)borates with hydrogen-substituted boron, in which R is equal to H and R' is equal to pyrazole or a substituted pyrazole. Particularly, our interest has been focused on isolation of highly electron deficient Tp coinage metal small molecular adducts and their use in homogeneous catalysis. Lack of such electron

deficient coinage metal complexes and their promising use in homogeneous catalysis led us to work on the synthesis of more electron deficient Tp coinage metal complexes.

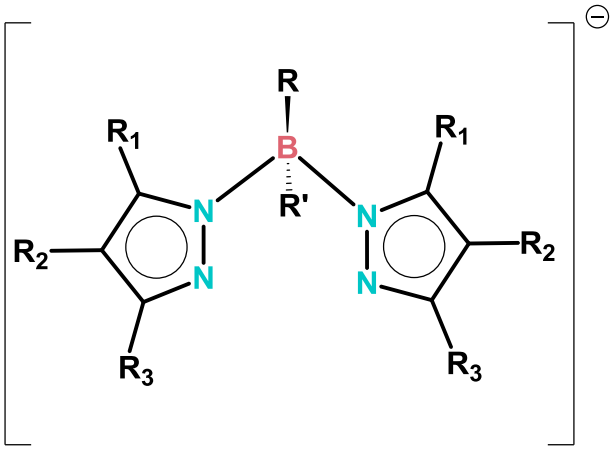

Figure 1.2 Poly(pyrazolyl)borate ligand

The monoanionic tris(pyrazolyl)borate ligand has been used as a cyclopentadiene (Cp) mimic, which donates six electrons to the metal center. The parent ligand, simple hydrogen-substituted $[HB(Pz)_3]$-, was first used to synthesize a TpMTp type sandwich complex with manganese. In 1967, Trofimenco reported the first TpML type complex based on the parent ligand $[HB(Pz)_3]^-$ to synthesis the complex $\{[HB(Pz)_3]Mn(CO)_3\}NEt_4$.[2] Subsequently, $[HB(Pz)_3]^-$ and $[HB(3,5\text{-}(Me)_2Pz)_3]^-$ governed this chemistry until the introduction of $[HB(3\text{-}(t\text{-}Bu)Pz)_3]^-$ in 1986.[3] Following the introduction of the *t*-Bu group, Tp chemistry was further expanded to other bulky substituents. Figure 1.3 illustrates a few examples of bulky Tp ligands.

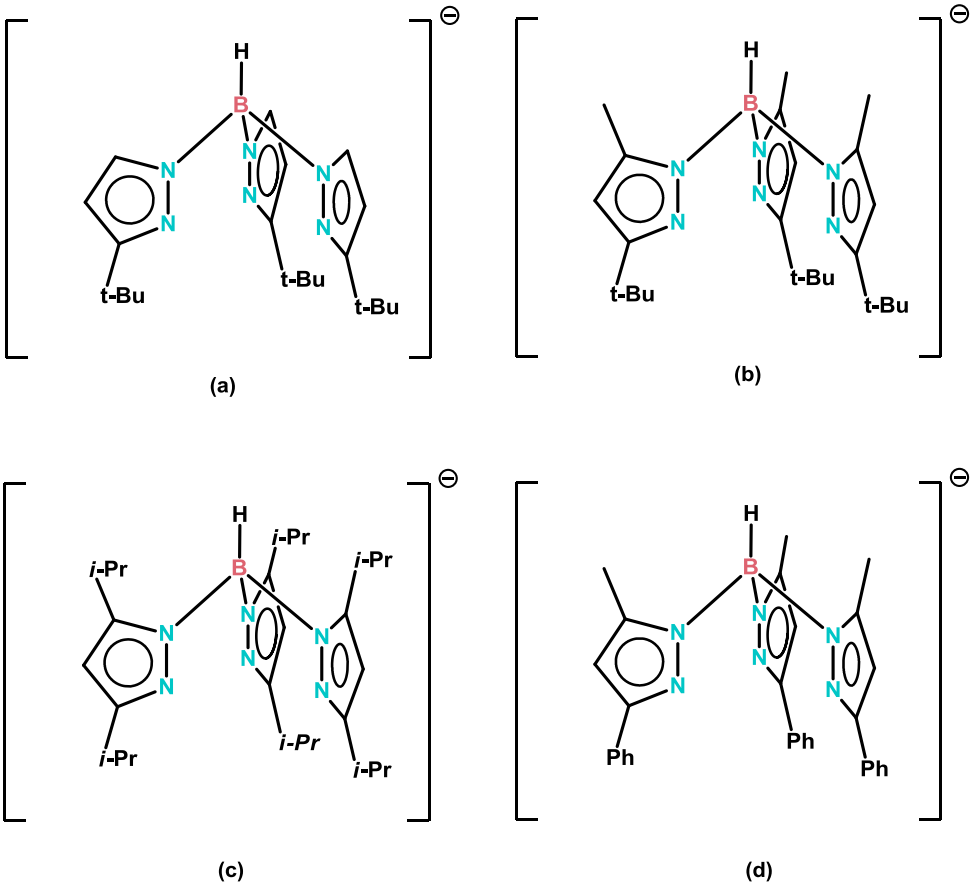

Figure 1.3 Tp ligands bearing hydrocarbon substituents. $[HB(3\text{-}(t\text{-}Bu)Pz)_3]^-$ (a), $[HB(3\text{-}(Me)\text{-}5\text{-}(t\text{-}Bu)_2Pz)_3]^-$ (b), $[HB(3,5\text{-}(i\text{-}Pr)_2Pz)_3]^-$ (c), $[HB(3\text{-}(Me)\text{-}5\text{-}(Ph)_2Pz)_3]^-$

1.1.2 Fluorinated tris(pyrazolyl)borate coinage metal complexes

Even though the Tp chemistry was further expanded with various bulky substituents, most of the substituent groups were limited to hydrocarbons.[1] The hydrocarbon substituents lead to electron rich, strongly coordinating Tp ligands. However the electron deficient Tps are fascinating due to their outstanding properties (we will discuss this in detail later in the text). To obtain such ligands, use of fluorinated substituents is a viable option. Fluorinated substituents also make the ligand more

electrons deficient, higher in thermal stability and higher in volatility. Hence, we have dealt with many fluorinated Tp ligands; mostly with hydrogen-substituted boron and few with alkyl or aryl substituted boron.[4-9] Figure 1.4 illustrates some of the fluorinated Tp molecules reported by our group. Among all, $[HB(3,5\text{-}(CF_3)_2Pz)_3]^-$ was the most common Tp we used due to its appealing properties.[10-21]

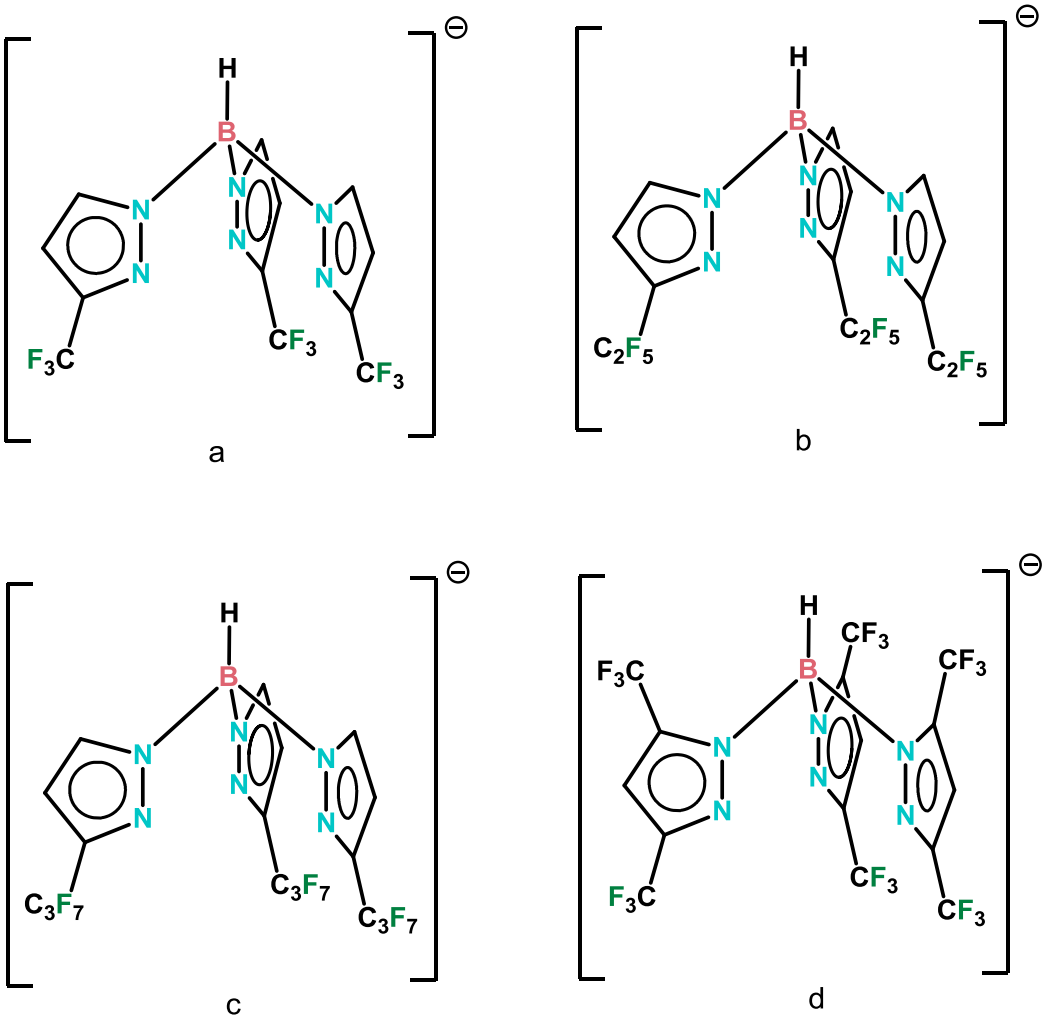

Figure 1.4 Fluorinated Tp ligands $[HB(3\text{-}(CF_3)Pz)_3]^-$ (a), $[HB(3\text{-}(C_2F_5)Pz)_3]^-$ (b), $[HB(3\text{-}(C_3F_7)Pz)_3]^-$ (c), $[HB(3,5\text{-}(CF_3)_2Pz)_3]^-$ (d)

The $[HB(3,5\text{-}(CF_3)_2Pz)_3]^-$ is the most electron deficient ligand among all fluorinated Tps. IR frequency of Tp copper carbonyl complexes is a tool to understand the electronic properties of the ligand. For example, $[HB(3,5\text{-}(CF_3)_2Pz)_3]CuCO$ shows carbonyl IR stretching at 2137 cm^{-1} whereas it's hydrocarbon version $[HB(3,5\text{-}(CH_3)_2Pz)_3]CuCO$, shows carbonyl IR stretching at 2066 cm^{-1} (Table 1.1). IR stretching frequency for uncoordinated or "free" CO appears at 2143 cm^{-1}. Metal coordinated CO stretch shows lower frequency compared to the "free" CO, in the classical metal carbonyl complexes. However, IR frequencies move closer to 2143 cm^{-1} and even go beyond that as the metals get more and more electron deficient. The IR frequency reported for $[HB(3,5\text{-}(CF_3)_2Pz)_3]CuCO$ is the highest value that was reported for the Tp supported copper carbonyl complexes. It has been used in isolation of many rare small molecular adducts of coinage metal complexes, such as $[HB(3,5\text{-}(CF_3)_2Pz)_3]CuCO$,[22] $[HB(3,5\text{-}(CF_3)_2Pz)_3]AuCO$,[10] $[HB(3,5\text{-}(CF_3)_2Pz)_3]AgCO$,[11] $[HB(3,5\text{-}(CF_3)_2Pz)_3]Cu(C_2H_4)$,[23] $[HB(3,5\text{-}(CF_3)_2Pz)_3]Ag(C_2H_4)$,[11] $[HB(3,5\text{-}(CF_3)_2Pz)_3]Au(C_2H_4)$.[24] The weakly coordinating nature of the ligand plays a key role in assembling these complexes. For example $[HB(3,5\text{-}(CF_3)_2Pz)_3]Au(C_2H_4)$ is one of first reported thermally stable neutral gold(I) ethylene adduct. Moreover $[HB(3,5\text{-}(CF_3)_2Pz)_3]Cu(C_2H_4)$ is a vacuum stable ethylene adduct which is extremely stable compared to its hydrocarbon substituted sister $[HB(3,5\text{-}(CH_3)_2Pz)_3]Cu(C_2H_4)$ which loose ethylene easily under vacuum.

Table 1.1 Tp copper carbonyl IR frequencies

Complex	vCO (cm^{-1})	Reference
[HB(3,5-(*i*-Pr)$_2$Pz)$_3$]CuCO	2056	[25]
[HB(3,5-(CH$_3$)$_2$Pz)$_3$]CuCO	2066	[26]
[HB(3-(CF$_3$)Pz)$_3$]CuCO	2100	[27]
[HB(3-(C$_3$F$_7$)Pz)$_3$]CuCO	2102	[7]
[HB(3-(CF$_3$),5-(Ph)Pz)$_3$]CuCO	2103	[5]
[HB(3-(CF$_3$),5-(CH$_3$)Pz)$_3$]CuCO	2109	[28]
[HB(3-(C$_2$F$_5$)Pz)$_3$]CuCO	2110	[7]
[PhB(3-(CF$_3$)Pz)$_3$]CuCO	2112	[29]
[HB(3,5-(CF$_3$)$_2$Pz)$_3$]CuCO	2137	[27]
CO	2143	[30]

Besides the synthesis of isolable small molecular adducts of coinage metal complexes, silver and copper complexes with electron deficient Tp ligands showed promising results in the chemistry of carbene insertion into unfunctionalized C-H bonds (Table 1.1).[31] For example, [HB(3,5-(CF$_3$)$_2$Pz)$_3$]Ag(C$_2$H$_4$) resulted in complete consumption of ethyl diazoacetate (EDA) and 99% of C-H activated products in the carbene insertion reaction of 2,3-dimethylbutane (Figure 1.5). However, more electron rich [HB(3,5-(Mes)$_2$Pz)$_3$]Ag(C$_2$H$_4$) complex resulted only 50% consumption of the carbene source and resulted only 80% C-H activated products (Table 1.2). The better catalytic activity of the more acidic metal center can be explained with the use of proposed reaction mechanism given below (Figure1.6).[31,32] The transition state (y) is facilitated by

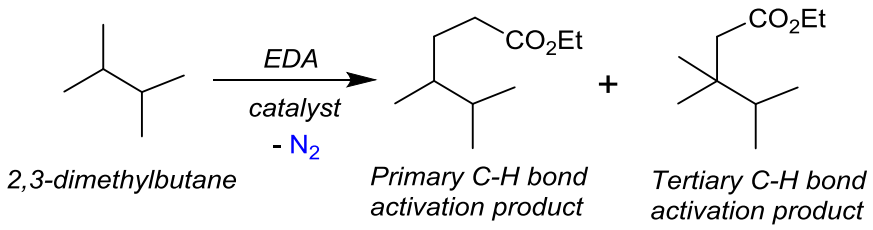

Figure 1.5 Silver catalyzed carbene insertion into 2,3-dimethylbutane

more electron deficient metal centers. Additionally, more electron deficient metal centers tend to activate a higher percentage of primary C-H bonds compared to a less acidic one (Table 1-2). Over again, electron deficient metal center in transition state (y) has extra potential to abstract a hydrogen from energetically less feasible primary C-H bond (Figure 1.6) where the order of C-H Bond dissociation energies are: primary > secondary > tertiary. Even though electron deficiency promotes catalytic activity and selectivity, use of AgOTf has resulted weaker performance. This indicates the necessity of a supporting ligand.

Table 1.2 Silver catalyzed carbene insertion into 2,3-dimethylbutane

Catalyst	EDA consumed (%)	C–H insertion products (%)	C-H insertion products selectivity		Carbene dimers[a] (%)
			Primary insertion	Tertiary insertion	
$[MeB(3\text{-}(CF_3)Pz)_3]Ag(C_2H_4)$	100	93	68	32	7
$[HB(3,5\text{-}(CF_3)_2Pz)_3]Ag(C_2H_4)$	100	99	79	21	1
$[MeB(3\text{-}(Mes)Pz)_3]Ag(C_2H_4)$	50	90	49	51	10
AgOTf	10	48	85	15	52

[a] Carbene dimer byproducts are diethyl fumarate and diethyl maleate.

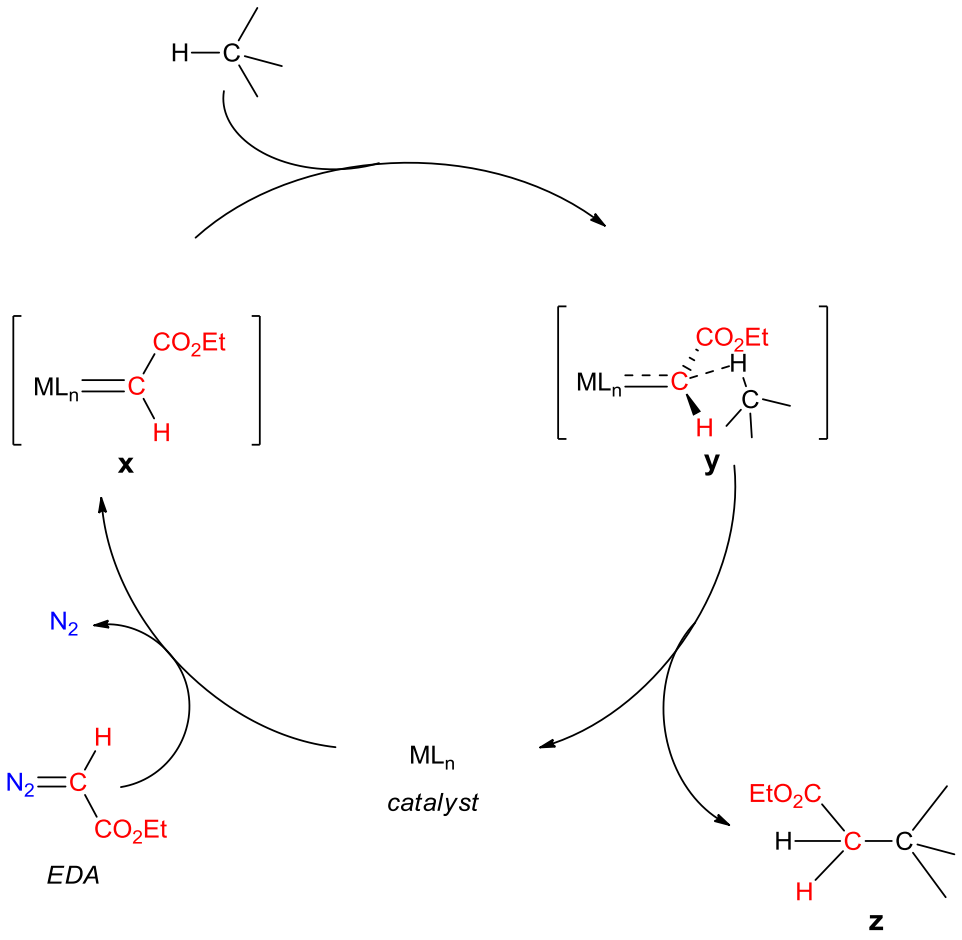

Figure 1.6 Proposed catalytic cycle for C-H bond activation

Based on the outstanding properties of the weakly coordinating fluorinated Tp ligands discussed, we set out to synthesize more electron deficient Tp ligands bearing additional electron withdrawing group at the 4th position of the pyrazole ring.

1.2 Copper and silver small molecular adducts of $[HB(3,4,5\text{-}(CF_3)_3Pz)_3]^-$

Naleen B. Jayaratna, Igor I. Gerus, Roman V. Mironets, Pavel K. Mykhailiuk,

Muhammed Yousufuddin, and H. V. Rasika Dias.

(Part of this work has been published in *Inorganic Chemistry* **2013**, *52*, 1691)

1.2.1 Introduction

Tris(pyrazolyl)borates are very popular auxiliary ligands in inorganic and organometallic chemistry.[34-36] It is possible to vary the steric and electronic properties of these ligands quite easily by changing the substituents on the boron atom or pyrazolyl moiety. In fact, a large number of tris(pyrazolyl)borate ligand varieties are now known. An area of research focus on in one of our laboratories concerns the development of fluorinated versions of these ligands and their use in various applications.[35] For example, we have reported the synthesis of several polyfluorinated tris(pyrazolyl)borates including $[HB(3\text{-}(CF_3)Pz)_3]^-$, $[HB(3,5\text{-}(CF_3)_2Pz)_3]^-$ (Figure 1.7) and boron-substituted varieties such as $[MeB(3\text{-}(CF_3)Pz)_3]^-$.[35] Metal adducts of fluorinated tris(pyrazolyl)borates feature more electrophilic metal sites and display interesting properties and reactivity compared to the non-fluorinated electron-rich tris(pyrazolyl)borate analogs.[37-39]

Recently, a practical route to 3,4,5-tris(trifluoromethyl)pyrazole ($3,4,5\text{-}(CF_3)_3PzH$) was reported.[40] It is one of the most acidic pyrazoles known with a pK_a value of 4.5 (which is more acidic than acetic acid, $pK_a = 4.7$) ! Considering the importance of weakly coordinating ligands like $[HB(3,5\text{-}(CF_3)_2Pz)_3]^-$ (which is based on $3,5\text{-}(CF_3)_2PzH$ with a pK_a of 7.1)[41] in metal coordination chemistry and catalysis,[35] we set out to develop poly(pyrazolyl)borates based on $3,4,5\text{-}(CF_3)_3PzH$. In this section, we describe the

synthesis of $[HB(3,4,5\text{-}(CF_3)_3Pz)_3]^-$, which has nine trifluoromethyl groups on the periphery (Figure 1.7) and some of its copper and silver complexes.

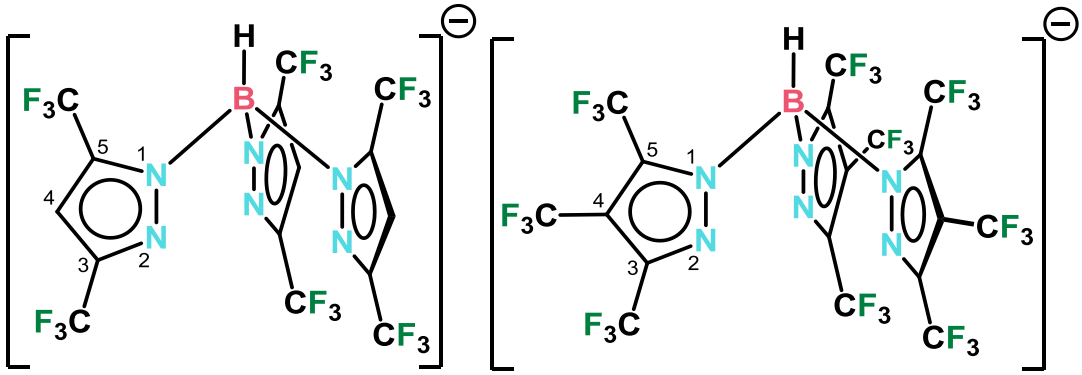

Figure 1.7 $[HB(3,5\text{-}(CF_3)_2Pz)_3]^-$ and $[HB(3,4,5\text{-}(CF_3)_3Pz)_3]^-$

Recently, a practical route to 3,4,5-tris(trifluoromethyl)pyrazole ($3,4,5\text{-}(CF_3)_3PzH$) was reported.[40] It is one of the most acidic pyrazoles known with a pK_a value of 4.5 (which is more acidic than acetic acid, $pK_a = 4.7$) ! Considering the importance of weakly coordinating ligands like $[HB(3,5\text{-}(CF_3)_2Pz)_3]^-$ (which is based on $3,5\text{-}(CF_3)_2PzH$ with a pK_a of 7.1)[41] in metal coordination chemistry and catalysis,[35] we set out to develop poly(pyrazolyl)borates based on $3,4,5\text{-}(CF_3)_3PzH$. In this section, we describe the synthesis of $[HB(3,4,5\text{-}(CF_3)_3Pz)_3]^-$, which has nine trifluoromethyl groups on the periphery (Figure 1.7) and some of its copper and silver complexes.

1.2.2 Results and discussion

The sodium salt $[HB(3,4,5\text{-}(CF_3)_3Pz)_3]Na$ was readily synthesized by the reaction of $NaBH_4$ with $3,4,5\text{-}(CF_3)_3PzH$ at *ca*. 190 °C in a solventless process. It was isolated as its tetrahydrofuran (THF) adduct after a workup involving THF. ^{19}F NMR spectrum of $[HB(3,4,5\text{-}(CF_3)_3Pz)_3]Na(THF)$ displays three peaks centered at δ -55.1, -57.0, and -62.3

corresponding to the fluorine atoms of CF_3 groups on pyrazolyl moieties. For comparison, fluorines of the starting material, 3,4,5-$(CF_3)_2$PzH in $CDCl_3$ give rise to two peaks at δ -56.1 and -61.3 (1:2 ratio).

The treatment of [HB(3,4,5-$(CF_3)_3Pz)_3$]Na(THF) with AgOTf in THF under an atmosphere of ethylene affords the silver(I) ethylene complex [HB(3,4,5-$(CF_3)_3Pz)_3$]Ag(C_2H_4). It is a white powder and stable to loss of ethylene in a nitrogen atmosphere. The X-ray structure of [HB(3,4,5-$(CF_3)_3Pz)_3$]Ag(C_2H_4) is illustrated in Figure 1.8. Such structurally characterized silver(I) ethylene complexes are of interest because of their relevance in various industrial and biological processes.[35,42] The silver atom of [HB(3,4,5-$(CF_3)_3Pz)_3$]Ag(C_2H_4) adopts a pseudo-tetrahedral geometry. Interestingly, the ethylene moiety coordinates to the metal center in η^2-fashion but somewhat asymmetrically having one short and one long Ag-C bonds, 2.294(4) and 2.337(4) Å. This asymmetric arrangement is atypical for ethylene even though that is common in arene silver complexes.[43,44] The [HB(3,4,5-$(CF_3)_3Pz)_3$]$^-$ moiety shows κ^3 coordination but with three different Ag-N distances (2.369(3), 2.399(3), and 2.444(3) Å). Such variations in metal-N distance are not unusual and there are even κ^2 ligated tris(pyrazolyl)borates, as we observed in [HB(3,5-$(CF_3)_2Pz)_3$]Au(C_2H_4).[45,46] Detailed analysis of the ethylene C=C distance is not very useful because the C=C bond distance change as a result of coordination to silver(I) in these (and many of other reported) adducts is small and is often overshadowed by experimental errors associated with routine X-ray crystallography, high estimated standard deviation values, libration effects, and the anisotropy of the electron density.[42,47]

The ^{1}H NMR signal of the protons of silver bound ethylene of [HB(3,4,5-$(CF_3)_3Pz)_3$]Ag(C_2H_4) appears at δ 5.65. It is a notable downfield shift compared to the free ethylene signal (δ 5.40). The ^{13}C NMR spectrum of [HB(3,4,5-$(CF_3)_3Pz)_3$]Ag(C_2H_4) in

CD_2Cl_2 shows a resonance at δ 111.6, which is assigned to carbon atoms of the silver-coordinated ethylene moiety. This is the smallest upfield shift relative to the free ethylene signal (δ 123.3) observed thus far for a coinage metal ethylene adduct supported by

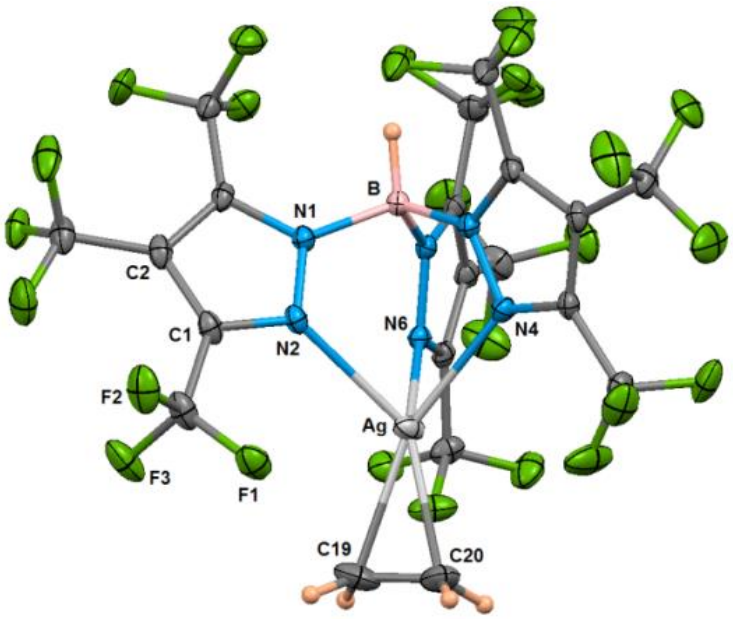

Figure 1.8 Molecular structure of $[HB(3,4,5\text{-}(CF_3)_3Pz)_3]Ag(C_2H_4)$

Thermal ellipsoids at 40% probability. Selected distances (Å) and angles (deg): Ag-C20 2.294(4), Ag-C19 2.337(4), C19-C20 1.305(8), Ag-N4 2.369(3), Ag-N2 2.399(3), Ag-N6 2.444(3), Ag.....B 3.39; C20-Ag-C19 32.73(19), N4-Ag-N2 80.76(10), N4-Ag-N6 78.74(10), N2-Ag-N6 82.61(10)

tris(azolyl)borates (Table 1.3). The related $[HB(3,5\text{-}(CF_3)_2Pz)_3]Ag(C_2H_4)$, for example, exhibits a corresponding signal at δ 104.9.[43] The ^{13}C data suggest that the silver-ethylene interaction in these adducts is much closer to the T-shaped bonding extreme than the metallacyclopropane regime.[46] For comparison, $[Ni(i\text{Pr}_2\text{Im})_2(\eta^2\text{-}C_2H_4)]$, which

features a high degree of metal→ethylene back-bonding [leading to near-metallacyclopropane-type bonding and a C-C distance of 1.420(4) Å] displays its ethylene carbon resonance at δ 24.85.[48] Bubbling excess ethylene into a $CDCl_3$ solution of $[HB(3,4,5\text{-}(CF_3)_3Pz)_3]Ag(C_2H_4)$ at room temperature led to coalescence of the ^1H NMR signals of the coordinated ethylene, with the free ethylene producing a broad new signal at a weighted average position. This indicates that the bound ethylene exchanges rapidly with the free ethylene in the solution on the NMR timescale. The removal of excess ethylene by purging with nitrogen led to the reappearance of the ethylene peak of $[HB(3,4,5\text{-}(CF_3)_3Pz)_3]Ag(C_2H_4)$.

Solid $[HB(3,4,5\text{-}(CF_3)_3Pz)_3]Ag(C_2H_4)$ displays a sharp band in the Raman spectrum at 1581 cm^{-1}, which can be assign to the C=C stretch of the ethylene moiety.

Table 1.3 Selected copper(I)-ethylene and silver(I)-ethylene complexes of tris(pyrazolyl)borate and tris(triazolyl)borate ligands, and some of their structural and spectroscopic parameters

Compound	^1H, ppm	^{13}C, ppm	Av. M-C, Å	$\upsilon_{C=C}$, cm^{-1}	Ref
$[HB(3,4,5\text{-}(CF_3)_3Pz)_3]Cu(C_2H_4)$	5.06 (CD_2Cl_2)	94.9 (CD_2Cl_2)			This work
$[HB(3,5\text{-}(CF_3)_2Tz)_3]Cu(C_2H_4)$	5.12 ($CDCl_3$)	92.6 (CD_2Cl_2)	2.045(8)	1551	49
$[HB(3,5\text{-}(CF_3)_2Pz)_3]Cu(C_2H_4)$	4.96 ($CDCl_3$)	89.5 (C_6D_{12})	2.022(6)		23
$[HB(3,5\text{-}(CH_3)_2Pz)_3]Cu(C_2H_4)$	4.41 (CD_2Cl_2)		2.014(5)		50
$[HB(3,4,5\text{-}(CF_3)_3Pz)_3]Ag(C_2H_4)$	5.65 (CD_2Cl_2)	111.6 (CD_2Cl_2)	2.294(4) 2.337(4)	1581	This work
$[HB(3,5\text{-}(CF_3)_2Tz)_3]Ag(C_2H_4)$	5.70 ($CDCl_3$)	109.7 ($CDCl_3$)	2.296(6) 2.285(8)	1576	49
$[HB(3,5\text{-}(CF_3)_2Pz)_3]Ag(C_2H_4)$	5.52 ($CDCl_3$)	104.9 (C_6D_{12})	2.301(7)	1573	43
C_2H_4	5.40 (CD_2Cl_2)	123.3		1623	42

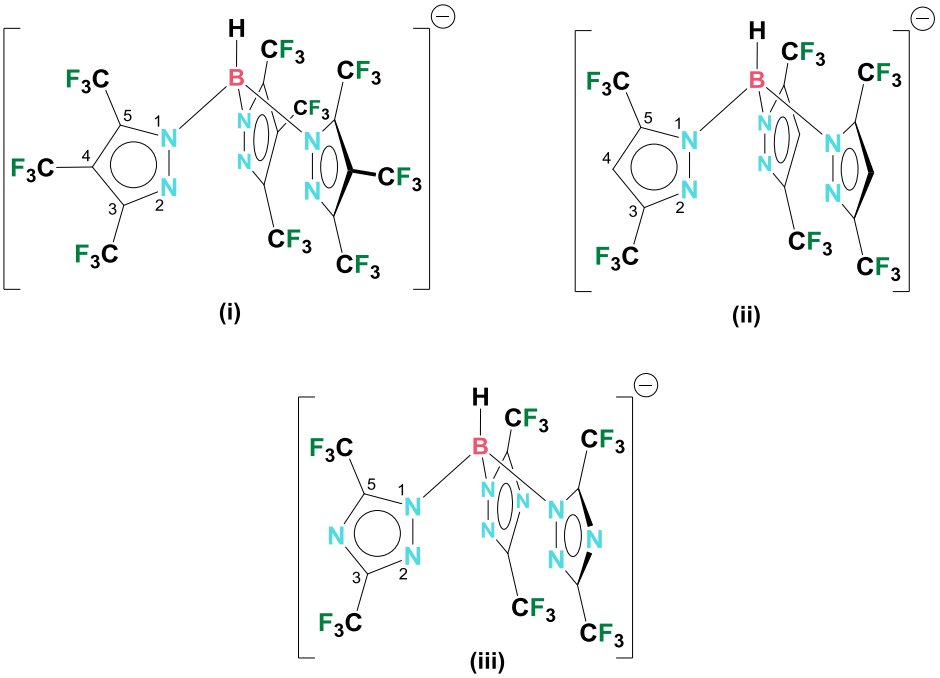

$[HB(3,4,5\text{-}(CF_3)_3Pz)_3]^-$ (i), $[HB(3,5\text{-}(CF_3)_2Pz)_3]^-$ (ii) and $[HB(3,5\text{-}(CF_3)_2Tz)_3]^-$ (iii)

This points to only a 42 cm^{-1} reduction from the C=C stretch of free ethylene (1623 cm^{-1}) as a result of Ag(I) coordination. For comparison, $[HB(3,5\text{-}(CF_3)_2Pz)_3]Ag(C_2H_4)$ and the related tris(triazolyl)borate $[HB(3,5\text{-}(CF_3)_2Tz)_3]Ag(C_2H_4)$ (Tz = triazolyl) display the $\nu_{C=C}$ band at 1573 and 1576 cm^{-1}, respectively.[49] Overall, Raman data are in agreement with the findings from NMR spectroscopy and indicate only minor changes to the ethylene moiety in $[HB(3,4,5\text{-}(CF_3)_3Pz)_3]Ag(C_2H_4)$ compared to the free state. These data also point to the presence of a very electrophilic and only weakly back-bonding silver site and a weakly donating tris(pyrazolyl)borate ligand in $[HB(3,4,5\text{-}(CF_3)_3Pz)_3]Ag(C_2H_4)$.

The related copper analog $[HB(3,4,5\text{-}(CF_3)_3Pz)_3]Cu(C_2H_4)$ was synthesized by treating $[HB(3,4,5\text{-}(CF_3)Pz)_3]Na(THF)$ with $[CuOTf]_2{\bullet}C_6H_6$ in the presence of ethylene. It is also possible to obtain this adduct by the metathesis of $[HB(3,4,5\text{-}(CF_3)_3Pz)_3]Ag(C_2H_4)$ with CuCl. ^1H NMR spectrum of the crude sample indicates the presence of two metal-

bound ethylene adducts out of which $[HB(3,4,5\text{-}(CF_3)_3Pz)_3]Cu(C_2H_4)$ is the major product. $[HB(3,4,5\text{-}(CF_3)_3Pz)_3]Cu(C_2H_4)$ is stable in air at least for several days at room temperature. The ^1H NMR spectrum of $[HB(3,4,5\text{-}(CF_3)_3Pz)_3]Cu(C_2H_4)$ exhibits a resonance at δ 5.06, which is due to the protons of the coordinated ethylene. This is a small but an upfield shift from the free ethylene ^1H NMR signal that appears at δ 5.40. The related silver adduct, as noted earlier, shows a downfield shift of the ethylene ^1H resonance. The ^{13}C NMR spectrum of the $[HB(3,4,5\text{-}(CF_3)_3Pz)_3]Cu(C_2H_4)$ in $CDCl_3$ displays the ethylene carbon signal at δ 94.9 (Table 1.3). It is also the highest ^{13}C chemical shift value observed for copper ethylene adducts of poly(azolyl)borates. The corresponding signal for the $[HB(3,5\text{-}(CF_3)_2Pz)_3]Cu(C_2H_4)$ was observed at δ 89.5, while $[HB(3,5\text{-}(CF_3)_2Tz)_3]Cu(C_2H_4)$ shows this resonance at δ 92.6.[23,49] Similar to the $[HB(3,4,5\text{-}(CF_3)_3Pz)_3]Ag(C_2H_4)$, a $CDCl_3$ solution of $[HB(3,4,5\text{-}(CF_3)_3Pz)_3]Cu(C_2H_4)$ also shows rapid exchange of bound ethylene with added external ethylene on the NMR timescale. $[HB(3,4,5\text{-}(CF_3)_3Pz)_3]Cu(C_2H_4)$ is a crystalline solid, but the crystals we managed to obtain thus far show severe disorder.

It is also possible to synthesize the silver(I) carbonyl adduct supported by $[HB(3,4,5\text{-}(CF_3)_3Pz)_3]^-$. $[HB(3,4,5\text{-}(CF_3)_3Pz)_3]Ag(CO)$ was obtained by replacing ethylene of $[HB(3,4,5\text{-}(CF_3)_3Pz)_3]Ag(C_2H_4)$ with CO (this is, however, a reversible process; the ethylene adduct can be regenerated by treating $[HB(3,4,5\text{-}(CF_3)_3Pz)_3]Ag(CO)$ with ethylene in $CDCl_3$). $[HB(3,4,5\text{-}(CF_3)_3Pz)_3]Ag(CO)$ is a stable white powder at room temperature under nitrogen. The X-ray structure of $[HB(3,4,5\text{-}(CF_3)_3Pz)_3]Ag(CO)$ is illustrated in Figure 1.9. It features a κ^3-bonded tris(pyrazolyl)borate with three somewhat similar Ag-N distances. The Ag-C-O moiety is essentially linear. The Ag-C bond distance 2.083(3) Å is longer than the corresponding distance observed for compounds like $[HB(3,5\text{-}(CF_3)_2Pz)_3]Ag(CO)$ [2.037(5) Å][43] and $[MeB(3\text{-}(Mes)Pz)_3]Ag(CO)$ [1.994(3) Å].[51]

The IR spectrum of [HB(3,4,5-$(CF_3)_3Pz)_3$]Ag(CO) shows the ν_{CO} band at 2177 cm^{-1}. It is significantly higher than the C-O stretching frequency of the free carbon monoxide (2143 cm^{-1}).[52] It also suggests the presence of a very electrophilic metal site with relatively low levels of M→CO π-back-bonding and considerable M-CO electrostatic component.[52] Interestingly, despite the presence of two different pyrazolyl moieties on the supporting ligands, [HB(3,5-$(CF_3)_2Pz)_3$]Ag(CO) shows essentially identical C-O stretch value (2178 cm^{-1}) in the IR spectrum. However, the corresponding silver-ethylene adducts described above show two different chemical shifts for their ethylene carbons.

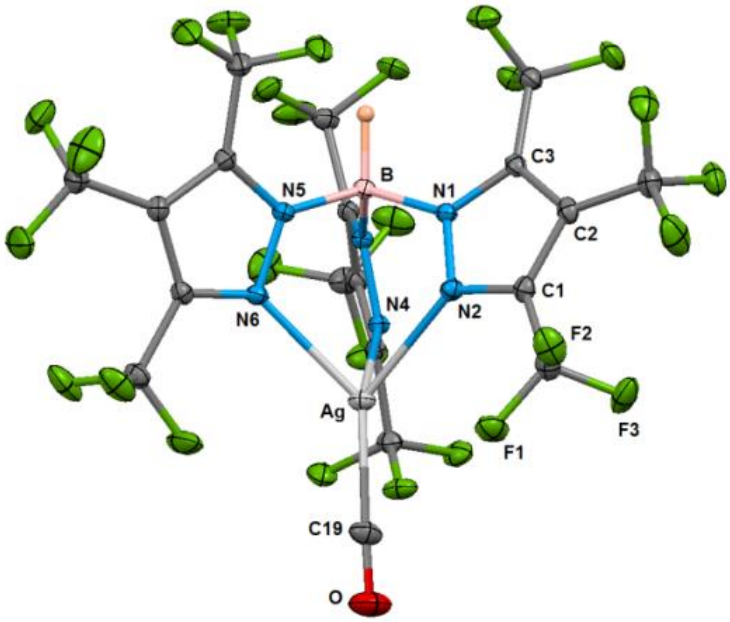

Figure 1.9 Molecular structure of [HB(3,4,5-$(CF_3)_3Pz)_3$]Ag(CO)

Thermal ellipsoids at 40% probability. Selected distances (Å) and angles (deg): Ag-C19 2.083(3), Ag-N6 2.352(2), Ag-N_2 2.3654(19), Ag-N4 2.3799(18), C19-O 1.109(3), Ag⋯B 3.38; N6-Ag-N2 82.12(6), N6-Ag-N4 80.08(6), N2-Ag-N4 81.26(6), O-C19-Ag 175.4(2), C19 Ag⋯B 174.5.

This shows that in contrast to the ethylene ^{13}C chemical shift, the CO stretching frequency value of these Ag-CO adducts lies in a region where CO stretch of silver tris(pyrazolyl)borates is relatively insensitive to the donor properties of the supporting ligand.

Most chemists use CO stretching frequency as a very convenient tool to probe the electronic properties at the metal site. It works well in the regions where M→CO π-back donation dominates. However, the findings presented here and computational studies on cationic $[M\text{-}CO]^+$ (M = Cu, Ag, Au) species reported by Frenking, Strauss and co-workers[53] suggest that one has to be cautious when relating CO stretching frequency data to the metal site electron densities of metal adducts when the $\bar{\upsilon}_{CO}$ values fall in the flatter region. This region is very likely unique to different classes of metal-ligand adducts and depends on many factors including the nature of metal, charge, and supporting ligand. In fact, our previous work involving tris(pyrazolyl)borate and tris(triazolyl)borate adducts suggest that this flatter region is different for copper systems.[54]

1.2.3 Conclusion

Overall, this section describes the isolation of a very highly trifluoromethylated tris(pyrazolyl)borate. Silver and copper ethylene adducts of $[HB(3,4,5\text{-}(CF_3)_3Pz)_3]^-$ are also reported and the weakly donating nature of the supporting ligand is reflected in their ethylene ^{13}C chemical shift. Although the CO stretching frequency of the silver adduct is significantly higher than that of free CO, it is not different from the corresponding parameter of the less fluorinated $[HB(3,5\text{-}(CF_3)_2Pz)_3]Ag(CO)$. We have shown that silver adducts of fluorinated tris(pyrazolyl)borates like $[HB(3,5\text{-}(CF_3)_2Pz)_3]^-$ are very promising catalysts for various processes including C-H and C-halogen bond activation.[35] The catalytic properties of $[HB(3,4,5\text{-}(CF_3)_3Pz)_3]^-$ supported metal adducts, and related ligands with longer fluorocarbons are presently under study.

1.3 Silver small molecular adducts of $[HB(4\text{-}(NO_2)\text{-}3,5\text{-}(CF_3)_2Pz)_3]^-$ and $[HB(4\text{-}Cl\text{-}3,5\text{-}(CF_3)_2Pz)_3]^-$

Naleen B. Jayaratna, Daniel B. Pardue, Sriparna Ray, Muhammed Yousufuddin, Krishna G. Thakur, Thomas R. Cundarib and H. V. Rasika Dias

(Part of this work has been published in *Dalton Transactions* **2013**, 42, 15399)

Reproduced from the reference [55] with permission from The Royal Society of Chemistry.

1.3.1 Introduction

Tris(pyrazolyl)borates (which belong to a family of metal ion chelators generally referred to as scorpionates) are very popular supporting ligands in inorganic, bioinorganic and organometallic chemistry.[1] It is possible to fine-tune their steric and electronic properties easily and over a large continuum of donor properties by changing the substituents on the pyrazolyl rings and on the boron. We are interested in the chemistry of highly fluorinated and weakly coordinating versions of these systems[5-9,22,33,56,57] because they serve as useful supporting ligands for improving resistance to oxidative degradation[58-60], and enhancing the thermal stability of rare examples of late transition metal complexes.[4,10,11,19,22,24,61] For example, $[HB(3,5\text{-}(CF_3)_2Pz)_3]^-$ (Figure 1.10 (a)) is an excellent ligand to stabilize coinage metal ethylene complexes like $[HB(3,5\text{-}(CF_3)_2Pz)_3]Cu(C_2H_4)$ and $[HB(3,5\text{-}(CF_3)_2Pz)_3]Au(C_2H_4)$.[23,24] The copper adduct $[HB(3,5\text{-}(CF_3)_2Pz)_3]Cu(C_2H_4)$ is significantly more thermally and air stable relative to the non-fluorinated analog $[HB(3,5\text{-}(CH_3)_2Pz)_3]Cu(C_2H_4)$. Fluorinated tris(pyrazolyl)borates are also useful auxiliary ligands in catalytic applications.[15-18,23,60,62] For instance, $[HB(3,5\text{-}(CF_3)_2Pz)_3]Ag(C_2H_4)$ and $[HB(3\text{-}(CF_3)\text{-}5\text{-}(CH_3)Pz)_3]Ni(\kappa^2\text{-mCPBA})$ (mCPBA = *m*-

chloroperbenzoate) are good catalysts for the activation of aliphatic C-H bonds *via* carbene and oxygen atom transfer, respectively.[16,17,31,60]

Taking into account the importance and current interest of fluorinated tris(pyrazolyl)borates and weakly coordinating anions in general,[19,63-66] we set out to develop two new tris(pyrazolyl)borates (Figure 1.10), $[HB(4\text{-}Cl\text{-}3,5\text{-}(CF_3)_2Pz)_3]^-$ (b) and $[HB(4\text{-}(NO_2)\text{-}3,5\text{-}(CF_3)_2Pz)_3]^-$ (c), that are not only highly fluorinated, but are also loaded with additional electron-withdrawing substituents. It is also noteworthy that most of the tris(pyrazolyl)borate ligand modification studies involve change in substituents at the pyrazolyl ring 3- and/or 5-positions and on the boron atom. For example, a search of Cambridge Crystallographic database shows that only about 5% of tris(pyrazolyl)borates contain a substituent other than hydrogen at the pyrazolyl ring 4-position.[67] Considering the pKa values of 7.1, 5.5, and 3.4 of the free pyrazoles $3,5\text{-}(CF_3)_2PzH$, $4\text{-}Cl\text{-}3,5\text{-}(CF_3)_2PzH$ and $4\text{-}(NO_2)\text{-}3,5\text{-}(CF_3)_2PzH$, respectively,[68] we anticipate $[HB(4\text{-}Cl\text{-}3,5\text{-}(CF_3)_2Pz)_3]^-$ and $[HB(4\text{-}(NO_2)\text{-}3,5\text{-}(CF_3)_2Pz)_3]^-$ to be weaker donors than $[HB(3,5\text{-}(CF_3)_2Pz)_3]^-$, which we have used effectively in several catalytic applications.

Herein, we report the successful synthesis of these ligands, their silver(I) *cis*-cyclooctene (*c*-COE) adducts, and an experimental and computational study of their electronic and spectral properties. The related $[HB(3,5\text{-}(CF_3)_2Pz)_3]Ag(c\text{-}COE)$ complex was also prepared for comparison. This research is further noteworthy in that structural data on silver *cis*-cyclooctene complexes are rare and heretofore been limited to $\{[\{(2,5\text{-}{}^tBu_2C_6H_3)N{=}CPh\}_2(C_5H_3N)]Ag(c\text{-}COE)\}[OTf]$.[69] In addition, we also describe the use of $[HB(4\text{-}(R)\text{-}3,5\text{-}(CF_3)_2Pz)_3]Ag(c\text{-}COE)$ as catalysts for the activation of C-H bonds of 2,3-dimethylbutane via the insertion of carbene moiety of ethyl diazoacetate (EDA).

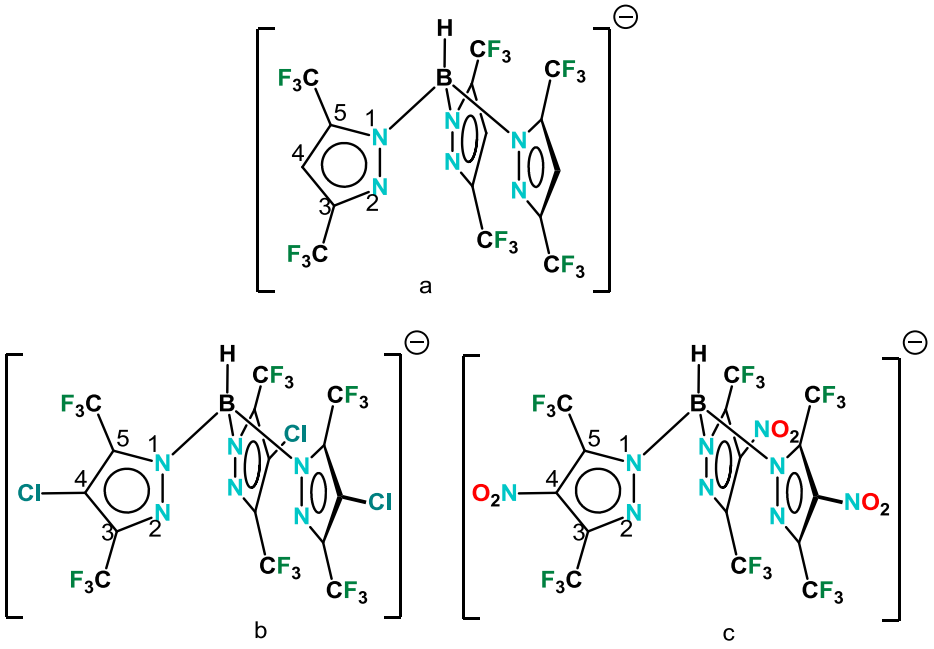

Figure 1.10 Highly fluorinated tris(pyrazolyl)borates $[HB(3,5\text{-}(CF_3)_2Pz)_3]^-$ (a), $[HB(4\text{-}Cl\text{-}3,5\text{-}(CF_3)_2Pz)_3]^-$ (b) and $[HB(4\text{-}(NO_2)\text{-}3,5\text{-}(CF_3)_2Pz)_3]^-$ (c)

1.3.2 Result and discussion

Sodium salts $[HB(4\text{-}Cl\text{-}3,5\text{-}(CF_3)_2Pz)_3]Na$ and $[HB(4\text{-}(NO_2)\text{-}3,5\text{-}(CF_3)_2Pz)_3]Na$ were prepared by reacting $4\text{-}Cl\text{-}3,5\text{-}(CF_3)_2PzH$ or $4\text{-}(NO_2)\text{-}3,5\text{-}(CF_3)_2PzH$ with $NaBH_4$ under nitrogen in a solvent-less process. After a work up involving tetrahydrofuran (THF and/or) diethyl ether (Et_2O), they were obtained as their THF or Et_2O adducts and used in the preparation of silver(I) complexes $[HB(4\text{-}Cl\text{-}3,5\text{-}(CF_3)_2Pz)_3]Ag(THF)$ and $[HB(4\text{-}(NO_2)\text{-}3,5\text{-}(CF_3)_2Pz)_3]Ag(THF)$ (Figure 1.11). The resulting silver adducts were characterized by NMR spectroscopy and elemental analysis. For example, ^1H NMR signals of the THF moiety in $[HB(4\text{-}Cl\text{-}3,5\text{-}(CF_3)_2Pz)_3]Ag(THF)$ appear at δ 1.99 and 3.94 ppm. ^1H NMR signals of free THF in $CDCl_3$ were observed at δ 1.85 and 3.76 ppm.[70] The

^{19}F NMR spectrum of [HB(4-Cl-3,5-$(CF_3)_2$Pz)$_3$]Ag(THF) displays two signals at δ -62.8 and -57.5 ppm for the CF_3 groups at the pyrazolyl ring 3- and 5-positions, respectively. For comparison, the free pyrazole 4-Cl-3,5-$(CF_3)_2$PzH shows just one peak at δ -61.8 ppm in the ^{19}F NMR spectrum. The ^{19}F NMR and ^{1}H NMR spectra of [HB(4-(NO_2)-3,5-$(CF_3)_2$Pz)$_3$]Ag(THF) are not very different from those observed for the [HB(4-Cl-3,5-$(CF_3)_2$Pz)$_3$]Ag(THF). [HB(4-Cl-3,5-$(CF_3)_2$Pz)$_3$]Ag(THF) shows a good solubility in common organic solvents like THF, hexane and dichloromethane whereas [HB(4-(NO_2)-3,5-$(CF_3)_2$Pz)$_3$]Ag(THF) shows good solubility only in relatively polar solvents like acetone and THF and low solubility in $CHCl_3$ and dichloromethane. We have used [HB(3,5-$(CF_3)_2$Pz)$_3$]Ag(THF) as a convenient source of "[HB(3,5-$(CF_3)_2$Pz)$_3$]Ag" motif since silver bound THF can be displaced quite easily with a number of other donors such as ethylene, adamantylazide, or pivalonitrile.[11-13] [HB(4-Cl-3,5-$(CF_3)_2$Pz)$_3$]Ag(THF) and [HB(4-(NO_2)-3,5-$(CF_3)_2$Pz)$_3$]Ag(THF) seem to behave in a similar manner based on the ligand exchange chemistry reported here.

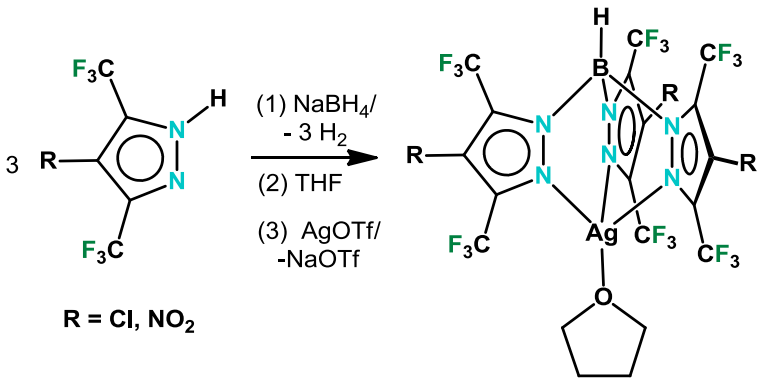

Figure 1.11 Synthesis of [HB(4-(R)-3,5-(CF3)$_2$Pz)$_3$]Ag(THF) (R = Cl, NO_2)

In addition to the synthesis of [HB(4-Cl-3,5-$(CF_3)_2$Pz)$_3$]$^-$ and [HB(4-(NO_2)-3,5-$(CF_3)_2$Pz)$_3$]$^-$, it was also of interest to probe the donor properties of these ligands that

contain a large number of powerful electron-withdrawing substituents (*meta*-substituent constant, σ_{meta} for H, Cl and NO_2 groups are 0.0, +0.37, and +0.71, respectively).[71] One possibility was to use the C-O stretching frequency of carbonyl adducts for this purpose. Preliminary work suggested that it was possible to prepare the silver-carbonyl adduct $[HB(4\text{-}(NO_2)\text{-}3,5\text{-}(CF_3)_2Pz)_3]AgCO$ by treating $[HB(4\text{-}(NO_2)\text{-}3,5\text{-}(CF_3)_2Pz)_3]Ag(THF)$ with CO as evidenced by the appearance of a 2177 cm^{-1} band in the IR spectrum for the CO stretch. However, the IR band for these adducts unfortunately appear in a region relatively insensitive to their ligand electronic properties.[33,56,72] A second option was to utilize silver-alkene adducts as it is known that NMR spectroscopic parameters (in particular the ^{13}C NMR chemical shifts of the olefinic carbons) of metal alkenes provide useful insights into the nature of metal-alkene bonds.[21,73-75] The chemical shift of coordinated carbons gives an estimate of the electron density around the olefinic carbon nuclei, which can be related to the electron density at the metal atom and thus indirectly to the donor properties of supporting ligands. In fact, we have used ^{13}C NMR resonance of coinage metal ethylene adducts to probe the bonding between Cu, Ag, or Au and ethylene[19,21,57] and also to estimate the donor properties of tris(pyrazolyl)borate *versus* tris(triazolyl)borate auxiliary ligands.[56]

Silver alkene complexes are of interest due to their importance in industrial processes and alkene separation chemistry.[19,20,76] Thus, we focused our initial efforts on the synthesis of the ethylene adduct $[HB(4\text{-}(NO_2)\text{-}3,5\text{-}(CF_3)_2Pz)_3]Ag(C_2H_4)$ using $[HB(4\text{-}(NO_2)\text{-}3,5\text{-}(CF_3)_2Pz)_3]Ag(THF)$ and ethylene. Although preliminary data suggest the formation of this adduct (silver bound ethylene signal at δ 5.69 ppm in $CDCl_3$), its low solubility in non-polar solvents has so far prevented us from making complete characterization. As an alternative, we decided to prepare a series of *cis*-cyclooctene (*c*-COE) adducts as these were thought to be more soluble in common, less polar organic

solvents. Stabilization of such adducts was also of interest because, compared to the *trans*-cyclooctene complexes of Ag(I), *cis*-cyclooctene analogs are less common. In fact, silver nitrate has been used very effectively to separate *cis*-cyclooctene from *trans*-cyclooctene because *trans*-cyclooctene preferentially coordinates to Ag(I) leaving *cis*-cyclooctene in solution.[77-81] The Ag(*c*-COE)(OTf) and {[$H_2C(3,5\text{-}(CF_3)_2Pz)_2$]Ag(*c*-COE)}[$BF_4$] represent Ag-(*c*-COE) compounds with detailed spectroscopic data while {[{(2,5-$^tBu_2C_6H_3$)N=CPh}$_2$(C_5H_3N)]Ag(*c*-COE)}[OTf] is the only silver(I) *cis*-cyclooctene adduct with X-ray structural data.[69,82]

The tris(pyrazolyl)boratosilver(I) adduct [HB(4-(NO_2)-3,5-(CF_3)$_2$Pz)$_3$]Ag(*c*-COE) can be obtained quite easily and in high yield by displacing the THF in [HB(4-(NO_2)-3,5-(CF_3)$_2$Pz)$_3$]Ag(THF) with *cis*-cyclooctene in a dichloromethane solution (Figure 1.12). Excess *cis*-cyclooctene is needed to ensure complete displacement of THF. A reaction between Ag(OTf) and [HB(4-(NO_2)-3,5-(CF_3)$_2$Pz)$_3$]Na(THF) in the presence of *cis*-cyclooctene in dichloromethane also yields the same product. [HB(4-(NO_2)-3,5-(CF_3)$_2$Pz)$_3$]Ag(*c*-COE) is a remarkably stable white powder that can be dried under vacuum at room temperature without any noticeable loss of coordinated *cis*-cyclooctene. Related [HB(4-Cl-3,5-(CF_3)$_2$Pz)$_3$]Ag(*c*-COE) and [HB(3,5-(CF_3)$_2$Pz)$_3$]Ag(*c*-COE) can also be obtained via a similar process. They are also thermally stable solids. Alternatively, the silver *cis*-cyclooctene adduct [HB(3,5-(CF_3)$_2$Pz)$_3$]Ag(*c*-COE) can be synthesized by replacing the ethylene in [HB(3,5-(CF_3)$_2$Pz)$_3$]Ag(C_2H_4). A lesser amount of *cis*-cyclooctene is sufficient for this route.

The silver(I) *cis*-cyclooctene adducts [HB(4-(R)-3,5-(CF_3)$_2$Pz)$_3$]Ag(*c*-COE) (R = H, Cl, NO_2) were characterized using several spectroscopic techniques and also by X-ray crystallography. The ^{19}F NMR spectra of these adducts display two signals attributable to

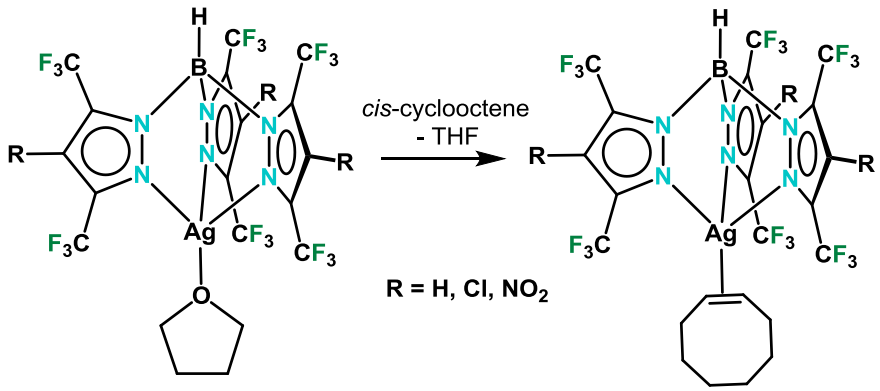

Figure 1.12 Synthesis of $[HB(4\text{-}(R)\text{-}3,5\text{-}(CF_3)_2Pz)_3]Ag$(c-COE) (R = H, Cl, NO_2)

the CF_3 groups at the pyrazolyl ring 3- and 5-positions, respectively, and the chemical shift values were not much different from the corresponding resonances of the THF adducts $[HB(4\text{-}(R)\text{-}3,5\text{-}(CF_3)_2Pz)_3]Ag$(THF). However, in all three $[HB(4\text{-}(R)\text{-}3,5\text{-}(CF_3)_2Pz)_3]Ag$(*c*-COE) adducts, the resonance assignable to CF_3 groups at the pyrazolyl ring 5-positions appeared as a doublet due to coupling to proton on the boron atom. We have observed such long-range coupling in several metal adducts involving $[HB(3,5\text{-}(CF_3)_2Pz)_3]^-$ ligand.[9]

^{1}H NMR spectra of $[HB(4\text{-}(R)\text{-}3,5\text{-}(CF_3)_2Pz)_3]Ag$(*c*-COE) display three sets of resonances for the protons of silver-bound *cis*-cyclooctene moiety. Vinylic protons appear in the region δ 6.29 - 6.18 ppm, which is a downfield shift of the corresponding resonance of the free *cis*-cyclooctene (δ 5.62 ppm). We have observed a similar downfield shift of ethylene proton signal in silver adducts like $[HB(3,5\text{-}(CF_3)_2Pz)_3]Ag(C_2H_4)$.[33,57,83] Addition of excess *cis*-cyclooctene to $CDCl_3$ solution of $[HB(4\text{-}(R)\text{-}3,5\text{-}(CF_3)_2Pz)_3]Ag$(*c*-COE) leads to line broadening and coalescence of the matching ^{1}H signals pointing to a ligand exchange process in solution at room temperature on the

NMR time scale. For comparison, vinylic protons of Ag(*c*-COE)(OTf) and {[$H_2C(3,5\text{-}(CF_3)_2Pz)_2$]Ag(*c*-COE)}[$BF_4$] appear at δ 6.07 (in $CDCl_3$) and 5.79 (in C_6D_6) ppm, respectively, while copper adducts like {[$H_2C(3,5\text{-}(CF_3)_2Pz)_2$]Cu(*c*-COE)}[OTf] show an upfield shift (δ 5.23 ppm in $CDCl_3$) relative to the corresponding resonance of the free *cis*-cyclooctene.[82,84,85]

To study the effect of the temperature on NMR spectra of theses complexes, we used [HB(4-Cl-3,5-$(CF_3)_2Pz)_3$]Ag(*c*-COE) (which shows good solubility in $CDCl_3$) as a model complex and collected ^1H and ^{13}C NMR data at –20 °C. At this temperature, the singlet observed at δ 2.38 ppm separated in to a doublet while the multiplet at δ 1.45–1.85 ppm became more complicated and displayed additional peak splitting. The better resolution of spin-spin coupling of the resonances corresponding to the -CH_2- protons in the ring perhaps indicates the restriction of free motion of the *cis*-cyclooctene at low temperature. The olefinic carbon resonance in ^{13}C displayed a small upfield shift from δ 123.4 to 122.7 ppm upon cooling from room temperature to -20 °C. $^{13}C\{1H\}$ NMR spectra of [HB(4-(R)-3,5-$(CF_3)_2Pz)_3$]Ag(c-COE) (R = H, Cl, NO_2) display the alkene carbon resonance in the δ 121.2 - 124.4 ppm region, which is a small but significant upfield shift compared to the δ 130.2 ppm (alkene carbon) signal observed for free cis-cyclooctene. These signals appear as doublets in the proton-coupled ^{13}C NMR spectra. For example, alkene carbons of [HB(4-(NO_2)-3,5-$(CF_3)_2Pz)_3$]Ag(c-COE) show up in the ^{13}C NMR spectrum as a doublet with $1J$(C-H) = 154 Hz. Interestingly, [HB(4-(NO_2)-3,5-$(CF_3)_2Pz)_3$]Ag(c-COE) displays the smallest upfield shift ($\Delta^{13}C$ = -5.8 ppm; $\Delta^{13}C$ = $\delta_{\text{coordinated olefin}} - \delta_{\text{free olefin}}$) of the alkene carbon peak (versus free alkene) followed by the [HB(4-Cl-3,5-$(CF_3)_2Pz)_3$]Ag(c-COE) ($\Delta^{13}C$ = -6.8 ppm) and [HB(3,5-$(CF_3)_2Pz)_3$]Ag(c-COE) ($\Delta^{13}C$ = -9.0 ppm). For comparison, cationic {[$H_2C(3,5\text{-}(CF_3)_2Pz)_2$]Ag(c-COE)}[$BF_4$] displays the olefinic carbon at δ 125.1 ppm ($\Delta^{13}C$ = -5.1 ppm) while the related copper

analog {[$H_2C(3,5\text{-}(CF_3)_2Pz)_2$]Cu(c-COE)}[OTf] exhibits this peak at a much lower chemical shift value of δ 106.3 ppm ($\Delta^{13}C$ = -23.9 ppm).[86] Overall, these data point to the presence of very electron poor silver(I) sites in [$HB(4\text{-}(R)\text{-}3,5\text{-}(CF_3)_2Pz)_3$]Ag(c-COE) with minimal Ag→(*cis*-cyclooctene) backbonding. Although the impact of R (H, Cl, NO_2) on the alkene carbon chemical shift of these adducts is small, the ^{13}C NMR data suggest that [$HB(4\text{-}(NO_2)\text{-}3,5\text{-}(CF_3)_2Pz)_3$]Ag(c-COE) possesses the most-electrophilic metal site, which correlates with the pKa values of the free pyrazoles quoted above.[68] Note also that while [$HB(3,5\text{-}(CF_3)_2Pz)_3$]$^-$ is a weak donor in many respects it is the "best" donor in this [$HB(4\text{-}(R)\text{-}3,5\text{-}(CF_3)_2Pz)_3$]$^-$ series.

The X-ray crystal structure of [$HB(3,5\text{-}(CF_3)_2Pz)_3$]Ag(*c*-COE) is illustrated in Figure 1.13. Selected bond distances and angles are presented in Table 1-5. There are two molecules in the asymmetric unit with somewhat different bond lengths and bond angles. Both molecules show a pseudo-tetrahedral geometry at the silver atom defined by the ligating nitrogen atoms of the scorpionate ligand and the centroid of the *cis*-cyclooctene double bond. The *cis*-cyclooctene is ligated to the silver ion in a η^2 fashion. The Ag-C distances for Ag(1) are 2.3349(14) and 2.3612(14) Å and for Ag(2) are 2.3271(13) and 2.3486(13) Å and thus indicate a slightly asymmetry in the coordination of the alkene to the silver. A similar coordination mode of the cyclooctene has been observed in {[{(2,5-^{t}Bu$_2$C$_6$H$_3$)N=CPh}$_2$(C_5H_3N)]Ag(*c*-COE)}[OTf] with Ag–C_{olefin} distances of 2.418(5) and 2.360(6) Å.[69]

The Ag(I) in [$HB(3,5\text{-}(CF_3)_2Pz)_3$]Ag(*c*-COE) coordinates to tris(pyrazolyl)borate in typical κ^3 fashion having two similar bond lengths and one unique bond length in each molecule, Ag(1): 2.4027(11), 2.4095(11), 2.3446(11) Å and Ag(2): 2.4391(11), 2.3567(11), 2.3578(11) Å. Interestingly in one molecule, two Ag-N bonds are longer and the third one is shorter whereas in the second molecule in the asymmetric unit, two

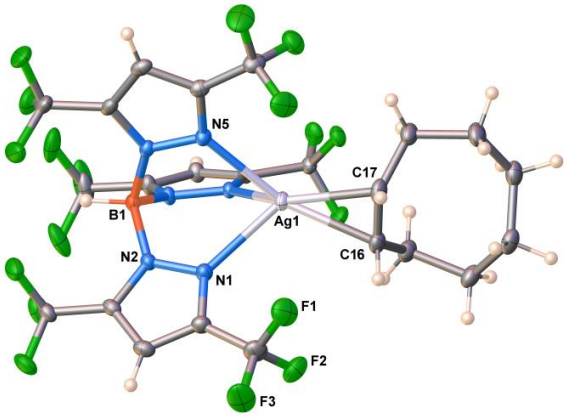

Figure 1.13 Molecular structure of [HB(3,5-$(CF_3)_2Pz)_3$]Ag(c-COE)

Thermal ellipsoids at 50% probability.

bonds are shorter and only one is longer (which is not an uncommon metal coordination mode for this family of metal complexes).

The X-ray crystal structure of [HB(4-Cl-3,5-$(CF_3)_2Pz)_3$]Ag(*c*-COE) is illustrated in Figure 1.14. The molecule shows pseudo-tetrahedral geometry at the silver atoms and features a κ^3-bound tris(pyrazolyl)borate moiety. There are two similar Ag-N bond distances 2.3636(16), 2.3870(15) Å and a fairly long Ag-N 2.5835(16) Å. The *cis*-cyclooctene ring is located on the same side of one of the pyrazolyl arms that has the longer Ag-N bond. The alkene is coordinated to the silver in η^2 fashion. [HB(4-(NO_2)-3,5-$(CF_3)_2Pz)_3$]Ag(*c*-COE) in general has a similar structure (Figure 1.15) to that of [HB(4-Cl-3,5-$(CF_3)_2Pz)_3$]Ag(*c*-COE), but with two longer and one shorter Ag-N bonds. In addition, there is an inter-molecular interaction at 3.02 Å between Ag and oxygen atoms of an adjacent nitro-group (which is within van der Waals contact distance of 3.24 Å). Overall, both of [HB(4-(NO_2)-3,5-$(CF_3)_2Pz)_3$]Ag(*c*-COE) and [HB(4-Cl-3,5-$(CF_3)_2Pz)_3$]Ag(*c*-COE) have very similar average Ag-N bond distances (2.441 and 2.445 Å) while [HB(3,5-$(CF_3)_2Pz)_3$]Ag(*c*-COE) with relatively better donating tris(pyrazolyl)borate has a somewhat

Table 1.4 Crystallographic data for [HB(4-(R)-3,5-$(CF_3)_2Pz)_3$]Ag(c-COE) (R = H, Cl, NO_2)

Compound	**[HB(3,5-$(CF_3)_2Pz)_3$]Ag(*c*-COE)**	**[HB(4-Cl-3,5-$(CF_3)_2Pz)_3$]Ag(*c*-COE)**	**[HB(4-(NO_2)-3,5-$(CF_3)_2Pz)_3$]Ag(*c*-COE)**
FW	839.11	942.44	1016.58
Temperature (*K*)	100	100	100
Crystal System	Triclinic	Triclinic	Triclinic
Space Group	$P\bar{1}$	$P\bar{1}$	$P\bar{1}$
Cell Dimensions	a = 10.5488(4) Å	a = 11.0504(7) Å	a = 9.1587(10) Å
	b = 16.9402(7) Å	b = 11.7809(7) Å	b = 10.6707(12) Å
	c = 17.4895(7) Å	c = 14.1755(9) Å	c = 19.284(2) Å
	α= 83.886(1)°	α= 112.159(1)°	α= 105.190(1)°
	β= 74.977(1)°	β= 99.295(1)°	β= 90.842(2)°
	γ = 81.857(1)°	γ = 101.201(1)°	γ = 105.294(1)°
V (Å)^3	2980.1(2)	1619.61(17)	1747.2(3)
Z	4	2	2
d_{calcd} (g cm^{-3})	1.870	1.933	1.932
abs coeff (mm^{-1})	0.817	1.003	0.804
F (000)	1648	920	998
θ range (deg)	2.79-34.14	1.93-29.37	2.05-28.29
reflns collected	58332	15682	16723
R_{int} (Ind reflns)	0.0207(24492)	0.0150(8054)	0.0317(8404)
data/restr/params	24492/0/891	8054/0/492	8404/13/554
GOF on F^2	1.039	1.045	1.019
*R*1 [$I > 2\sigma(I)$]/all data	0.0314/0.0444	0.0298/0.0323	0.0426/0.0555
w*R*2 [$I > 2\sigma(I)$]/all data	0.0712/0.0757	0.0772/0.0793	0.0970/0.1032

Table 1.5 Selected experimentally determined and DFT calculated (in italics) bond distances (Å) and angles (deg) of [HB(4-(R)-3,5-$(CF_3)_2Pz)_3$]Ag(c-COE) (R = H, Cl, NO_2). Calculated C=C distance of free cis-cyclooctene = 1.346 Å.

Compound	**Ag-N**	**Ag-C**	**C=C**	**C-Ag-C**	**N-Ag-N**
[HB(3,5-$(CF_3)_2Pz)_3$]Ag	*2.344* *2.343* *2.341*				*84.9* *84.9* *85.0*
[HB(3,5-$(CF_3)_2Pz)_3$]Ag(*c*-COE) *Molecule 1*	2.4027(11) 2.4095(11) 2.3446(11)	2.3349(14) 2.3612(14)	1.358(2)	33.62(5)	81.94(4) 79.47(4) 77.18(4)
[HB(3,5-$(CF_3)_2Pz)_3$]Ag(*c*-COE) *Molecule 2*	2.4391(11) 2.3567(11) 2.3578(11)	2.3271(13) 2.3486(13)	1.361(2)	33.84(5)	79.19(4) 80.33(4) 79.79(4)
[HB(3,5-$(CF_3)_2Pz)_3$]Ag(c-COE)	*2.405* *2.518* *2.371*	*2.329* *2.339*	*1.383*	*34.48*	*78.87* *82.28* *80.82*
[HB(4-Cl-3,5-$(CF_3)_2Pz)_3$]Ag(*c*-COE)	2.3636(16) 2.3870(15) 2.5835(16)	2.347(2) 2.375(2)	1.358(3)	33.41(8)	83.58(5) 77.18(5) 80.81(5)
[HB(4-Cl-3,5-$(CF_3)_2Pz)_3$]Ag(c-COE)	*2.399* *2.552* *2.433*	*2.331* *2.361*	*1.382*	*34.26*	*79.24* *82.87* *79.35*
[HB(4-(NO_2)-3,5-$(CF_3)_2Pz)_3$]Ag(*c*-COE)	2.472(2) 2.459(2) 2.393(2)	2.365(3) 2.374(3)	1.354(5)	33.22(11)	85.44(8) 74.48(8) 74.47(8)
[HB(4-(NO_2)-3,5-$(CF_3)_2Pz)_3$]Ag(c-COE)	*2.415* *2.552* *2.429*	*2.327* *2.358*	*1.384*	*34.34*	*78.39* *81.81* *79.05*

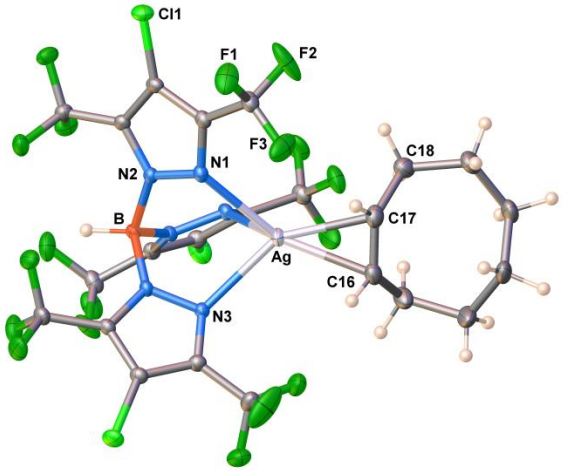

Figure 1.14 Molecular structure of [HB(4-Cl-3,5-$(CF_3)_2Pz)_3$]Ag(c-COE) (thermal ellipsoids at 50% probability).

shorter average Ag-N distance (2.385 Å). Average Ag-C_{olefin} bond distances 2.343, 2.361, and 2.396 Å of [HB(4-(R)-3,5-$(CF_3)_2Pz)_3$]Ag(*c*-COE) (R = H, Cl, NO_2, respectively) show a similar pattern. [HB(3,5-$(CF_3)_2Pz)_3$]Ag(C_2H_4) is known and it has a bit shorter Ag-C distance (average 2.301 Å), perhaps due to steric reasons. The C=C bond distance of coordinated *cis*-cyclooctene in these silver(I) adducts does not show a significant variation (range from 1.354(2)-1.361(2) Å). The C-Ag-C angles are also essentially the same among the three *cis*-cyclooctene adducts.

To further probe the structure and bonding of these novel Ag(I) complexes, density functional theory was employed using methods successfully calibrated in previous studies of coinage metal olefin complexes.[21] The *cis*-cyclooctene is coordinated to the Ag(I) ion in a η^2 fashion, as seen experimentally and as expected based on previous literature precedents. The computed Ag-C_{olefin} distances show a minute variation (2.327 Å to 2.361 Å), Table 1-5. There is a slight asymmetry in the Ag-C_{olefin} distances, *ca.* 0.02 Å on average, akin to that measured experimentally. Only a small (0.04 Å)

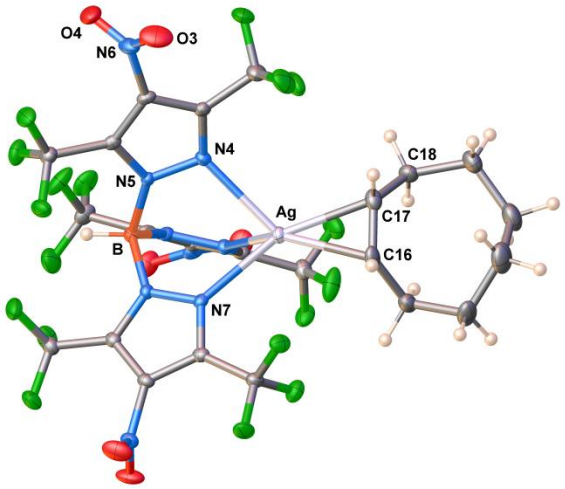

Figure 1.15 Molecular structure of [HB(4-(NO_2)-3,5-(CF_3)$_2$Pz)$_3$]Ag(*c*-COE)

(thermal ellipsoids at 50% probability).

lengthening of olefin C=C bond upon ligation to Ag(I) (compared to calculated C=C distance of 1.346 Å for free *cis*-cyclooctene) was observed, consistent with the formulation of these complexes as π-complexes rather than metallacyclopropanes. The Ag—(N1, N2, N3) distances consistently had interactions in which two of the three nitrogens (those trans to the olefinic carbons) are more closely ligated (by ~ 0.1 Å) to the silver in all three complexes. In the absence of the *cis*-cyclooctene, the Ag-N bond lengths (*ca*. 2.34 Å) were of equal distance, Table 1-5.

Computed ^{13}C NMR spectra (referenced to TMS) of [HB(4-(R)-3,5-(CF_3)$_2$Pz)$_3$]Ag(*c*-COE) (R = H, Cl, NO_2) display the alkene carbon resonance in the δ 122.8 – 125.7ppm region, depending on the substituents in the 4-position of the tris(pyrazolyl)borate. This is an upfield shift in comparison to the δ 141.1 ppm (average of alkene carbons) signal computed for “free” *cis*-cyclooctene. The calculated ~12 - 20 ppm

shift in ^{13}C δ mimics, but exaggerates the 6 – 9 ppm upfield shifts measured experimentally, perhaps due to neglect of solvent effects in the simulations.

The complexes [HB(3,5-$(CF_3)_2$Pz)$_3$]Ag(*c*-COE) and [HB(4-Cl-3,5-$(CF_3)_2$Pz)$_3$]Ag(*c*-COE) have computed average alkene carbon peaks of δ 122.8 ppm and δ 125.2 ppm, respectively. Complex [HB(4-(NO_2)-3,5-$(CF_3)_2$Pz)$_3$]Ag(*c*-COE) has an average alkene carbon peak of δ 125.7 ppm. Thus, as with experimental $\Delta^{13}C$ (*vide supra*), the 4-Cl and 4-NO_2 decorated scorpionates are more similar, while the adduct based on parent [HB(3,5-$(CF_3)_2$Pz)$_3$]$^-$ is more dissimilar. Computed ^1H NMR spectra (referenced to TMS) for the two vinylic protons of free *cis*-cyclooctene yield an average chemical shift of δ 6.2 ppm. The computed chemical shifts for vinylic protons in the silver *c*-COE complexes are downfield from free *cis*-cyclooctene. The complex [HB(3,5-$(CF_3)_2$Pz)$_3$]Ag(*c*-COE) has computed (average) δ of 7.3 ppm. Complexes [HB(4-Cl-3,5-$(CF_3)_2$Pz)$_3$]Ag(*c*-COE) and [HB(4-(NO_2)-3,5-$(CF_3)_2$Pz)$_3$]Ag(*c*-COE) have average vinylic H peaks of δ 7.1 ppm and δ 7.2 ppm, respectively. As seen experimentally, the ^1H shifts are less sensitive to silver coordination than the ^{13}C NMR chemical shifts. More significantly, the aggregate of experimental and computed NMR properties clearly point to very electron deficient Ag(I)-olefin complexes. Furthermore, this research suggests that the R = NO_2 complex has the most electrophilic/acidic metal site with the R = Cl complex possessing a slightly less electrophilic/acidic metal site, with the parent complex being the least acidic.

The electron populations (P_π and P_{π^*}) localized on the olefinic moiety of *cis*-cyclooctene were evaluated via a Natural Bond Order analysis, Table 1-6. The increased population in the π^*_{CC} of the C=C bond upon coordination to Ag(I) (ΔP_{π^*} ~ +0.06 e^-) is commensurate with the decline in the π_{CC} population for the complexes studied (ΔP_π ~ -0.06 e^-). These small numbers thus corroborate the other spectroscopic and structural

analyses in that there is minimal Ag-(*cis*-cyclooctene) σ-bonding and π-backbonding, indicating complexes that are much more heavily weighted toward π-complex than metallacyclopropane within the Dewar-Chatt-Duncanson spectrum of descriptions for olefin adducts.[19,87,88] Further support for the ionicity of the silver(I)-olefin moiety is found in the computed atomic charge of silver, which is *ca.* +0.61 e^- for all three [HB(4-(R)-3,5-$(CF_3)_2Pz)_3$]Ag(*c*-COE) complexes studied here. While the changes in orbital electron populations are very small, the largest decrease in π_{CC} population and the smallest increase in π^*_{CC} population were observed in [HB(4-(NO_2)-3,5-$(CF_3)_2Pz)_3$]Ag(*c*-COE) whereas [HB(3,5-$(CF_3)_2Pz)_3$]Ag(*c*-COE) shows smallest decrease in π_{CC} population and the largest increase in π^*_{CC} population. These data suggest that [HB(4-(NO_2)-3,5-$(CF_3)_2Pz)_3$]Ag(*c*-COE) has the weakest Ag→olefin π-backdonation and the strongest olefin→Ag σ-donation although the differences among the three systems are small. Interestingly, the net effect of σ/π-bonding (*e.g.*, calculated bond order) appears to be the same for all three adducts, which is also reflected in essentially identical C=C distances of silver coordinated *cis*-cyclooctene.

Silver complexes supported by weakly coordinating ligands such as tris(pyrazolyl)borates (scorpionates) are excellent catalysts for the insertion of carbene moiety of diazo reagents like ethyl diazoacetate (EDA) to unactivated C-H bonds of hydrocarbons (Figure 1.16).[16,17,19,31,32,89-91] The activation of primary C-H bonds in greater proportion has also been noted with the increased acidity at the silver center.[31] Such a study involving "[HB(4-(R)-3,5-$(CF_3)_2Pz)_3$]Ag" catalysts would be useful as it could provide additional evidence for the more weakly coordinating nature of the supporting ligands like [HB(4-(NO_2)-3,5-$(CF_3)_2Pz)_3]^-$ compared to the well-known [HB(3,5-$(CF_3)_2Pz)_3]^-$. Thus, carbene insertion chemistry catalyzed by [HB(4-Cl-3,5$(CF_3)_2Pz)_3$]Ag

Table 1.6 Calculated orbital population of *c*-COE and all three [HB(4-(R)-3,5-$(CF_3)_2Pz)_3$]Ag(*c*-COE) complexes (R = H, Cl, NO_2)

Compound	$\mathbf{P_\pi}$	$\mathbf{P_\pi^*}$	$\Delta\mathbf{P_\pi}$	$\Delta\mathbf{P_{\pi^*}}$
c-COE	1.951	0.0900	0.000	0.000
[HB(3,5-$(CF_3)_2Pz)_3$]Ag(*c*-COE)	1.893	0.159	0.058	-0.069
[HB(4-Cl-3,5-$(CF_3)_2Pz)_3$]Ag(*c*-COE)	1.890	0.156	0.061	-0.066
[HB(4-(NO_2)-3,5-$(CF_3)_2Pz)_3$]Ag(*c*-COE)	1.886	0.152	0.065	-0.062

Population of the π natural bond orbital (P_π, e^-) and population of the π^* natural bond orbital (P_π^*, e^-), variation with respect to free *cis*-cyclooctene (ΔP_π = P_π(free ligand) – P_π(metal complex, e^-); ΔP_{π^*} = P_{π^*}(free ligand) – P_{π^*}(metal complex), e^-).

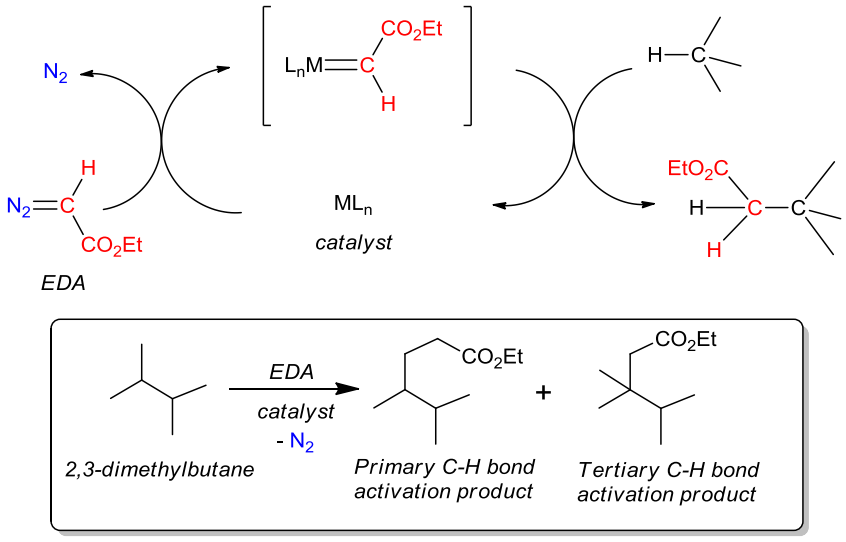

Figure 1.16 Transition metal mediated carbene insertion into C-H bonds and reactions involving 2,3-dimethylbutane

Table 1.7 Catalytic C-H bond activation of 2,3-dimethylbutane

Catalyst	EDA remaining	primary C-H bond activation product	tertiary C-H bond activation product
[HB(4-(NO_2)-3,5-(CF_3)$_2$Pz)$_3$]Ag(*c*-COE)	0.9	83.2	15.6
[HB(4-Cl-3,5-(CF_3)$_2$Pz)$_3$]Ag(*c*-COE)	0.5	79.8	18.8
[HB(4-Cl-3,5-(CF_3)$_2$Pz)$_3$]Ag(THF)	0.1	79.3	20.0
[HB(3,5-(CF_3)$_2$Pz)$_3$]Ag(THF)	0	79.0	20.4
AgOTf	97.8	0.9	0.7

Product distribution (based on GC and confirmed by NMR spectroscopy) as a percentage (average of two runs), obtained from the reaction of 2,3-dimethylbutane (excess) with EDA (1.0 mmol) with use of silver complexes (0.015 mmol) as the catalyst in octafluorotoluene after 12 hrs. See Figure 1.16 for primary and tertiary C-H bond activation products. The remainder of the products were carbene dimers (diethyl maleate and diethyl fumarate), and the total amounts were less than 1% in all the runs listed.

(*c*-COE) and [HB(4-(NO_2)-3,5-(CF_3)$_2$Pz)$_3$]Ag(*c*-COE) was probed using 2,3-dimethylbutane as the substrate (which contains both primary and tertiary C-H bonds) and ethyl diazoacetate as the carbene source. The catalyst [HB(3,5-(CF_3)$_2$Pz)$_3$]Ag(THF) was also included in the study for a comparison.

Often these C-H activation reactions are performed using the substrate (hydrocarbon) as the reaction medium. Indeed, the [HB(3,5-(CF_3)$_2$Pz)$_3$]Ag(THF)

catalyzed reaction could be performed effectively in neat 2,3-dimethylbutane. However, the solubility of [HB(4-(NO_2)-3,5-(CF_3)$_2$Pz)$_3$]Ag(*c*-COE) is poor in 2,3-dimethylbutane to perform a similar reaction effectively in neat 2,3-dimethylbutane. For example, even after 12 h, ~41% of unreacted EDA was left in the reaction mixture while the [HB(3,5-(CF_3)$_2$Pz)$_3$]Ag(THF) catalyzed reaction in neat 2,3-dimethylbutane was complete well within 6 h. We found that octafluorotoluene is a better solvent for [HB(4-(NO_2)-3,5-(CF_3)$_2$Pz)$_3$]Ag(*c*-COE). The related silver adducts [HB(4-(Cl)-3,5-(CF_3)$_2$Pz)$_3$]Ag(*c*-COE), [HB(4-(Cl)-3,5-(CF_3)$_2$Pz)$_3$]Ag(THF) and [HB(3,5-(CF_3)$_2$Pz)$_3$]Ag(THF) show even better solubility in octafluorotoluene. Since octafluorotoluene is also inert compared to the substrate 2,3-dimethylbutane, it was chosen as a reasonable solvent to use in this chemistry. Results are summarized in Table 1-7. All these fluorinated tris(pyrazolyl)borate ligand supported silver adducts show excellent catalytic activity. They efficiently transfer the carbene moiety to C-H bonds very effectively and cleanly with negligible carbene dimer (diethyl maleate and diethyl fumarate) formation. Interestingly, [HB(4-(NO_2)-3,5-(CF_3)$_2$Pz)$_3$]Ag(*c*-COE) gave the highest primary C-H bond activation product, suggesting that it indeed possesses the most acidic silver site. The product distribution between [HB(4-(Cl)-3,5-(CF_3)$_2$Pz)$_3$]Ag(*c*-COE) and [HB(3,5-(CF_3)$_2$Pz)$_3$]Ag(THF) is, however, not very different. The [HB(4-(Cl)-3,5-(CF_3)$_2$Pz)$_3$]Ag(*c*-COE) and [HB(4-(Cl)-3,5-(CF_3)$_2$Pz)$_3$]Ag(THF) gave essentially the same product distribution as expected indicating that the secondary ligand THF or *cis*-cyclooctene on the tris(pyrazolyl)boratosilver moiety has essentially no effect on the catalytic activity. When AgOTf was used as the catalyst under similar conditions, significant EDA activation was not observed.

1.3.3 Conclusions

In summary, we report the synthesis of [HB(4-Cl-3,5-(CF_3)$_2$Pz)$_3$]$^-$ and [HB(4-(NO_2)-3,5-(CF_3)$_2$Pz)$_3$]$^-$, which are not only highly fluorinated, but are also loaded with

additional electron-withdrawing substituents. The pyrazole precursors utilized for the synthesis of these ligands can be prepared quite easily from 3,5-$(CF_3)_2$PzH. They allow the isolation of thermally stable silver(I) *cis*-cyclooctene adducts. The ^{13}C NMR data of the olefinic carbons and NBO analysis of the silver bound π and π^* orbital populations of the *cis*-cyclooctene suggest that [HB(4-(NO_2)-3,5-$(CF_3)_2$Pz)$_3$]Ag(*c*-COE) possesses the most-electrophilic metal site among [HB(4-(R)-3,5-$(CF_3)_2$Pz)$_3$]Ag(*c*-COE) (R = H, Cl, NO_2), which correlates with the p*K*a values of the free pyrazoles. To some extent the impact of these 4-position modifications upon the metal ion and the olefin ligand is muted, as expected from inductive effects far separated by many bonds from the Ag(*c*-COE) active site. [HB(4-(R)-3,5-$(CF_3)_2$Pz)$_3$]Ag(*c*-COE) (R = H, Cl, NO_2) adducts mediate the transfer of carbene moiety of EDA very effectively to unfunctionalized C-H bond of 2,3-dimethylbutane. Although the difference was small, [HB(4-(NO_2)-3,5-$(CF_3)_2$Pz)$_3$]Ag(*c*-COE) gave the highest selectivity towards primary C-H bond activation product.

Chapter 2

Fluorinated coinage metal pyrazolate π-stacking complexes

2.1 Introduction

2.1.1 Pyrazolate ligand

In the previous chapter we discussed the tris(pyrazolyl)borate (Tp) ligand and its fascinating uses in organometallic chemistry and catalysis. The Tp ligand is built with the combination of three pyrazoles with a boron ion. Thus our interest was directed towards the chemistry of the primary building block of Tp, the pyrazolate ligand. This simple ligand has been widely used in inorganic, bioinorganic, and organometallic chemistry. In this chapter we will discuss a brief introduction to the pyrazolate ligand and chemistry of highly fluorinated coinage metal complexes, and the synthesis of novel coinage metal pyrazolate π-stacking complexes. One major reason for the fame of pyrazolate ligand among the scientists is its simple yet tunable nature (three possible sites) (Figure 2.1).

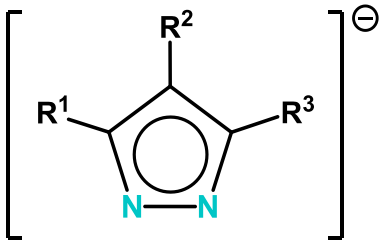

Figure 2.1 Pyrazolate ligand

Pyrazolate ligands play an important role in coinage metal chemistry. These ligands can strongly bind to the metal ions such as Cu(I), Ag(I) and Au(I).[92-96] The binding modes to the metals include but not limited to neutral monodentate (a), anionic monodentate (b) or exo/ endo (η^1- η^1 / η^2) bidentate (c/d) (Figure 2.2).[97] However, in this study we have concentrated only on exo-bidentate coinage metal pyrazolate complexes.

We are interested in the highly fluorinated pyrazolate coinage metal complexes due to the scarcity, their reversed π-stacking ability and the remarkable photophysical properties.[92,98]

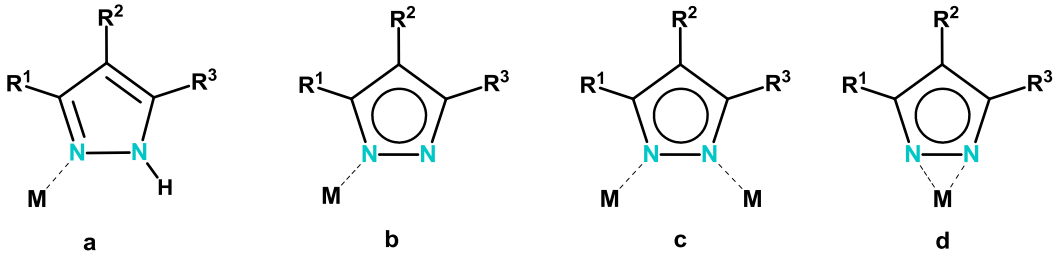

Figure 2.2 Coordination modes of the pyrazole ligand and the corresponding anionic ligand

The bidentate mode allows the pyrazolate ligand to coordinate to the metal in an exo-bidentate fashion, which allows the formation of polynuclear complexes such as trimers, tetramers, hexamers, or polymers. However, the formation of the metallocycles depends on the steric hindrance caused by the substituents on the ligand. Pyrazolate ligands have been used in organometallic field due to their correct geometry to hold the two metal atoms in close proximity.

2.1.2 Fluorinated coinage metal pyrazolates

Even though pyrazolates are widely used as ligands, the availability of fluorinated pyrazolate ligands are limited. Thus the fluorinated pyrazolate supported coinage metal complexes are not common. Nevertheless, these complexes (fluorinated coinage metal pyrazolates) not only show photophysical properties but also show other remarkable characteristics such as reversed π-stacking ability, thermal stability, and higher volatility.[99,95] Among the several pyrazolates we have used in our laboratory, $[3,5\text{-}(CF_3)_2Pz]^-$ was

the most extensively studied moiety in its coinage metal complexes.[6,95,100,101] Previous research in our lab introduced a convenient synthetic route to synthesize coinage metal adducts. The corresponding metal oxides and [3,5-$(CF_3)_2$Pz]H were used to obtain copper(I) and silver(I) adducts of {[3,5-$(CF_3)_2$Pz]Cu}$_3$, **[Cu$_3$]** and {[3,5-$(CF_3)_2$Pz]Ag}$_3$, **[Ag$_3$]** respectively, and {[3,5-$(CF_3)_2$Pz]Au}$_3$, **[Au$_3$]** was obtained by reacting [3,5-$(CF_3)_2$Pz]Na with Au(THT)Cl (Figure 2.3 and Figure 2.4 respectively). Photophysical properties[102,103,95], metallophilic bonding interactions[94,95,104,105], π-acid/π-base chemistry or π-acid/σ-donor interactions[106,100,107,94] and dissociation-aggregation behavior in solution[101,108,109] of such solid state structures are of significant interests. For example {[3,5-$(CF_3)_2$Pz]Cu}$_3$ can be sublimed at 80 °C whereas {[3,5-$(CH_3)_2$Pz]Cu}$_3$ need to be heated 245 °C for the sublimation.[95]

The luminescence properties of solids and solutions of the trimeric copper complexes in our previous studies showed fascinating trends with dramatic sensitivities to different factors such as temperature, solvent, concentration and excitation wavelengths. The trinuclear copper(I) pyrazolate adducts showed bright luminescence upon exposure to UV radiation.[15,95] The adduct **[Cu$_3$]** showed photoluminescence mainly due to the metal centered emission modified by inter-trimer Cu···Cu cuprophilic interactions.

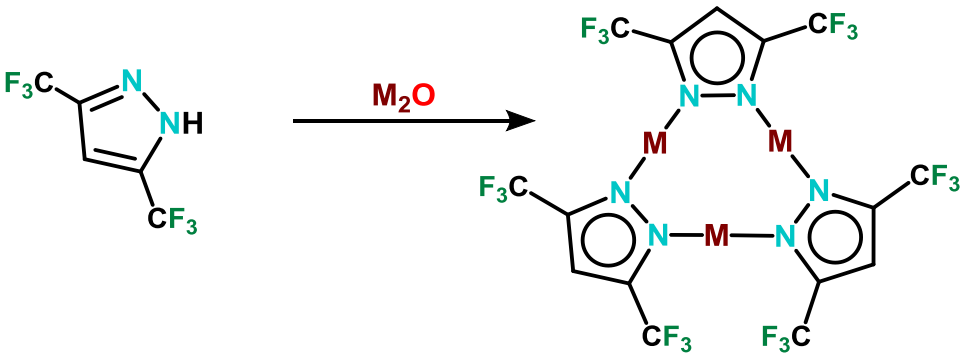

Figure 2.3 Synthetic route for the {[3,5-$(CF_3)_2$Pz]M}$_3$ where M = Cu/Ag

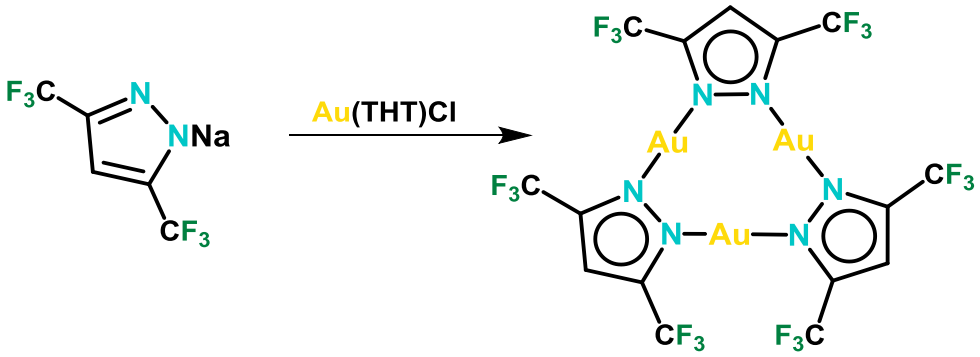

Figure 2.4 Synthetic route for the {[3,5-$(CF_3)_2$Pz]Au}$_3$

Many solid state materials of coinage metal complexes of pyrazolates have been shown photo luminescent properties.[95,102,103,110-113] We have studied the trinuclear and dinuclear, complexes of Cu(I) and Ag(I) with fluorinated pyrazolate ligands such as [3,5-(CF_3)2Pz]-. These complexes exhibit bright, tunable luminescence. For example we have reported that solids and glassy solutions of **[Cu_3]** [114] exhibits bright luminescence. The luminescence can be fine and coarse tuned to multiple bright visible colors by varying the solvent, concentration, temperature, and excitation wavelength.[15]

This type of neutral metal containing fluorinated ligands are gained attention as light emitting materials. The fluorination increases the volatility, which facilitated the thin-film fabrication.[95] The presence of the closed-shell transition metals provides enhanced phosphorescence respectively.[115,116] Fluorinated ligands possess some other beneficial properties such as improved thermal and oxidative stability, and reduced concentration quenching of luminescence to metal adducts. The properties described above, collectively make these complexes potential candidates for emitting materials in molecular light-emitting devices (LEDs) with predictable emission colors.

Another factor that governs the optoelectronic applications of trinuclear d^{10} pyrazolates comprise is the π acid−base/donor−acceptor nature.[6,15,95,100,117] For example **[Ag_3]**, a strong π-acid, forms crystalline solvates with benzene and its methylated derivatives.[100,96,118,119] Also our group has reported the on/off switching and sorption properties upon exposure of non-luminescent thin films of **[Ag_3]** to vapors of benzene, toluene, and mesitylene which are π-bases.[119]

The monovalent coinage metal complexes have fascinating structural, chemical and physical properties. There are some examples of these type of compounds that show very interesting π-acid/base properties that lead to the formation of extended binary stacks with arenes.[94,120] Usually, the π acid is an electron deficient arene while metal center is the base/donar. For example, 2001 Olmstead et al. reported that [{(MeNCOMe)Au}$_3$] or its dimer serves as the π base and nitro-9-fluorenones serve as the π acid.[121] The adduct formed between [{[(p-tolyl)NCOEt]Au}$_3$], a π base, and perfluoroarene acceptors such as hexafluorobenzene and octafluoronaphthalene has also been reported.[122]

The π basicity trend of the trinuclear pyrazolate complexes of coinage metals is as Au>Cu>Ag for a given pyrazolate.[6] However the fluorination in the pyrazolate allows the polarity of the metal complex to be reversed (Figure 2.5). As a consequence π bases such as aromatic hydrocarbons can be used for the adduct formation with π-acidic [M_3L_3] complexes. For example, our group revealed that even the most basic member of the coinage metal family, gold(I) pyrazolate, **[Au_3]** forms stack with toluene, **[Tol]** (where toluene is a π base) (Figure 2.6).[94] These assemblies may exhibit the forms of trinuclear metal trimers, [M_3L_3], and its dimers, [$(M_3L_3)_2$], with arenes such as $(AB)_\infty$, $(AAB)_\infty$, $(ABB)_\infty$ (Figure 2.7).

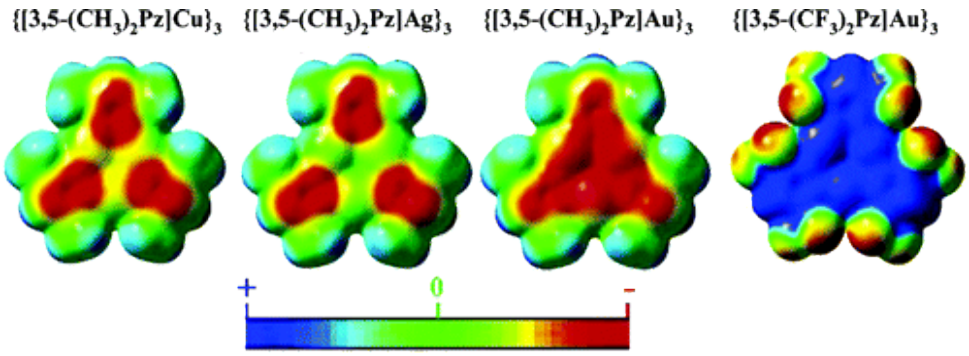

Figure 2.5 DFT-derived molecular electrostatic potentials (MEP) mapped onto the electron density surfaces of selected $\{[3,5\text{-}(R)_2Pz]M\}_3$ models.

Adopted with the permission from the Metal Effect on the Supramolecular Structure, Photophysics, and Acid−Base Character of Trinuclear Pyrazolato Coinage Metal Complexes M. A. Omary, Manal A. Rawashdeh-Omary,M. W. Alexander Gonser,Oussama Elbjeirami,Tom Grimes, and, Thomas R. Cundari, Himashinie V. K. Diyabalanage,Chammi S. Palehepitiya Gamage, and, and H. V. Rasika Dias *Inorganic Chemistry* **2005** *44* (23), 8200-8210. Copyright (2005) American Chemical Society.

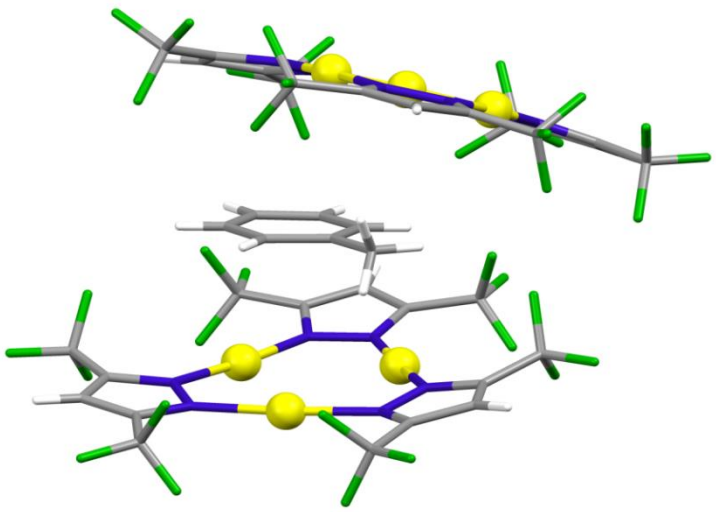

Figure 2.6 X-ray crystal structure of **$\{[Tol][Au_3]_2\}_\infty$**

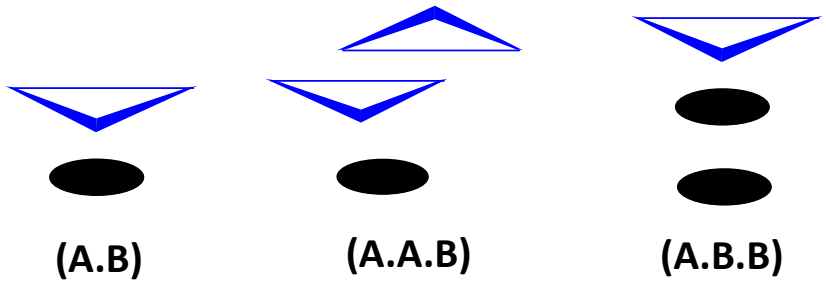

Figure 2.7 Different types of sandwich structures, which result from the π acid/base chemistry of trinuclear d^{10} metal complexes (triangles) with arenes (ovals).

Taking into account the fascinating chemistry of coinage metal pyrazolates and their arene adducts, we set out to work on filling the missing blocks, copper pyrazolate arene adducts and coinage metal adducts of C_{60} fullerene. Despite many C_{60} – metal adducts reported, there are no literature reports for coinage metal adducts of C_{60} fullerene, to the best of our knowledge.

2.2 Isolable arene sandwiched copper(I) pyrazolates

Naleen B. Jayaratna, Champika V. Hettiarachchi, Muhammed Yousufuddin, and H. V. Rasika Dias.

(Part of this work has been published in New Journal of Chemistry 2015,**39**, 5092)

Reproduced from reference [123] with permission from the Centre National de la Recherche Scientifique (CNRS) and The Royal Society of Chemistry.

2.2.1 Introduction

Copper(I) pyrazolates have attracted significant interest in recent years.[106,124-132, 95] They show diverse structures, fascinating luminescent properties and are useful in catalysis and serve as excellent precursors for mixed ligand complexes of copper. For instance, $[Cu(Pz)]_n$ (Pz = pyrazolate) is a polymer,[133] whereas $\{[3,5\text{-}(Me)_2Pz]Cu\}_3$ and $\{[3,5\text{-}(i\text{-}Pr)_2Pz]Cu\}_3$ adopt trinuclear structures[95] and $\{[3,5\text{-}(t\text{-}Bu)_2Pz]Cu\}_4$ is a tetramer.[134] Some copper(I) pyrazolates aggregate further, often through Cu···Cu interactions, forming dimers of trimers or even extended chains of trimers.[95] Solid samples of $\{[3,5\text{-}(i\text{-}Pr)_2Pz]Cu\}_3$ emits orange light upon photo-excitation at room temperature, while the emitted color changes to green upon cooling to 77 K.[95] Aida *et al.* has reported the development of rewritable media by exploiting the self-assembling process of trinuclear copper pyrazolate luminophors.[110]

An area of research focus in our laboratory concerns the chemistry of copper and related heavier coinage metal (Ag, Au) complexes featuring fluorinated pyrazolates.[14,94,95,98,125] The $\{[3,5\text{-}(CF_3)_2Pz]Cu\}_3$ (Figure 2.8) is a particularly interesting molecule.[14,98] It forms chains of trimers in the solid state and exhibits bright luminescence in the solid state and glassy solutions upon irradiation with UV radiation that can be fine

and coarse-tuned to multiple bright visible colors by varying the solvent, concentration, temperature, and excitation wavelength. Here we demonstrate yet another aspect of $\{[3,5\text{-}(CF_3)_2Pz]Cu\}_3$; its π-acid character.[135] In particular, we report the isolation and structural characterization of π-acid/base sandwich adducts of copper(I) pyrazolate $\{[3,5\text{-}(CF_3)_2Pz]Cu\}_3$, **[Cu$_3$]** with simple hydrocarbon π-bases benzene, mesitylene and naphthalene.

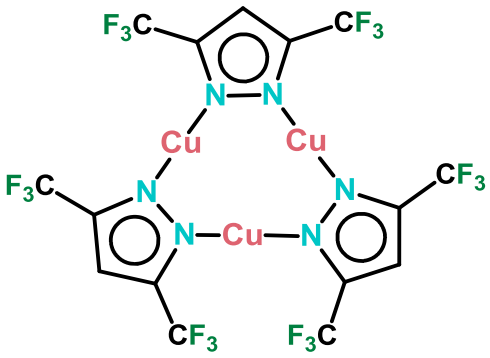

Figure 2.8 Trinuclear copper pyrazolate $\{[3,5\text{-}(CF_3)_2Pz]Cu\}_3$, **[Cu$_3$]**.

2.2.2 Results and discussion

The benzene adduct of **[Cu$_3$]** was prepared by treating a chloroform solution of **[Cu$_3$]** with benzene. The mixture was kept at −20 °C for several days to afford a colorless crystalline solid. X-ray analysis at 150 K revealed that it is a π-acid/base sandwich adduct of the type **{[Bz][Cu$_3$]$_2$}$_\infty$** consisting of alternating benzene **[Bz]** and **[Cu$_3$]$_2$** dimer of trimer units (Figure 2.9). Detailed analysis shows that there are two crystallographically different **{[Bz][Cu$_3$]$_2$}$_\infty$** chains in the crystal lattice resulting from minor differences in orientations of **[Bz]** and **[Cu$_3$]$_2$**. The**[Cu$_3$]** units sandwich benzene rather symmetrically with benzene carbon centroid and Cu_3-core centroid distances of 3.16, 3.16 Å and 3.20, 3.20 Å for the two **{[Bz][Cu$_3$]$_2$}$_\infty$** chains. The shortest Cu···C(benzene) distances are 3.17 and 3.22 Å. These distances are slightly

longer than sum of the Bondi's van der Waals radii of copper and carbon 1.40 + 1.70 = 3.10 Å. However, more recent work from Alveraz[136] places van der Waals contact distance of copper and carbon at 4.15 Å implying noteworthy interactions between **[Bz]** and **[Cu$_3$]$_2$** in **{[Bz][Cu$_3$]$_2$}$_\infty$**. These Cu···C(benzene) distances, however are significantly longer than those observed for cationic Cu(I) arene adducts like [Cu(η^2-Me$_6$C$_6$)$_2$][PF$_6$] (2.092(2), 2.192(2) Å) or [Ph$_3$PCu(η^6-Me$_6$C$_6$)][PF$_6$] (2.284(5), 2.293(5) Å).[137]

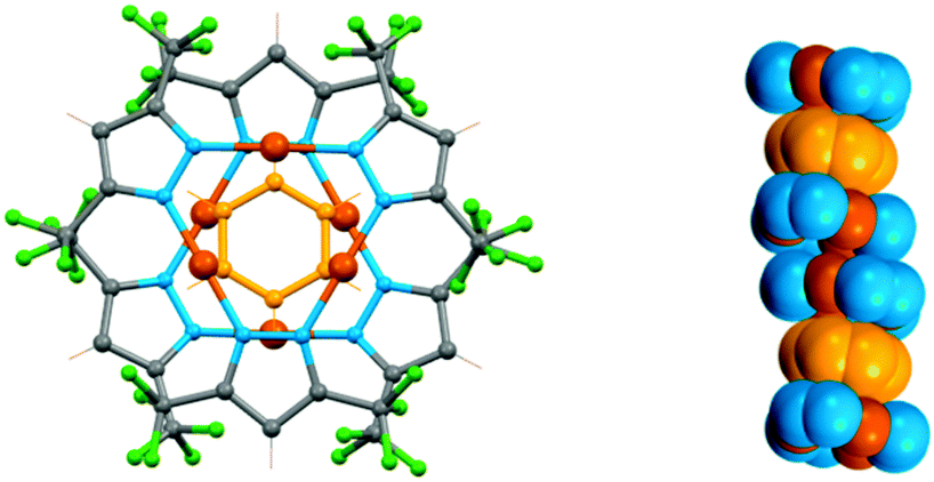

Figure 2.9 Left: molecular structure of **{[Bz][Cu$_3$]$_2$}$_\infty$** showing the repeating unit [Bz][Cu$_3$]$_2$ ({[3,5-(CF$_3$)$_2$Pz]Cu}$_3$ = **[Cu$_3$]** and benzene = **[Bz]**). Right: portion of the supramolecular chain of **{[Bz][Cu$_3$]$_2$}$_\infty$**

(carbon and fluorine atoms of the pyrazolyl moieties and hydrogen atoms have been omitted for clarity).

Each **[Cu$_3$]** dimer in **{[Bz][Cu$_3$]$_2$}$_\infty$** also shows two close inter-trimer Cu···Cu contacts (Figure 2.10) at 3.031, 3.031 and 3.091, 3.091 Å (for two crystallographically different **[Cu$_3$]$_2$** units). The pyrazolyl moieties turn outward from the Cu$_3$N$_6$ core to facilitate this close approach of **[Cu$_3$]** units. The benzene free **[Cu$_3$]** crystallizes as zig-zag chains with much longer inter-trimer Cu···Cu separations (closest Cu···Cu distances

of adjacent **[Cu$_3$]** trimers are at 3.813 and 3.987 Å at 100 K).[95] This shows that the presence of benzene affects the cuprophilic interactions of **[Cu$_3$]**. It is probably one of the reasons for changes in **[Cu$_3$]** luminescence observed in its glassy solutions of benzene.[95]

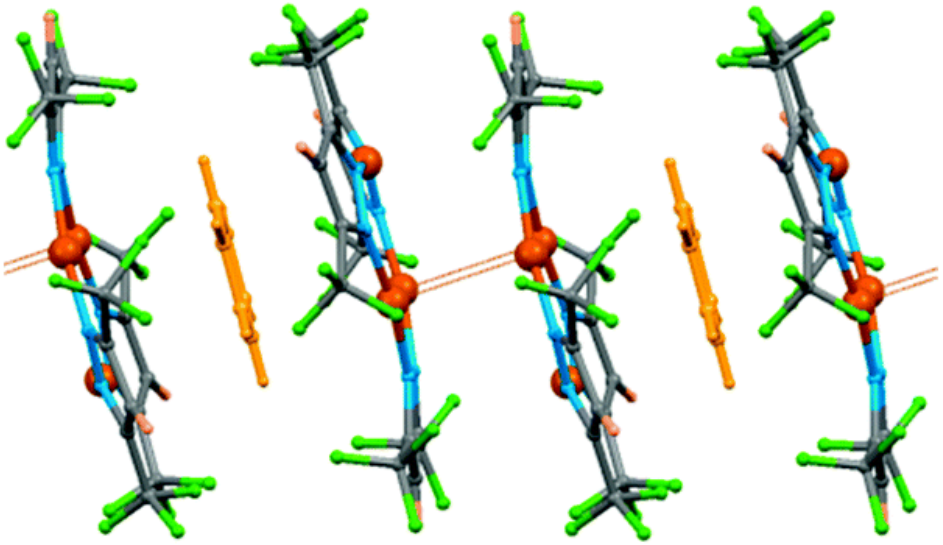

Figure 2.10 Portion of **{[Bz][Cu$_3$]$_2$}∞** showing inter trimer Cu···Cu contacts.

The **{[Bz][Cu$_3$]$_2$}$_\infty$** crystals lose benzene quite easily at room temperature upon air drying or under reduced pressure affording the **[Cu$_3$]**, as evident from NMR spectroscopic and elemental analysis data. This suggests that **[Bz]** and **[Cu$_3$]** interactions are rather weak. In contrast, {[3,5-(CF$_3$)$_2$Pz]Ag}$_3$, **[Ag$_3$]**, which is the strongest π-acid of the {[3,5-(CF$_3$)$_2$Pz]M}$_3$series (M = Cu, Ag, Au)[94] and features the largest metal ion, forms isolable and more robust adducts with benzene and other arenes much easily.[96,100,119] Computational data show that **[Cu$_3$]** is a relatively weak π-acid.[94] **[Cu$_3$]** also has the smallest metal atom of group 11 series, and therefore more prone to adverse steric effects and weaker side-on (face-to-face) interactions. Thus obtaining isolable adducts of **[Cu$_3$]** with volatile arenes are particularly challenging and

above observations are not surprising. For comparison, **[Ag_3]** is known to form **[Bz][Ag_3]$_2$[Bz]** type adducts with benzene.

Synthesis of **[Cu_3]-**mesitylene adduct was accomplished by mixing a chloroform solution of **[Cu_3]** with mesitylene **[Mes]**. This mixture was kept at −20 °C for several days to obtain crystalline **{[Mes][Cu_3]}$_\infty$** which has a columnar structure (Figure 2.11). It is a common stacking pattern for arene sandwiches of **[Ag_3]**,[96,118] and trinuclear Hg^{II}.[138,139] The **[Ag_3]** for comparison, also forms π-acid/base adducts with mesitylene, affording **{[Mes][Ag_3]}$_\infty$** aggregates. The **[Cu_3][Mes]** unit in **{[Mes][Cu_3]}$_\infty$** sits on a three-fold rotation axis. Two mesitylene ring carbon centroid and Cu_3-core centroid distances are 3.30 and 3.34 Å while the shortest Cu···C(mesitylene) distance is 3.34 Å. These distances are slightly longer than the corresponding distances observed for the **{[Bz][Cu_3]$_2$}$_\infty$** adduct. It could be a result of having larger mesitylene because otherwise more electron rich π-base mesitylene should have closer interactions with **[Cu_3]**. The steric repulsions of methyl groups of mesitylene with CF_3-bearing pyrazolyl moieties of **[Cu_3]** lead to distortions as illustrated in Figure 2.12, which perhaps hinder the closer approach of a second **[Cu_3]** and formation of inter-trimer Cu···Cu interactions, as observed in **{[Bz][Cu_3]$_2$}$_\infty$** (Figure 2.10).

The crystalline naphthalene adduct of [Cu_3] was isolated from a chloroform solution of [Cu_3] containing benzene and naphthalene at −20 °C. It forms extended binary stacks of {[Nap][Cu_3]}∞ consisting of alternating [Cu_3] and naphthalene [Nap] moieties (Figure 2.13). In contrast to the benzene and mesitylene adducts of [Cu_3], {[Nap][Cu_3]}∞ is more robust and does not lose the sandwiched arene easily even under reduced pressure. Also note that {[Nap][Cu_3]}∞ crystallized out from a solution containing benzene. The shortest Cu···C(naphthalene) distance in{[Nap][Cu_3]}∞ is 3.09 Å, which is shorter than those observed in the [Cu_3] benzene and

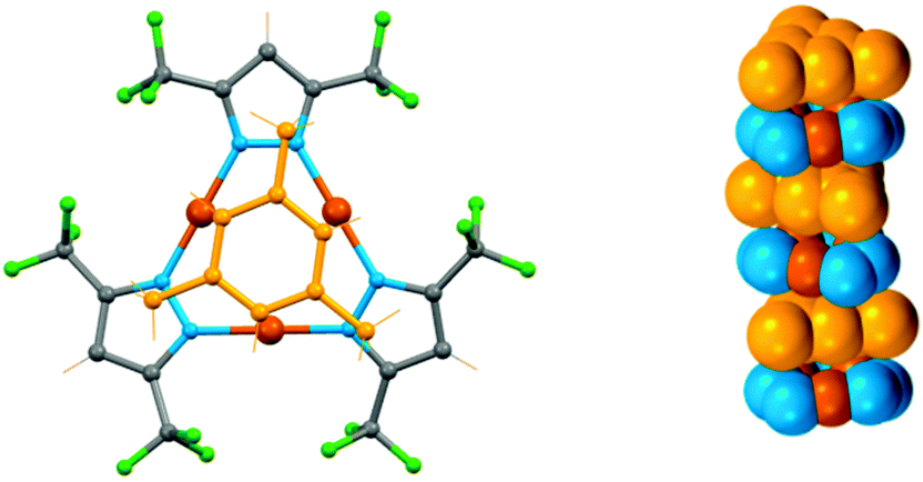

Figure 2.11 Left: molecular structure of **{[Mes][Cu_3]}∞** showing the repeating unit **[Mes][Cu_3]** (mesitylene = [Mes]). Right: portion of the supramolecular chain of **{[Mes][Cu_3]}∞**

(carbon and fluorine atoms of the pyrazolyl moieties and hydrogen atoms have been omitted for clarity)

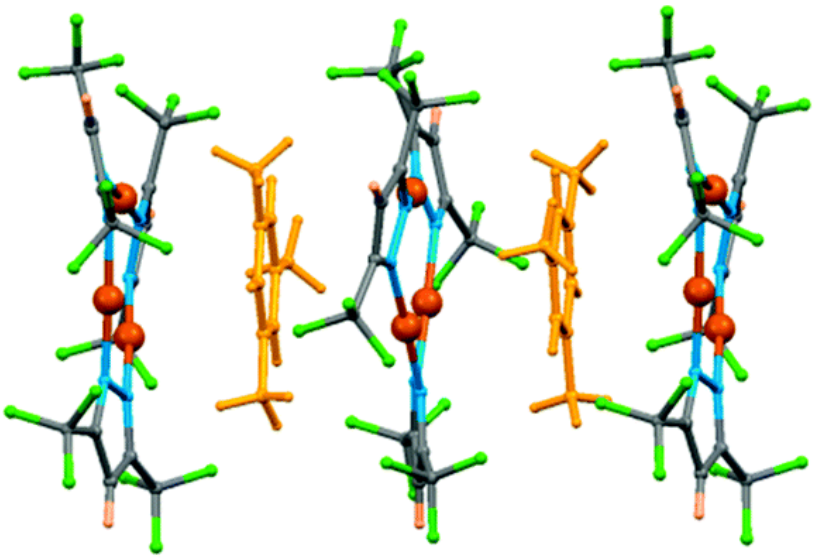

Figure 2.12 Portion of **{[Mes][Cu_3]}∞** showing distortions of **[Cu_3]** moiety.

mesitylene adducts. For comparison, the shortest Ag···C(naphthalene) distance in {[Nap][Ag_3]}∞ is 3.00 Å, which is slightly shorter than that observed in {[Nap][Cu_3]}∞ despite the larger atomic radius of silver. This points to the presence of relatively stronger π-acid/base interactions in the silver adduct.

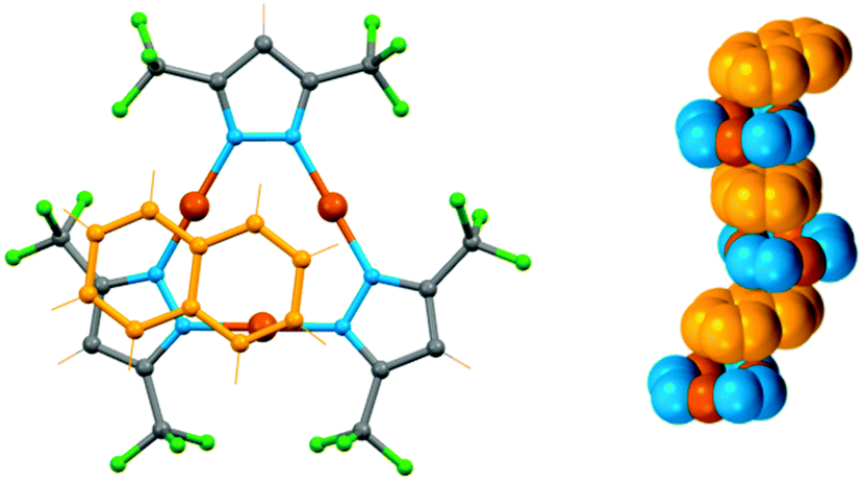

Figure 2.13 Left: molecular structure of **{[Nap][Cu_3]}∞** showing the repeating unit **[Nap][Cu_3]** (naphthalene = **[Nap]**). Right: portion of the supramolecular chain of **{[Nap][Cu_3]}∞**

(carbon and fluorine atoms of the pyrazolyl moieties and hydrogen atoms have been omitted for clarity)

Room temperature ^{1}H NMR spectra of **[Cu_3]** containing sub-molar quantities of benzene, mesitylene or naphthalene taken in $CDCl_3$ show no notable chemical shift difference between the aromatic proton signals of adducts and the free components, **[Cu_3]** and arene. This suggests that these π-acid/base adducts are too weak to survive (*i.e.*, they dissociate) in solution, or to influence the solution chemical shifts significantly. Similar observations were noted in adducts involving more π-acidic **[Ag_3]**.[96]

We have reported several types of arene adducts with **[Ag_3]** and the use of **[Ag_3]** to prepare a vapochromic sensor for benzene and its alkylated derivatives,[119] as well as strong sensitization of the triplet state of naphthalene.[118] This work shows that **[Cu_3]** may also serve as a viable option for such applications. At the room temperature, the arene free **[Cu_3]** adduct shows bright orange emissions centered at 645 nm. Although we could not study the photoluminescence of crystalline **{[Bz][Cu_3]$_2$}$_\infty$** due to the easy loss of benzene, preliminary studies show that **{[Mes][Cu_3]}$_\infty$** and **{[Nap][Cu_3]}$_\infty$** display bright green photoluminescence (Figure 2.14). The emission maximum of **{[Mes][Cu_3]}$_\infty$** was centered at 546 nm (Figure 2.15) whereas the **{[Nap][Cu_3]}$_\infty$** shows three bands at 497, 526, 564 (sh) nm (Figure 2.16) at the room temperature pointing to significant blue shift relative to that of the arene free **[Cu_3]**. Removal of mesitylene from **{[Mes][Cu_3]}$_\infty$**leads for the reappearance of **[Cu_3]** based emission signal.

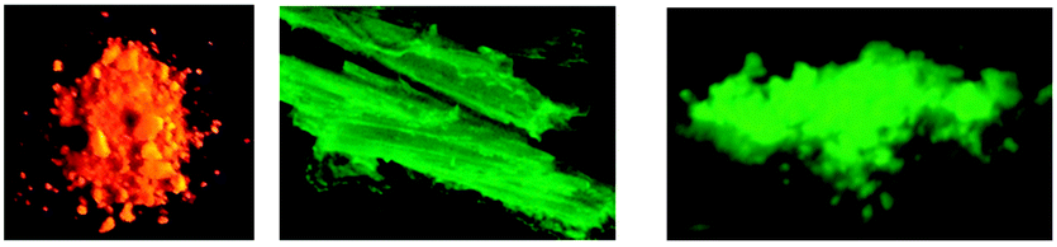

Figure 2.14 Photos (from left to right) showing the emission colors of **[Cu_3]**, **{[Mes][Cu_3]}∞** and **{[Nap][Cu_3]}∞**.

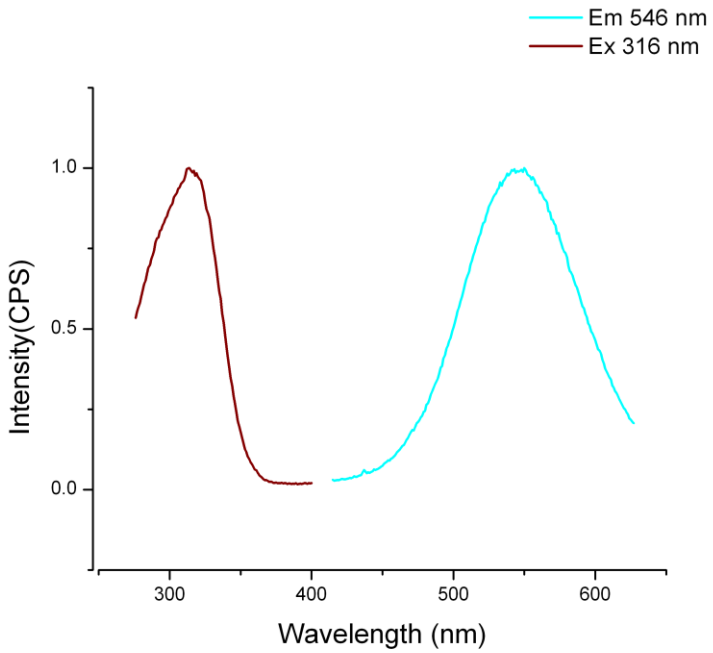

Figure 2.15 **{[Mes][Cu_3]}$_\infty$** photo luminescence spectra

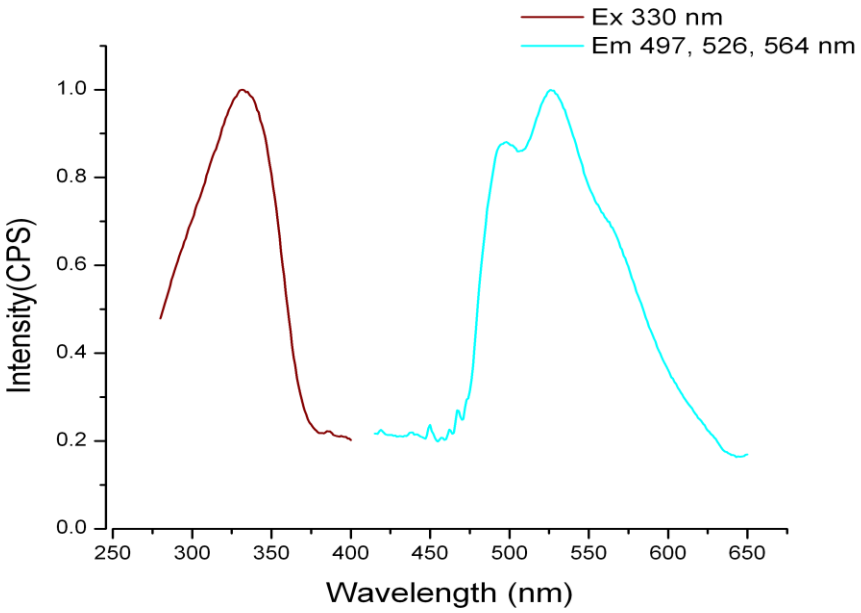

Figure 2.16 **{[Nap][Cu_3]}$_\infty$** photo luminescence spectra

2.2.3 Conclusions

In summary, here we report the isolation of supramolecular stacks involving π-acidic [Cu_3] and electron rich aromatic π systems. They represent rare, isolable sandwich complexes of copper(I) pyrazolates and aromatic hydrocarbons. Recently, somewhat related [Cu_3] sandwiched ferrocene was reported.[107] We are currently expanding this π-acid/base chemistry of [Cu_3]and probing their photoluminescence properties and coinage metal family group trends in detail.

2.3 π-stacking complexes of gold(I), silver(I) and copper(I) pyrazolate with C_{60} fullerene

2.3.1 Introduction

Pyrazolate ligand plays a vital role in coinage metal chemistry.[94,95,98,105,128] Homoleptic, tri-nuclear exo-bidentate copper pyrazolates are well known for their photophysical properties. Some of these complexes show fascinating π-acid/base properties leading to π stacks formation with electron rich arenes. For example we have synthesized hydrocarbon arene adducts of all three coinage metals (Cu, Ag and Au), with the support of $[3,5\text{-}(CF_3)_2Pz]^-$ ligand (Figure 2.17).[94,96,123] Use of the highly fluorinated pyrazolate ligand let us reverse the electronic properties of the M_3N_6 core. For example $\{[3,5\text{-}(CF_3)_2Pz]Au\}_3$, **$[Au_3]$** retain positively charged core, compared to $\{[3,5\text{-}(CH_3)_2Pz]Au\}_3$, where the core is negatively charged, according to the DFT-derived molecular electrostatic potentials (MEP).[94] **$[Au_3]$** form π stacks with π bases such as aromatic hydrocarbons where electron rich cyclic trinuclear gold complex, $[(bzim)_3Au]_3$ complexes with π acids like 7,7,8,8-tetracianoquinodimeathane. Aromatic hydrocarbon π –stacking complexes of $\{[3,5\text{-}(CF_3)_2Pz]Ag\}_3$, **$[Ag_3]$** and $\{[3,5\text{-}(CF_3)_2Pz]Cu\}_3$, **$[Cu_3]$** have shown interesting properties such as sensing small molecules and act as tunable molecular light emitters.[119,123]

Fullerene C_{60} is a molecule with 60 π electrons which was first discovered by Kroto *et al.* in 1985.[140] It forms various metal complexes by acting as a π ligand. Metal complexes of C_{60} bearing van der Waals forces are one class of complexes which shows fascinating properties. For example, metalloporphyrine fullerene complexes exhibit many attractive properties such as optoelectronic properties, magnetic and conductivity properties. However there are no reports of coinage metal pyrazolate fullerene complexes reported to the best of our knowledge. Here we report crystallographically

characterized, full series of C_{60} coinage metal pyrazolate complexes. These complexes are of interested not only they are the first coinage metal pyrazolate C_{60} complexes but also due to several other reasons. For example there are not many C_{60} complexes reported with gold and most of the metallo C_{60} complexes co-crystalize with solvents (not found in pure form). Further, these coinage metal C_{60} adducts show very similar packing to that of pure $C_{60,}$ which is very rare for any C_{60} metal complex.

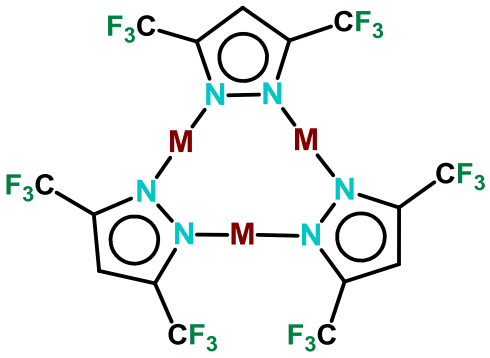

Figure 2.17 Copper(I), silver(I), and gold(I) complexes of $[3,5\text{-}(CF_3)_2Pz]^-$ **[Cu$_3$]**, **[Ag$_3$]**, **[Au$_3$]** respectively (M = Cu/Ag/Au).

2.3.2 Results and discussion

Treatment of C_{60} with **[Ag$_3$]** in stoichiometric ratio afforded the π-stacking complex $C_{60}\{[(3,5\text{-}(CF_3)_2Pz)Ag]_3\}_4$, **C$_{60}$[Ag$_3$]$_4$** as air stable purple crystals (appeared black to naked eye) from CS_2 (Figure 2.18). Presence of C_{60} in excess does not alter the product formation (this might be explained by the stability of highly symmetric crystal packing nature of the complex). The complex is moderately soluble in CS_2, and slightly soluble in CH_2Cl_2 and $CHCl_3$. However the solubility of the **C$_{60}$[Ag$_3$]$_4$** is less compared to that of "free" C_{60} in CS_2. The complex is very slightly soluble in hexane in which sonication was necessary. Nevertheless, the complex formation increased the solubility of C_{60} twice

compared to that of "free" C_{60}. Solubility was determined by direct weight measurements of dried solutions.

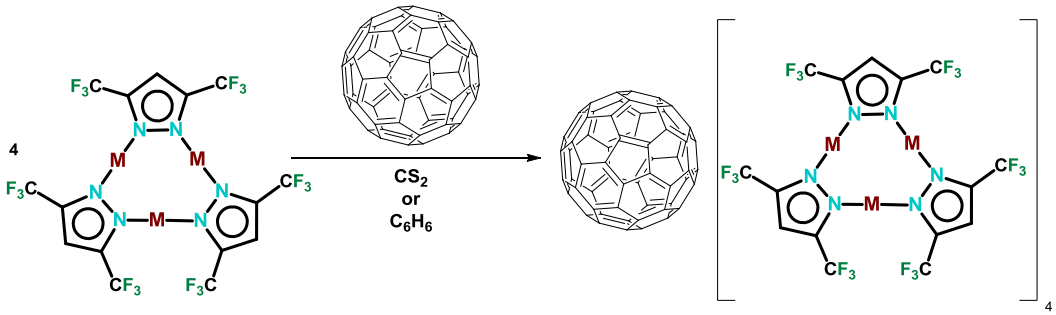

Figure 2.18 General reaction for synthesis of $\mathbf{C_{60}[M_3]_4}$ where M = Cu/Ag/Au

The complex $\mathbf{C_{60}[Cu_3]_4}$ was also obtained by a similar procedure to its silver sister and the basic properties of the copper complex is not significantly varied from those of silver complex. However the gold complex of the family, $\mathbf{C_{60}[Au_3]_4}$ shows different solubility. It is quite insoluble in any solvent but shows little solubility in benzene. The initial complex $\mathbf{[Au_3]}$, by itself possesses low solubility. All three complexes, slowly decompose upon prolong exposure to the light, particularly silver and gold complexes.

The crystal structure of $\mathbf{C_{60}[Ag_3]_4}$ involved four dimer of trimer (hexamer) units, $\mathbf{[Ag_3]_2}$, around one C_{60} molecule in a tetrahedral fashion (Figure 2.19). However, each of the dimer unit, $\mathbf{[Ag_3]_2}$ is shared with another C_{60} molecule granting the molecular formula of $\mathbf{C_{60}[Ag_3]_4}$ (Figure 2.20 and Figure 2.21). Interestingly, it shares the face centered cubic space group (Figure 2.22) similar to that of "free" C_{60} crystals structure, however, with more than twice larger lattice constant. For example, lattice constant a, of $\mathbf{C_{60}[Ag_3]_4}$ is 36.964(3) Å, compared to that of "free" C_{60} which is 14.052 (5) Å. [141] Both $\mathbf{C_{60}[Cu_3]_4}$ and $\mathbf{C_{60}[Au_3]_4}$ complexes also possess very similar crystal packing along with noticeably close unit cell dimensions.

The distance between the centroid of closest six membered ring of the C_{60} to centroid of the **[Ag_3]** is 3.243 Å which is considerably shorter than the sum of the Bondi's van der Waal radii of Ag and C (1.72 + 1.70 = 3.42 Å). This indicates that there are well established van der Waal interactions exist in between the silver trimer and C_{60}. These interactions are somewhat stronger than the interactions of **[Ag_3]$_2$** to the benzene (in that case centriodal separation was 3.28 Å).[96] However the closest contacts between the silver and carbon atom of the aromatic ring of each adduct are surprisingly close (3.182 Å and 3.187 Å in **C_{60}[Ag_3]$_4$** and **{[Bz][Ag_3]$_2$}$_\infty$** respectively). Interestingly **[Ag_3]$_2$** dimer unit in the **C_{60}[Ag_3]$_4$** shows almost equal Ag···Ag separation of trimers, to that of the free **[Ag_3]$_2$** (3.2047(7) Å and 3.2037(3) Å respectively). However in the "free" silver pyrazolate complex there are only four Ag(I) ions showed Ag···Ag interactions, while in the complex **C_{60}[Ag_3]$_4$**, all six Ag(I) are involved. This is not very common for these dimer units, nevertheless such interactions were observed in {[(4-Br-3,5-(*i*-Pr)$_2$Pz)Ag]$_3$}$_2$.[142]

C_{60}[Cu_3]$_4$ shares most of the basic structural (packing) properties with some variations in distances, angles, etc (Figure 2.23). For example, **[Cu_3]** shows very similar packing to that of **[Ag_3]$_2$**, however with some variations in distances. Cu···Cu separation of two adjacent trimers is 3.158 Å. The "free" **[Cu_3]** shows much longer Cu···Cu interactions (closest Cu···Cu interactions of the adjacent trimers are 3.813 and 3.987 Å). However in the **[Cu_3]$_2$** stack formed with benzene showed an average Cu···Cu interaction of 3.061 Å which is somewhat shorter compared to what we observed in **C_{60}[Cu_3]$_4$**. In both instances (stacking with benzene and C_{60}), the pyrazolyl moieties turn outward from the Cu_3N_6 core to facilitate this close approach of [Cu_3] units. Similar to **C_{60}[Ag_3]$_4$**, **C_{60}[Cu_3]$_4$** also shows Cu···Cu interactions in-between all six Cu(I) ions of the **[Cu_3]$_2$** core which is unusual for **[Cu_3]$_2$**.

The distance between closest C_6 face centroid of the C_{60} to the centroid of **[Cu_3]**

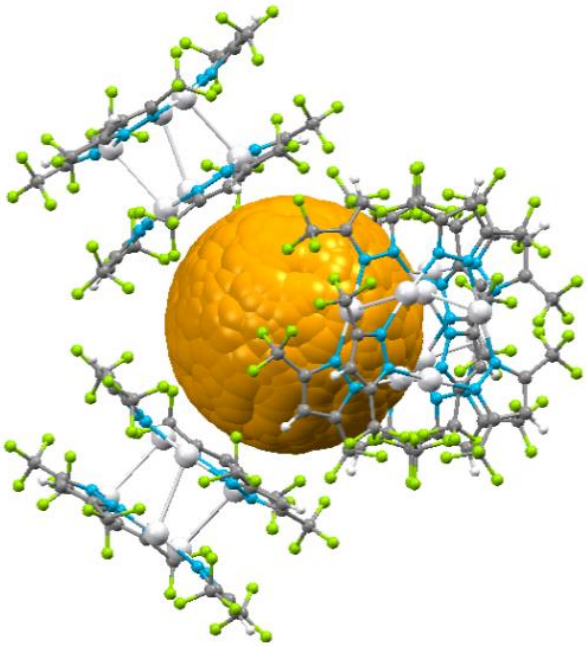

Figure 2.19 X-ray structure showing four **$[Ag_3]_2$** units around C_{60}

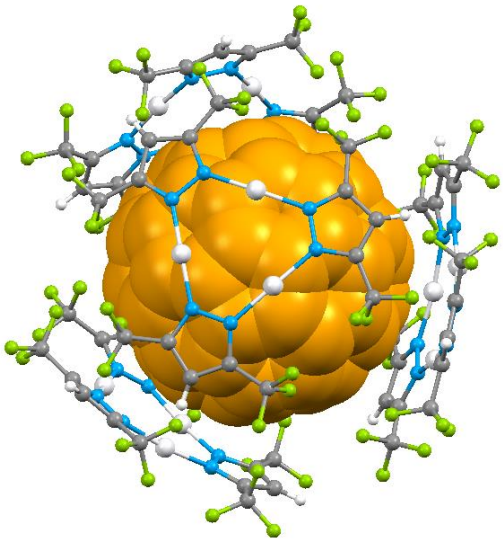

Figure 2.20 X-ray crystal structure of **$C_{60}[Ag_3]_4$**

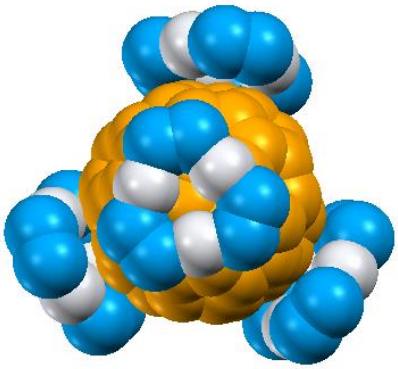

Figure 2.21 X-ray structure of **$C_{60}[Ag_3]_4$** showing only four Ag_3N_6 metallacycles around the C_{60}.

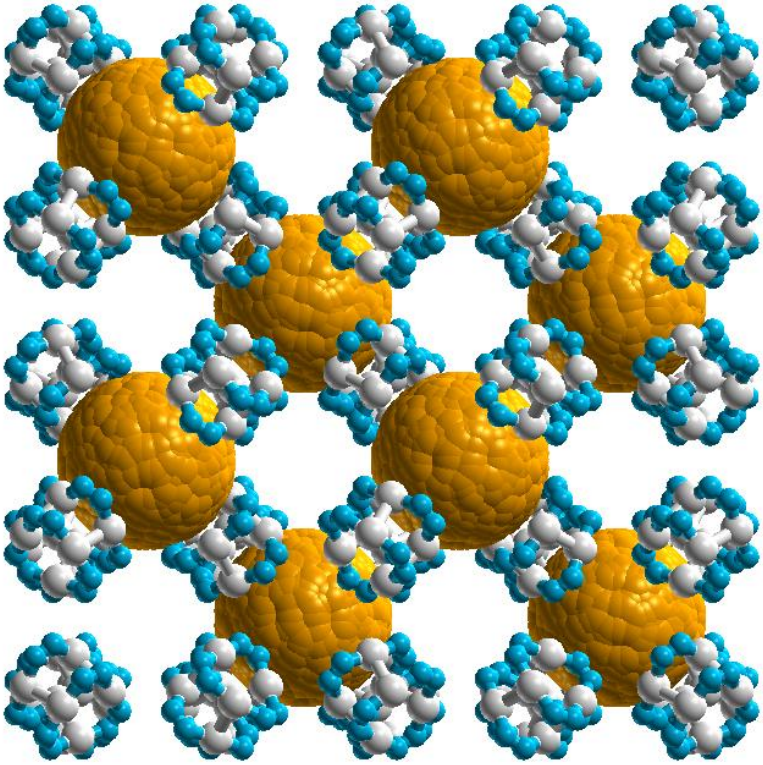

Figure 2.22 Unit cell of the X-ray structure of **$C_{60}[Ag_3]_4$**, showing only four Ag_3N_6 of the **$[Ag_3]_2$** unit.

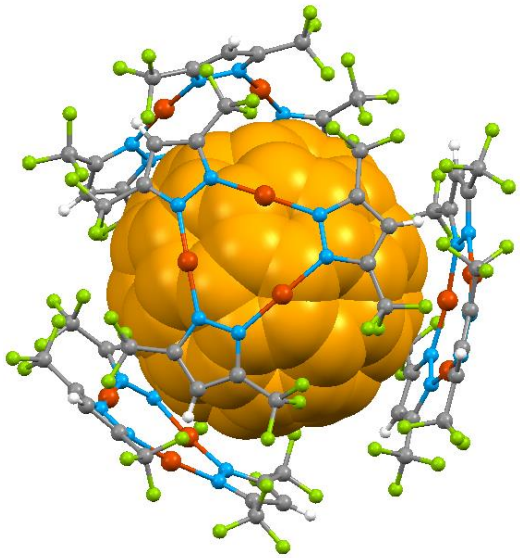

Figure 2.23 X-ray crystal structure of **$C_{60}[Cu_3]_4$**

is 3.264 Å. These distances are slightly longer than sum of the Bondi's van der Waals radii of copper and carbon 1.40 + 1.70 = 3.10 Å. However, more recent work from Alveraz[136] put van der Waals contact distance of copper and carbon at 4.15 Å indicating notable interactions between C_{60} and **$[Cu_3]_2$** in **$C_{60}[Cu_3]_4$**. Such interactions were also observed in benzene **$[Cu_3]_2$** adducts. In that case the average centroidal distance was 3.18 Å. **$C_{60}[Au_3]_4$** also shows similar basic structural properties with certain variations in distances and angles (Figure 2.24).

In solution state C_{60} to metal complexes demonstrate no interaction or very weak interactions. This was evidenced by the proton signal of the metal – pyrazolate remaining unchanged or insignificantly changed. For example in ^{1}H NMR of **$C_{60}[Cu_3]_4$** shows a peak at δ 7.01 for the pyrazolate proton compared to that of **$[Cu_3]$** appeared at δ 7.02. Also $^{13}C\{^1H\}$ NMR resonances for the metal – pyrazolates and the C_{60} are equal or very closer to their original forms. For example, the $^{13}C\{^1H\}$ NMR resonance corresponding to

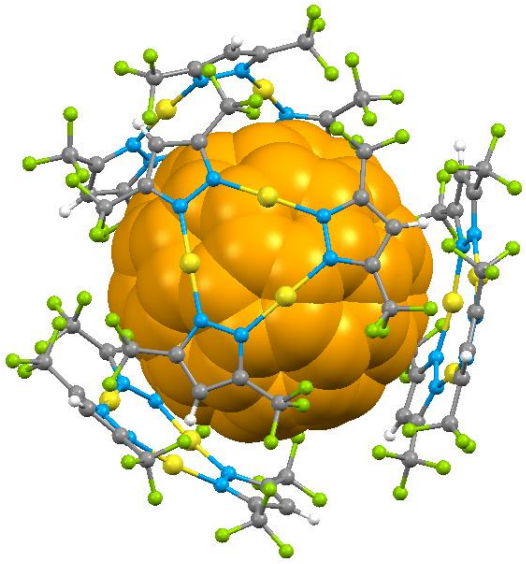

Figure 2.24 X-ray crystal structure of **$C_{60}[Au_3]_4$**

unchanged or insignificantly changed. For example in ^{1}H NMR of **$C_{60}[Cu_3]_4$** shows a peak at δ 7.01 for the pyrazolate proton compared to that of **$[Cu_3]$** appeared at δ 7.02. Also $^{13}C\{^{1}H\}$ NMR resonances for the metal – pyrazolates and the C_{60} are equal or very closer to their original forms. For example, the $^{13}C\{^{1}H\}$ NMR resonance corresponding to the C_{60} in the complex, arises at δ 143.0 compared to that of "free" C_{60} appears at δ 143.6. The silver complex **$C_{60}[Ag_3]_4$** , also showed very similar observations for NMR in solutions. Unfortunately, **$C_{60}[Au_3]_4$** did not show a fair solubility to perform a $^{13}C\{^{1}H\}$ NMR.

Raman spectra of **$C_{60}[Au_3]_4$** and **$C_{60}[Ag_3]_4$** exhibited resonances only corresponding to the C_{60}. There were no signals appeared for the trimers. **$C_{60}[Au_3]_4$** showed three resonance 266, 490 and 1466 cm^{-1}. These are not significantly different from those of "free" C_{60} (free C_{60} : 273, 499, 1468 cm^{-1}). There was only one resonance for the **$C_{60}[Ag_3]_4$**, appeared at 1468 cm-1 which is very similar to that of "free" C_{60}. Unfortunately **$C_{60}[Cu_3]_4$** did not give a decent Raman spectra.

These C_{60} metal adducts decompose at elevated temperatures, which was observed in the melting point determination and confirmed by thermogravimetric analysis (TGA). All three complexes decompose by releasing the metal-pyrazolate, leaving only C_{60}. This is actually the reverse of what we have seen with the other coinage metal pyrazolate stacks. In the arene adducts, the arene is kicked off from the complex leaving the metal pyrazolate. However it is not a surprise that retaining of C_{60} since it owns a high sublimating temperature (~600 °C).[143] For example, **$C_{60}[Cu_3]_4$** starts decomposition at 175 °C and lose 80.4% of its total weight by 309 °C in which mass content of the metal pyrazolate is equal to 81.6%. The two values are close enough to attribute to the weight loss to the metal pyrazolate.

Table 2.1 Calculated M3 weight percentages and observed by the thermogravimetric analysis.

Complex	**M_3 weight %**	**Combined weight loss (1^{st} +2^{nd}) %**
$C_{60}\{[(3,5\text{-}(CF_3)_2Pz)Cu]_3\}_4$	81.6	80.4
$C_{60}\{[(3,5\text{-}(CF_3)_2Pz)Ag]_3\}_4$	83.8	82.0
$C_{60}\{[(3,5\text{-}(CF_3)_2Pz)Au]_3\}_4$	87.0	82.8

Also the decomposition occurs at fairly close but little lower temperature to the melting point of **$[Cu_3]$** (188-189 °C). Interestingly this weight loss occur by two steps, 74.6% and 5.9%, nevertheless a fair match of molecular fragment weights are not available. This prevents the prediction of a mechanism for the decomposition. **$C_{60}[Ag_3]_4$** also behaves very similarly except the little higher starting and ending temperatures of decomposition. However it seems sensible since **$[Ag_3]$** has somewhat higher melting point (212 °C). Decomposition of **$C_{60}[Au_3]_4$** also occurs in two steps, adding up to 82.8%

which is a closer value to weight percentage of four **[Au_3]** units. Nevertheless, in the first step the weight loss is 60.6% and in the second step it is 22%. The first weight loss closely matches to lose of three **[Au_3]** molecules from the complex and the second weight loss is equal to lose of one **[Au_3]** unit (after the experiment some gold plating was observed on the pan and the hang-down wire. This might be the reason for the observed difference of calculated and experimental weight loses). Fascinatingly, decomposition of the **$C_{60}[Au_3]_4$** starts at fairly lower temperature (170 °C) compared to the melting point of **$[Au_3]_4$** (210 °C) and end at extremely higher temperature. The reason for the high end temperature might be the strong interactions of the last **$C_{60}[Au_3]_4$** molecule leaving the C_{60}. All the decompositions started a temperature little lower to the corresponding metal-pyrazolate melting point. The reason for this could be in the M_3 complexes exist in a columnar structure in which dimer of trimer units also show some interaction. In the **$C_{60}[M_3]_4$** complexes M_3 to C_{60} interaction is weaker. **$[Au_3]_4$** shows the strongest interaction in the columnar structure which in **$C_{60}[M_3]_4$** possesses the largest drop of the decomposition temperature.

2.3.3 Conclusions

In summary, we have synthesized a series of three novel coinage metal complexes, **$C_{60}[Cu_3]_4$**, **$C_{60}[Ag_3]_4$** and **$C_{60}[Au_3]_4$**, which represents the first coinage metal – pyrazolate fullerene adducts to the best of our knowledge. These adducts show fantastic crystallographic properties including extremely high symmetry, possessing the same space group as the “free” C_{60} and tetrahedral arrangement of metal complexes around C_{60}. These “super” packed complexes are formed mainly due to the match by the packing rather than the interactions. It was suggested by non-interacting nature in NMR solutions as well as insignificant change in Raman spectra in solid state.

Chapter 3

Experimental details

Experimental:

All manipulations were carried out under an atmosphere of purified nitrogen using standard Schlenk techniques or in a Vacuum Atmospheres single-station glovebox equipped with a -25 °C refrigerator. Solvents were purchased from commercial sources, purified using Innovative Technology SPS-400 PureSolv solvent drying system or by distilling over conventional drying agents prior to use. NMR spectra were recorded at 25 °C (unless specified) on a JEOL Eclipse 500 spectrometer (^{1}H, 500.16 MHz; ^{13}C, 125.77 MHz, ^{19}F, 470.62). Proton and carbon chemical shifts are reported in ppm, and referenced using the residual proton or carbon signals of the deuterated solvent.^{19}F NMR values were referenced to external $CFCl_3$. Elemental analyses were performed at Intertek QTI laboratory (Whitehouse, NJ). IR spectra were collected on a Bruker ALPHA FT-IR spectrometer with an attenuated total reflection (ATR) attachment. Raman spectra were recorded at room temperature on a Horiba Jobin Yvon LabRAM Aramis instrument using a 633 nm laser source. Crystals of the compound under study were placed on a glass slide for Raman analysis. Different experimental settings (laser intensity, level of magnification, time of exposure, number of cycles) were used for each compound in order to obtain the best signal-to-noise ratio. Melting points were obtained on a Mel-Temp II apparatus. Silver(I) triflate (Alfa Aesar), $NaBH_4$ (Aldrich), 2,3-dimethybutane (Aldrich), ethyl diazoacetate (EDA) (Aldrich), *cis*-cyclooctene (Acros Organics) and C_{60} (Aldrich) were purchased from commercial sources. 3,4,5-$(CF_3)_3$PzH, 4-Cl-3,5-$(CF_3)_2$PzH, 4-(NO_2)-3,5-$(CF_3)_2$PzH, [HB(3,5-$(CF_3)_2$Pz)$_3$]Ag(THF), **[Cu$_3$]**, **[Ag$_3$]** and **[Au$_3$]** were prepared as reported.[14,41,43] Catalytic reactions were monitored and analyzed by GC (Shimadzu GC-17A) and GC/MS (GC-MS QP 2010 SE). Thermo gravimetric analysis was performed

in a Shimadzu TGA-51 analyzer using a platinum crucible. Prior to the experiments, the thermo gravimetric equipment was calibrated by following the Shimadzu's Instruction Manual.

3.1 Synthesis of copper and silver small molecular adducts of $[HB(3,4,5\text{-}(CF3)]^-$

3,4,5-$(CF_3)_3$PzH : This compound was synthesized using the reported procedure.[40] By crystallization from hexane the pyrazole was obtained as a semihydrate, off-white crystals with m.p. 82-83 °C. The treatment of CH_2Cl_2 solution of the pyrazole by anhydrous Na_2SO_4 for 24 hr gave a mixture of crystals and oil after solvent evaporation as a result of partial removing of hydrate water. Anhydrous pyrazole for this work was obtained via slow sublimation through a layer of Drierite under reduced pressure. ^{1}H NMR (500 MHz; $CDCl_3$; Me_4Si): δ 12.30 (br. s, NH). ^{13}C NMR (125 MHz; $CDCl_3$; Me_4Si): δ 138.0 [br. m, 3,5-($\underline{C}CF_3)_2$], 119.8 (q, J = 268.8 Hz, 4-CF_3), 118.6 [br. q, J = 271.0 Hz, 3,5-$(CF_3)_2$], 111.2 (qm, J = 42.3 Hz, 4-$\underline{C}CF_3$). ^{19}F NMR (470 MHz; $CDCl_3$; $CFCl_3$): δ -56.1 (sept, 3F, 4-CF_3, J = 6.3 Hz), -61.3 [br. s, 6F, 3,5-(C$F_3)_2$].

[HB(3,4,5-$(CF_3)_3$Pz)$_3$]Na(THF) : Freshly dried 3,4,5-$(CF_3)_3$PzH (1030 mg, 3.8 mmol) and $NaBH_4$ (38 mg, 1.0 mmol) were combined in a Schlenk flask attached to a reflux condenser and slowly raised the temperature to 190 °C and kept at 190–200 °C for 4 h under nitrogen. The molten mixture was removed from heat and allowed to solidify, and then sublimed at 95–100 °C to remove excess pyrazole. The off-white solid was cooled to room temperature, washed with a small amount of hexane (~5 mL), and dissolved in 15 mL of THF. It was stirred overnight and the solvent was removed under reduced pressure to obtain [HB(3,4,5-$(CF_3)_3Pz)_3$]Na(THF) as a white powder (553 mg, 60 % based on $NaBH_4$). Anal. Calc. for $C_{22}H_9N_6NaBOF_{27}$: C, 28.72; H, 0.99. Found: C,

28.98; H, 0.90. M.p. = 230-235 ^{o}C (decomposition). ^{1}H NMR ($CDCl_3$): δ 3.78 (m), 1.90 (m); ^{19}F NMR ($CDCl_3$): δ -55.1 (m), -57.0 (br s), -62.3 (q, J = 8.0 Hz).

$[HB(3,4,5\text{-}(CF_3)_3Pz)_3]Ag(C_2H_4)$: $[HB(3,4,5\text{-}(CF_3)_3Pz)_3]Na(THF)$ (170 mg, 0.18 mmol) and AgOTf (51 mg, 0.20 mmol) were placed in a Schlenk flask with 10 mL of THF. The resulting mixture was covered with aluminum foil to protect from light and stirred overnight at room temperature. Ethylene was bubbled into the solution and the solution was concentrated to ~2 mL and dried by means of a gentle ethylene flow. The residue was extracted with hexane, filtered through a bed of Celite and the filtrate was collected. Ethylene was bubbled in for a few minutes and the solvent was removed under reduced pressure to obtain $[HB(3,4,5\text{-}(CF_3)_3Pz)_3]Ag(C_2H_4)$ as a white powder (150 mg, 70% based on $[HB(3,4,5\text{-}(CF_3)_3Pz)_3]Na(THF)$). The colorless X-ray quality crystals were grown from hexane layered CH_2Cl_2 at -5 ^{o}C. Anal. Calc. for $C_{20}H_5N_6AgBF_{27}$: C, 25.00; H, 0.52. Found: C, 25.69; H, 0.55. M.P. = 130-134 ^{o}C (decomposition). ^{19}F NMR (CD_2Cl_2): δ -55.4 (m), -57.5 (br s), -61.2 (qd, J = 3.2 Hz and 8.8 Hz); ^{1}H NMR (CD_2Cl_2): δ 5.65 (s, CH_2=CH_2); $^{13}C\{^{1}H\}$ NMR (CD_2Cl_2): selected peaks δ 111.6 (s, CH_2=CH_2). ^{13}C NMR (CD_2Cl_2): selected peaks δ 111.1 (t, $^{1}J(CH)$ = 164 Hz); Raman, cm^{-1}: selected peaks 1581 (CH_2=CH_2), 1460.

$[HB(3,4,5\text{-}(CF_3)_3Pz)_3]Cu(C_2H_4)$: $[HB(3,4,5\text{-}(CF_3)_3Pz)_3]Na(THF)$ (100 mg, 0.11 mmol) and $[CuOTf]_2.C_6H_6$ (65 mg, 0.13 mmol) were placed in a Schlenk flask with 12 mL of THF and stirred overnight at room temperature. The solvent was removed under reduced pressure and the residue was dissolved 12 mL of CH_2Cl_2. Ethylene was bubbled through the solution for few minutes, concentrated to ~2 mL and dried by means of a gentle ethylene flow. The resulting solid was extracted with hexane twice, filtered through a bed of Celite, ethylene was bubbled for few minutes and the solvent was removed

under reduced pressure to obtain a solid that has $[HB(3,4,5\text{-}(CF_3)_3Pz)_3]Cu(C_2H_4)$ and some by-products. For example, 1H NMR spectrum of the crude mixture suggests the presence of two metal-ethylene adducts [δ 5.06 (major) and 4,97 (minor)]. It was washed with a small amount of CH_2Cl_2 (~5 mL) to remove by-products and dried under reduced pressure to obtain $[HB(3,4,5\text{-}(CF_3)_3Pz)_3]Cu(C_2H_4)$ as a white powder (55 mg, 54% based on $[HB(3,4,5\text{-}(CF_3)_3Pz)_3]Na(THF)$). Anal. Calc. for $C_{20}H_5N_6CuBF_{27}$: C, 26.21; H, 0.55. Found: C, 26.22; H, 0.14. M.p. = 154-159 ^oC (decomposition). ^{19}F NMR ($CDCl_3$): δ -54.7 (m), -56.5 (br s) -59.6 (q, J = 9.9 Hz); ^1H NMR ($CDCl_3$): δ 5.06 (s, $CH_2=CH_2$); $^{13}C\{^1H\}$ NMR ($CDCl_3$): selected peaks δ 94.9 (s, $CH_2=CH_2$). We are yet to identify the minor product that displayed a ^1H NMR signal at δ 4.97 noted above.

$[HB(3,4,5\text{-}(CF_3)_3Pz)_3]Ag(CO)$: $[HB(3,4,5\text{-}(CF_3)_3Pz)_3]Ag(C_2H_4)$ (100 mg, 0.10 mmol) was dissolved in 25 mL of CH_2Cl_2 and CO (1 atm) was bubbled for few minutes and concentrated to ~2 mL and dried by means of gentle CO flow. Residue was extracted with hexane twice, filtered through a bed of Celite, CO was bubbled for few minutes and the solvent was removed under reduced pressure to obtain $[HB(3,4,5\text{-}(CF_3)_3Pz)_3]Ag(CO)$ as a white powder (70 mg, 70% based on $[HB(3,4,5\text{-}(CF_3)_3Pz)_3]Ag(C_2H_4)$). The colorless X-ray quality crystals were grown from hexane layered CH_2Cl_2 at -5 ^oC. Anal. Calc. for $C_{19}HN_6AgBF_{27}O$: C, 23.75; H, 0.10. Found: C, 23.30; H, 0.13. M.p. = 117-120 ^oC (decomposition). ^{19}F NMR ($CDCl_3$): δ -55.0 (m), -56.9 (br s), -60.9 (qd, J = 3.6 Hz, 8.7 Hz). IR (only selected peaks are given), in KBr, cm^{-1}: 2177 (CO, s); Raman (solid sample in sealed capillary), cm^{-1}: selected peaks 2179 (CO, weak), 1461.

X-ray crystallographic data:

A suitable crystal covered with a layer of cold hydrocarbon oil was selected and mounted with paratone-N oil in a cryo-loop and immediately placed in the low-temperature nitrogen stream. The X-ray intensity data were measured at 100(2) K on a Bruker SMART APEX CCD area detector system equipped with an Oxford Cryosystems 700 Series cooler, a graphite monochromator, and a Mo Kα fine-focus sealed tube (λ = 0.710 73 Å). The data frames were integrated with the Bruker SAINT-Plus software package. Data were corrected for absorption effects using the multi-scan technique (SADABS). All the non hydrogen atoms were refined anisotropically.

3.2 Synthesis of copper and silver small molecular adducts of [HB(4-NO_2-3,5-$(CF_3)_2Pz)_3]^-$and [HB(4-Cl-3,5$(CF_3)_2Pz)_3]^-$

[HB(4-Cl-3,5-$(CF_3)_2$Pz)$_3$]Na(THF) : Freshly sublimed 4-Cl-3,5-$(CF_3)_2$PzH (1380 mg, 5.8 mmol) and $NaBH_4$ (50 mg, 1.3 mmol) were combined in a Schlenk flask attached to a reflux condenser and slowly raised the temperature to 170 ^oC holding 1 h at 130 ^oC and 1 h at 160 ^oC. Temperature was maintained at 170–175 ^oC for 2 h under nitrogen. The molten mixture was removed from heat and allowed to solidify, and sublimed at 95–100 ^oC to remove excess pyrazole. The off-white solid was cooled to room temperature, dissolved in 20 mL of THF and stirred overnight. The solvent was removed under reduced pressure, residuals were extracted into hexane (2x20 mL), filtered through a bed of Celite and solvent was evaporated to obtain [HB(4-Cl-3,5-$(CF_3)_2Pz)_3$]Na(THF) as a white powder, 690 mg, 64 % based on $NaBH_4$; M.p. = 129 – 132 ^oC. ^{19}F NMR ($CDCl_3$): δ -57.5 (d, J = 3.6 Hz), -63.4 (s). ^1H NMR ($CDCl_3$): δ 5.02 (br s, 1H, B*H*), 3.78 (m, 4H, OCH_2), 1.92 (m, 4H, CH_2). This was used directly in the synthesis of the corresponding silver adduct.

[HB(4-Cl-3,5-$(CF_3)_2$Pz)$_3$]Ag(THF) : [HB(4-Cl-3,5-$(CF_3)_2$Pz)$_3$]Na(THF) (325 mg, 0.40 mmol) and AgOTf (104 mg, 0.40 mmol) were placed in a Schlenk flask with 45 mL of THF. The resulting mixture was covered with aluminum foil to protect it from light and stirred overnight at room temperature. The solution was filtered through a bed of Celite; the filtrate was collected and solvent was removed under reduced pressure. The residue was extracted into dichloromethane, filtered through a bed of Celite, the filtrate was collected and solvent was removed under reduced pressure to obtain [HB(4-Cl-3,5-$(CF_3)_2$Pz)$_3$]Ag(THF) as a white powder (254 mg, 70 % based on [HB(4-Cl-3,5-$(CF_3)_2$Pz)$_3$]Na(THF)). Anal. Calc. for $C_{19}H_9N_6OAgBCl_3F_{18}$: C, 25.23; H, 1.00; N, 9.29. Found: C, 25.66; H, 0.98; N, 9.48. M.p., decomposition started around 125 ^oC, melted with complete decomposition at 132 – 137 ^oC. ^{19}F NMR ($CDCl_3$): δ -57.5 (d, J = 4.0 Hz), -62.8 (d, J = 2.9 Hz). ^1H NMR ($CDCl_3$): δ 5.01 (br s, 1H, BH) 3.94 (m, 4H, OCH_2), 1.99 (m, 4H, CH_2). $^{13}C\{^1H\}$ NMR ($CDCl_3$): δ 25.7 (s, CH_2), 71.7 (s, OCH_2), 111.5 (s, CCl), 119.0 (q, ^1J(C,F) = 270.5 Hz, CF_3), 119.8 (q, ^1J(C,F) = 272.2 Hz, CF_3), 136.8 (q, ^1J(C,F) = 38.8 Hz, CCF_3), 141.2 (q,^1J(C,F) = 37.2 Hz, CCF_3). ATR-IR (neat, cm^{-1}): 2963, 2889, 2648 (w BH), 1541, 1500, 1462, 1379, 1359, 1271, 1240, 1213, 1171, 1140, 1131, 1049, 1021.

[HB(4-(NO_2)-3,5-$(CF_3)_2$Pz)$_3$]Na(Et_2O) : Freshly sublimed 4-(NO_2)-3,5-$(CF_3)_2$PzH (2300 mg, 9.2 mmol) and $NaBH_4$ (90 mg, 2.4 mmol) were combined in a Schlenk flask attached to a reflux condenser and slowly raised the temperature to 170 ^oC holding 1 h at 145 ^oC and 1 h at 162 ^oC. The temperature was maintained 170 - 177 ^oC for 2 h under nitrogen. The molten mixture was removed from heat and allowed to solidify, and sublimed at 100 ^oC to remove excess pyrazole. The light-brown solid was cooled to room temperature, dissolved in 20 mL of THF and stirred overnight, and then filtered through a bed of Celite. The solvent was removed under reduced pressure, residuals were

extracted into diethyl ether (Et_2O) and dichloromethane was added to obtain a precipitate. Solvents were decanted and vacuum dried to obtain [HB(4-(NO_2)-3,5-(CF_3)$_2$Pz)$_3$]Na(OEt_2) as an off-white powder (1406 mg, 69 % based on $NaBH_4$; M.p. = 286 - 288 ^oC; ^{19}F NMR (DMSO): δ -58.6 (d, J = 8.0 Hz), -62.2 (s). ^1H NMR (DMSO): δ 4.90 (br, 1H, BH), 3.37 (q, $^1J(CH)$ = 6.9 Hz, 2H, OCH_2), 1.08 (t, $^1J(CH)$ = 6.9 Hz, 3H, CH_3)). That was used directly in the synthesis of the corresponding silver(I) adduct.

[HB(4-NO_2-3,5-(CF_3)$_2$Pz)$_3$]Ag(THF) : [HB(4-(NO_2)-3,5-(CF_3)$_2$Pz)$_3$]Na(Et_2O) (121 mg, 0.14 mmol) and AgOTf (40 mg, 0.16 mmol) were placed in a Schlenk flask with 25 mL of THF. The resulting mixture was covered with aluminum foil to protect from light and stirred overnight at room temperature. The solution was filtered through a bed of Celite; the filtrate was collected and solvent was removed under reduced pressure. The residue was extracted into dichloromethane, filtered through a bed of Celite; the filtrate was collected and solvent was removed under reduced pressure to obtain [HB(4-(NO_2)-3,5-(CF_3)$_2$Pz)$_3$]Ag(THF) as a white powder (98 mg, 74 % based on [HB(4-NO_2-3,5-(CF_3)$_2$Pz)$_3$]Na(Et_2O)). Anal. Calc. for $C_{19}H_9N_9O_7AgBF_{18}$: C, 24.38; H, 0.97; N, 13.47, Found: C, 23.82; H, 0.67; N, 13.65. M.p., decomposition started around 140 ^oC, melted with complete decomposition at 180 - 184 ^oC. ^{19}F NMR ($CDCl_3$): δ -57.7 (s), -62.1 (s). ^1H NMR ($CDCl_3$): δ 3.80 (m, 4H, OCH_2), 1.90 (m, 4H, CH_2). ATR-IR (neat, cm^{-1}): 2988, 2903, 2665 (w BH), 1693, 1673, 1548, 1462, 1372, 1252, 1209, 1176, 1151, 1056, 1034.

[HB(3,5-(CF_3)$_2$Pz)$_3$]Ag(*c*-COE) : [HB(3,5-(CF_3)$_2$Pz)$_3$]Ag(THF) (112 mg, 0.16 mmol) was placed in a Schlenk flask, dissolved in 20 mL of dichloromethane and *cis*-cyclooctene (300 mg, 2.72 mmol) was syringed into the Schlenk flask. The resulting mixture was covered with aluminum foil to protect it from light and stirred overnight at room temperature. The solution was filtered through a bed of Celite; the filtrate was

collected and solvent was removed under reduced pressure to obtain [HB(3,5-$(CF_3)_2Pz)_3$]Ag(*c*-COE) as a white powder (118 mg, 90 % based on [HB(3,5-$(CF_3)_2Pz)_3$]Ag(THF)). The colorless X-ray quality crystals were grown from the mixed solvent hexane/CH_2Cl_2 at -5 ^oC. M.p. = 107-109 ^oC. ^{19}F NMR ($CDCl_3$): δ -59.1 (d, J = 3.6 Hz), -61.7 (s). ^1H NMR ($CDCl_3$): δ 6.91 (s, 3H, C*H*), 6.29 (m, 2H, CH_2-CH=CH), 5.09 (br, 1H, B*H*), 2.48 (br s, 4H, CH_2=CH), 1.4 – 1.9 (m, 8H, CH_2). $^{13}C\{^1H\}$ NMR ($CDCl_3$): δ 26.0 (s, *C*H_2), 26.1 (s, *C*H_2), 30.1 (s, *C*H_2), 106.7 (s, *C*H), 119.3 (q, $^1J(C,F)$ = 270.2 Hz, *C*F_3), 120.5 (q, $^1J(C,F)$ = 269.1 Hz, *C*F_3), 121.2 (s, *C*H=*C*H), 140.5 (q, $^1J(C,F)$ = 42.0 Hz, *C*CF_3), 143.7 (q, $^1J(C,F)$ = 38.4 Hz, *C*CF_3). ^{13}C NMR ($CDCl_3$): δ 26.1 (t, $^1J(CH)$ = 128.3 Hz, *C*H_2), 30.1 (t, $^1J(CH)$ = 126.5 Hz, *C*H_2), 106.7 (d, $^1J(CH)$ = 185.9 Hz, *C*H), 119.3 (q, $^1J(C,F)$ = 272.3 Hz, *C*F_3), 120.5 (q, $^1J(C,F)$ = 269.1 Hz, *C*F_3), 121.2 (d, $^1J(CH)$ = 154.7 Hz, *C*H=*C*H), 140.5 (q, $^1J(C,F)$ = 45.6 Hz, *C*CF_3), 143.7 (q, $^1J(C,F)$ = 37.6 Hz, *C*CF_3); ATR-IR (neat, cm^{-1}): 3161, 2926, 2859, 2631 (w, BH), 1579 (sh), 1556, 1498, 1471, 1388, 1365, 1265, 1246, 1174, 1128, 1078, 1037, 1003.

[HB(4-Cl-3,5-$(CF_3)_2Pz)_3$]Ag(*c*-COE) : [HB(4-Cl-3,5-$(CF_3)_2Pz)_3$]Ag(THF) (116 mg, 0.13 mmol) was dissolved in a Schlenk flask with 20 mL of dichloromethane and *cis*-cyclooctene (250 mg, 2.27 mmol) was syringed into the Schlenk flask. The resulting mixture was covered with an aluminum foil to protect from light and stirred overnight at room temperature. The solution was filtered through a bed of Celite; the filtrate was collected and solvent was removed under reduced pressure to obtain [HB(4-Cl-3,5-$(CF_3)_2Pz)_3$]Ag(*c*-COE) as a white powder (108 mg 90 % based on [HB(4-Cl-3,5-$(CF_3)_2Pz)_3$]Ag(THF)). The colorless X-ray quality crystals were grown from the mixed solvent hexane/CH_2Cl_2 at -5 ^oC. Anal. Calc. for $C_{23}H_{15}N_6AgBCl_3F_{18}$: C, 29.31; H, 1.60; N, 8.92, Found: C, 29.93; H, 1.43; N, 8.83. M.p., decomposition started around 128 ^oC,

turned to completely dark brown around 145 ^{o}C, melted 158 – 162 ^{o}C. ^{19}F NMR ($CDCl_3$): δ (ppm) -57.8 (d, J = 4.0 Hz), -61.8 (d, J = 1.8 Hz); ^{1}H NMR ($CDCl_3$): δ 6.18 (m, 2H, C*H*=C*H*), 4.95 (br, 1H, B*H*), 2.38 (br s, 4H, CH_2-CH=CH), 1.45 – 1.85 (m, 8H, CH_2). ^{13}C{^{1}H} NMR ($CDCl_3$): δ 26.0 (s, *C*H_2), 26.1 (s, *C*H_2), 29.9 (s, *C*H_2), 111.8 (s, *C*Cl), 119.0 (q, ^{1}J(C,F) = 272.3 Hz, *C*F_3), 119.8 (q, ^{1}J(C,F) = 270.7 Hz, *C*F_3), 123.4 (s, *C*H=*C*H), 136.8 (q, ^{1}J(C,F) = 42.0 Hz, *C*CF_3), 141.6 (q, ^{1}J(C,F) = 37.2 Hz, *C*CF_3). ^{13}C NMR ($CDCl_3$): δ 26.0 (t, ^{1}J(CH) = 128.4 Hz, *C*H_2), 29.9 (t, ^{1}J(CH) = 127.1 Hz, *C*H_2), 111.8 (s, *C*Cl), 119.0 (q, ^{1}J(C,F) = 273.4 Hz, *C*F_3), 119.8 (q, ^{1}J(C,F) = 270.5 Hz, *C*F_3), 123.7 (d, ^{1}J(CH) = 149.9 Hz, *C*H=*C*H), 136.8 (q, ^{1}J(C,F) = 40.8 Hz, *C*CF_3), 141.6 (q, ^{1}J(C,F) = 37.2 Hz, *C*CF_3). ATR-IR (neat, cm^{-1}): 2933, 2862, 2652 (w BH), 1584, 1542, 1501, 1464, 1377, 1359, 1271, 1243, 1212, 1183, 1168, 1136, 1048, 1021. Raman (only selected peaks are given), cm^{-1}: 1584, 1503, 1465, 1358, 1269, 1245, 1213.

[HB(4-(NO_2)-3,5-(CF_3)$_2$Pz)$_3$]Ag(*c*-COE) : [HB(4-(NO_2)-3,5-(CF_3)$_2$Pz)$_3$]Ag(THF) (225 mg, 0.24 mmol) was placed in a Schlenk flask, dissolved in 30 mL of dichloromethane and *cis*-cyclooctene (600 mg, 5.45 mmol) was syringed into the Schlenk flask. The resulting mixture was covered with aluminum foil to protect from light and stirred overnight at room temperature. The solution was filtered through a bed of Celite, the filtrate was collected and solvent was removed under reduced pressure to obtain [HB(4-(NO_2)-3,5-(CF_3)$_2$Pz)$_3$]Ag(*c*-COE) as a white powder (215mg, 92 % based on [HB(4-(NO_2)-3,5-(CF_3)$_2$Pz)$_3$]Ag(THF)). The colorless X-ray quality crystals were grown from CH_2Cl_2 at -5 ^{o}C. Anal. Calc. for $C_{23}H_{15}N_9O_6AgBF_{18}$: C, 28.36; H, 1.55; N, 12.94. Found: C, 28.60; H, 1.57; N, 12.14. M.p., decomposition started around 165 ^{o}C, melted with complete decomposition at 217 – 221 ^{o}C. ^{19}F NMR ($CDCl_3$): δ -57.9 (d, J = 4.3 Hz), -61.6 (d, J = 2.1 Hz). ^{1}H NMR ($CDCl_3$): δ 6.27 (m, 2H, C*H*=C*H*), 4.99 (br, 1H, B*H*), 2.42 (br

s, 4H, CH_2-CH=CH), 1.4 – 2.0 (m, 8H, CH_2). $^{13}C\{^1H\}$ NMR ($CDCl_3$): δ 25.9 (s, *C*H_2), 26.3 (s, *C*H_2), 30.0 (s, *C*H_2), 117.6 (q, $^1J(C,F)$ = 272.3 Hz, *C*F_3), 118.5 (q, $^1J(C,F)$ = 272.3 Hz, *C*F_3), 124.4 (s, *C*H=*C*H), 133.1 (s, *C*NO_2), 135.3 (q, $^1J(C,F)$ = 41.2 Hz, *C*CF_3), 138.4 (q, $^1J(C,F)$ = 40.0 Hz, *C*CF_3). ^{13}C NMR ($CDCl_3$): selected peaks δ 124.3 (d, $^1J(CH)$ = 153.5 Hz, *C*H); ATR-IR (neat, cm^{-1}): 2963, 2941, 2916, 2858, 2667 (w, BH), 1551, 1533, 1459, 1365, 1258, 1190, 1777, 1154, 1094, 1059, 1026. Raman, cm^{-1}: 1583, 1552, 1539, 1514, 1463, 1366, 1269.

General procedure for C–H activation reactions : The silver complex (catalyst: [HB(4-(NO_2)-3,5-(CF_3)$_2$Pz)$_3$]Ag(*c*-COE), [HB(4-Cl-3,5-(CF_3)$_2$Pz)$_3$]Ag(*c*-COE), [HB(4-Cl-3,5-(CF_3)$_2$Pz)$_3$]Ag(THF) or [HB(3,5-(CF_3)$_2$Pz)$_3$]Ag(THF)) (0.015 mmol) was mixed in with octafluorotoluene (4 mL) under N_2 in a flask protected from light (using aluminium foil) and stirred for 5 min. A 2 mL aliquot of 2,3-dimethylbutane (substrate) was injected to the stirred solution of the catalyst. EDA (containing 13% w/w CH_2Cl_2) (131 mg, 1.00 mmol) in octafluorotoluene (2 mL) was added to the mixture over a period of ~15 min at the room temperature and the resulting mixture was stirred for 12 hrs in the absence of light. An aliquot of the reaction mixture was taken out, filtered through a short plug of Celite, and the filtrate was analysed using GC and NMR spectroscopy. Compounds in this filtrate (left over starting material and products) were also confirmed by the GC-MS data. GC analyses show that the EDA consumption is essentially complete within 2-3 hrs in [HB(4-Cl-3,5-(CF_3)$_2$Pz)$_3$]Ag(*c*-COE) and [HB(3,5-(CF_3)$_2$Pz)$_3$]Ag(THF) catalyzed reactions. However, [HB(4-(NO_2)-3,5-(CF_3)$_2$Pz)$_3$]Ag(*c*-COE) catalyzed reaction took a longer time (about 12 hrs) for complete EDA consumption (6% of unreacted EDA was observed after 6 hrs). Note that the reaction catalysed by [HB(3,5-(CF_3)$_2$Pz)$_3$]Ag(THF) could be performed in neat 2,3-dimethylbutane. This could be done by dissolving the catalyst in 6

mL of 2,3-dimethylbutane (instead of a mixture containing catalyst in 4 mL octafluorotoluene and 2 mL of 2,3-dimethylbutane) and treating it with 1.00 mmol EDA in 2 mL of 2,3-dimethylbutane (rather than 2 mL octafluorotoluene) as described above. The solubility of [HB(4-(NO_2)-3,5-(CF_3)$_2$Pz)$_3$]Ag(*c*-COE) is poor in 2,3-dimethylbutane to perform a similar reaction effectively in neat 2,3-dimethylbutane. For example, even after 12 hrs, ~41% of unreacted EDA was observed in the reaction mixture while [HB(3,5-(CF_3)$_2$Pz)$_3$]Ag(THF) catalyzed reaction in neat 2,3-dimethylbutane was complete within 6 hrs. Solubility of [HB(4-(NO_2)-3,5-(CF_3)$_2$Pz)$_3$]Ag(*c*-COE) is relatively low even in octafluorotoluene, compared to the solubility of the other two silver adducts in the same solvent.

X-ray Crystallographic Data : A suitable crystal covered with a layer of hydrocarbon/Paratone-N oil was selected and mounted on a Cryo-loop, and immediately placed in the low temperature nitrogen stream. The X-ray intensity data for [HB(3,5-(CF_3)$_2$Pz)$_3$]Ag(*c*-COE) were measured at 100(2) K on a Bruker D8 Quest with a Photon 100 CMOS detector equipped with an Oxford Cryosystems 700 series cooler, a Triumph monochromator, and a Mo Kα fine-focus sealed tube (λ = 0.71073 Å). X-ray intensity data for [HB(4-Cl-3,5-(CF_3)$_2$Pz)$_3$]Ag(*c*-COE) and [HB(4-(NO_2)-3,5-(CF_3)$_2$Pz)$_3$]Ag(*c*-COE) were measured at 100(2) K on a SMART APEX II CCD area detector system equipped with an Oxford Cryosystems 700 series cooler, a graphite monochromator, and a Mo Kα fine-focus sealed tube (λ = 0.71073 Å). Intensity data were processed using the Saint Plus program. All the calculations for the structure determination were carried out using the SHELXTL package (version 6.14).[144] Initial atomic positions were located by direct methods using XS, and the structures of the compounds were refined by the least-squares method using XL. Absorption corrections were applied by using SADABS. Hydrogen atoms except those on the boron atom were placed at calculated positions and

refined riding on the corresponding carbons. The hydrogen atom attached to boron was located from residual electron density and refined. All the non-hydrogen atoms were refined anisotropically. X-ray structural figures were generated using Olex2.[145] Further details are given in Tables 1-2. The 941720-941722 contain the supplementary crystallographic data. These data can be obtained free of charge *via* http://www.ccdc.cam.ac.uk/conts/retrieving.html or from the Cambridge Crystallographic Data Centre (CCDC), 12 Union Road, Cambridge, CB2 1EZ, UK).

[HB(3,5-$(CF_3)_2$Pz)$_3$]Ag(*c*-COE) crystallizes in the $P\bar{1}$ space group with two molecules in the asymmetric unit (for a Z value of 4). [HB(4-Cl-3,5-$(CF_3)_2$Pz)$_3$]Ag(*c*-COE) crystallizes in the $P\bar{1}$ space group. The cyclooctene ring backbones show positional disorder, which was modeled satisfactorily. [HB(4-(NO_2)-3,5-$(CF_3)_2$Pz)$_3$]Ag(*c*-COE) crystallizes in the $P\bar{1}$ space group. This compound co-crystallizes with a molecule of dichloromethane. The dichloromethane demonstrated occupancy disorder near an inversion center which was modeled satisfactorily.

Computational Methods : Density functional theory (DFT) within the Gaussian 09 package[146] was used for geometry optimization and vibrational frequency calculations. The Becke-Perdew (BP86)[147] functional was employed. Ag atoms were modeled with a CEP-31G pseudopotential and valence basis set plus a set of six uncontracted p functions (from Couty and Hall)[148] and also with Frenking *et al.*'s f polarization function.[149] All other atoms were calculated using the Pople all-electron triple-zeta basis set, 6-311++G(d,p).[150] NMR shielding tensors were computed with the Gauge-Independent Atomic Orbital (GIAO) method.[151] A full population analysis was performed with a Natural Bond Orbital (NBO) analysis, using NBO version 3.[152-154]

3.3 Synthesis of isolable arene sandwiched copper(I) pyrazolates

$\{[Bz][Cu_3]_2\}_\infty$: $[Cu_3]$ (100 mg, 0.125 mmol) was dissolved in 1 mL of benzene and 0.5 mL of $CDCl_3$ was added. The solution was kept at -20 °C to obtain X-ray quality colorless crystals of **$\{[Bz][Cu_3]_2\}_\infty$**. Crystals were separated from mother liquor and immediately covered with a layer of hydrocarbon/Paratone-N oil and used for X-ray crystallography. Crystals used in NMR spectroscopy were dried under reduced pressure for about 30 mins at room temperature. ^{1}H NMR ($CDCl_3$): δ (ppm) 7.03 (s), 7.36 (s). ^{19}F NMR ($CDCl_3$): δ (ppm) -61.0 (s). $^{13}C\{^1H\}$ NMR ($CDCl_3$): δ (ppm) 104.5 (s, *C*H), 120.0 (q, $^1J(C,F)$ = 269.1 Hz, *C*F_3), 128.5 (s, *C*H, *C*$_6H_6$), 144.6 (m, *C*CF_3). ^{1}H NMR signal integration indicated the presence of 6.4% benzene in dried sample. Data from elemental analysis agree with the calculated values for **$[Cu_3]$** containing traces of benzene. This observation is consistent with NMR data and indicates the loss of benzene under reduced pressure. Anal. Calc. for **$\{[Bz][Cu_3]_2\}_\infty$**, $C_{36}H_{12}N_{12}Cu_6F_{36}$: C, 25.77; H, 0.72; N, 10.02; Anal. Calc. for **$[Cu_3]$**, $C_{15}H_3N_6Cu_3F_{18}$: C, 22.52; H, 0.38; N, 10.51; Found: C, 22.45; H, 0.25; N,10.56 (indicates the loss of most benzene and the presence of **$[Cu_3]$** with about 6% benzene). Mp: 199-202 ^{o}C (decomposition).

$\{[Mes][Cu_3]\}_\infty$: $[Cu_3]$ (100 mg, 0.125 mmol) was dissolved in 1mL of mesitylene **[Mes]** and 4 mL of $CDCl_3$ was added. The solution was kept at -20 °C to obtain X-ray quality colorless crystals of **$\{[Mes][Cu_3]\}_\infty$**. Crystal were separated from mother liquor and immediately covered with a layer of hydrocarbon/Paraton-N oil and used for X-ray crystallography. Crystals used in NMR spectroscopy were air dried for few mins at room temperature. ^{1}H NMR ($CDCl_3$): δ (ppm) 2.27 (s), 6.80 (s), 7.02 (s). ^{19}F NMR ($CDCl_3$): δ (ppm) -61.0 (s). $^{13}C\{^1H\}$ NMR ($CDCl_3$): δ (ppm) 21.3 (S, CH_3), 104.5 (s, *C*H), 120.0 (q, $^1J(C,F)$ = 269.1 Hz, *C*F_3), 127.06 (s, *C*H, *C*$_9H_{12}$), 137.92 (s, *C*CH_3, *C*$_9H_{12}$), 144.6 (q, $^2J(C,F)$ = 38.0 Hz, *C*CF_3). Anal. Calc. for $C_{24}H_{15}N_6Cu_3F_{18}$: C, 31.33; H, 1.64; N, 9.13;

Found: C, 32.07; H, 1.70; N, 9.35. M.p. of sample shows two melting temperature events, first partial melting at 126-130 °C and second melting process at 188-192 °C.

{[Nap][Cu_3]}∞: [Cu_3] (200 mg, 0.25 mmol) and Naphthalene **[Nap]** (32 mg, 0.25 mmol) were dissolved in 1.5 mL of benzene and 1.5 mL of $CDCl_3$ was added. The solution was kept at -20 °C to obtain X-ray quality colorless crystals of **{[Nap][Cu_3]}∞**. Crystal were separated from mother liquor and immediately covered with a layer of hydrocarbon/Paraton-N oil and used for X-ray crystallography. Crystals used in NMR spectroscopy were dried under reduced pressure for 2 h at room temperature. Anal. Calc. for $C_{25}H_{11}N_6Cu_3F_{18}$ C, 32.36; H, 1.19; N, 9.06; Found: C, 31.88; H, 0.44; N, 9.49. ^{1}H NMR ($CDCl_3$): δ (ppm) 7.02 (s), 7.40 (m), 7.76 (m). ^{19}F NMR ($CDCl_3$): δ (ppm) -61.0 (s). $^{13}C\{^{1}H\}$ NMR ($CDCl_3$): δ (ppm) 104.4 (s, *C*H), 120.0 (q, $^{1}J(C,F)$ = 269.1 Hz, *C*F_3), 126.06 (s, *C*H, Nap), 128.0 (s, *C*H, Nap), 133.5 (s, *C*-CH, Nap), 144.4 (q, $^{2}J(C,F)$ = 38.0 Hz, *C*CF_3).

Photophysical measurements: Steady state luminescence spectra were acquired using a Horiba J-Y Fluoromax 3 with upgrades for lifetime fluorescence studies. The excitation and emission spectra were corrected using factors supplied by the manufacturer. Solid samples were placed in a solid sample cell and covered with a quarts plate for measurements. Photophysical data of arene free **[Cu3]** has been reported (see: H. V. R. Dias, H. V. K. Diyabalanage, M. G. Eldabaja, O. Elbjeirami, M. A. Rawashdeh-Omary and M. A. Omary, *J. Am. Chem. Soc.*, 2005, **127**, 7489-7501).

X-ray crystallographic data: A suitable crystal covered with a layer of hydrocarbon/paratoneN oil was selected and mounted on a Mitigen loop, and immediately placed in the low temperature nitrogen stream. The X-ray intensity data were measured on a Bruker D8 Quest with a Photon 100 CMOS detector equipped with an Oxford Cryosystems 700 series cooler, a Triumph monochromator, and a Mo Kα fine-focus sealed tube (λ = 0.71073 Å). Crystals of {[Nap][Cu3]}∞ appeared to crack at 100 K

but diffraction pattern was satisfactory. Data were taken at a slightly higher temperature of 150(2) K for {[Bz][Cu_3]$_2$}∞ and {[Mes][Cu_3]}∞ to prevent crystal cracking upon cooling to 100 K. Intensity data were processed using the Saint Plus program. Initial calculations for the structure determination were carried out using the SHELXTL package (version 6.14) and finalized with Olex2 (version 1.2.5). Initial atomic positions were located by direct methods using XS, and the structures of the compounds were refined by the least-squares method using XL. Absorption corrections were applied by using SADABS. Hydrogen atoms were placed at calculated positions and refined riding on the corresponding carbons.

{[Bz][Cu_3]$_2$}∞ crystallizes in the P-1 space group with one Cu containing molecule and one half molecule of benzene in the asymmetric unit (for a Z value of 2). The center of the benzene molecule is located on an inversion center. Two CF3 groups demonstrated rotational disorder. It was modeled and the atoms were treated with a combination of SADI, DELU, SIMU, and ISOR restraints as well as occupancy refinements. All the non-hydrogen atoms were refined anisotropically.

{[Mes][Cu_3]}∞ crystallizes in the R3c space group with one-third Cu molecule and one-third molecule of mesitylene in the asymmetric unit (for a Z value of 6). The centers of both molecules are located at the convergence of three glide planes which effectively creates 3-fold rotational symmetry. All the non-hydrogen atoms were refined anisotropically.

{[Nap][Cu_3]}∞ crystallizes in the P-1 space group with one Cu molecule and two half molecules of naphthalene in the asymmetric unit (for a Z value of 2). The naphthalene molecules are located on an inversion center. One CF3 group demonstrated rotational disorder and was modeled successfully as well as occupancy refinement. All the non-hydrogen atoms were refined anisotropically.

3.4 Synthesis of π-stacking complexes of gold(I), silver(I) and copper(I) pyrazolate with C_{60} fullerene

$C_{60}[Cu_3]_4$: C_{60} (48 mg, 0.067 mmol) was dissolved in 35 mL of carbon disulfide, $[(3,5\text{-}CF_3)_2PzCu]_3$ (200 mg, 0.25 mmol) was dissolved in 10 mL of carbon disulfide and transferred to the C_{60} solution by means of a cannula. Resulting solution was covered with an aluminum foil to protect from light, stirred for 1 hour, hand warmed to get rid of tiny precipitate and let stand at room temperature to obtain X-ray quality dark purple crystals of $C_{60}\{[(3,5\text{-}(CF_3)_2Pz)Cu]_3\}_4$ (almost black to naked eye). Solvent evaporated to half a volume, let stand to get the second and third crops of similar crystals and the collected crystals were completely dried under reduced pressure (combined crops: 225 mg. 92% yield based on $[(3,5\text{-}(CF_3)_2Pz)Cu]_3$). Mp: *ca* 280°C decomposition started and completely decomposed *ca* 315 °C (Metallic copper formation observed). Anal. Calc. for $C_{120}H_{12}N_{24}F_{72}Cu_{12}$: C, 36.77; H, 0.31; N, 8.58 Found: C, 36.46; H, 0.19; N, 9.34. ^{1}H NMR ($CS_2/CDCl_3$, 2:1): δ 7.01 (s), ^{19}F NMR ($CS_2/CDCl_3$, 2:1): δ -60.7 (s). $^{13}C\{^1H\}$ NMR ($CS_2/CDCl_3$, 2:1): δ 103.8 (s)*C*H), 119.5 (q, $^1J(C,F)$ = 269.9 Hz, *C*F_3), 142.9 (s, *C*-C_{60}) 144.3 (m).

$C_{60}[Ag_3]_4$: C_{60} (18 mg, 0.025 mmol) was dissolved in 8 mL of carbon disulfide, $[(3,5\text{-}(CF_3)_2Pz)Ag]_3$ (93 mg, 0.1 mmol) was dissolved in 4 mL of carbon disulfide and transferred to the C_{60} solution by means of a cannula. Resulting solution was covered with an aluminum foil to protect from light, stirred for 2 hours, hand warmed to get rid of tiny precipitate and let stand at room temperature to obtain X-ray quality dark purple crystals of $C_{60}\{[(3,5\text{-}(CF_3)_2Pz)Ag]_3\}_4$ (almost black to naked eye). Solvent evaporated to half a volume and let stand to get the second and third crops of similar crystals (combined crops: 100 mg. 90% yield based on $[(3,5\text{-}(CF_3)_2Pz)Ag]_3$ – *crystal structure unit cell was used to confirm the composition of later crops*). Mp: *ca* 70°C decomposition

started and completely decomposed *ca* 280 °C. Anal. Calc. for $C_{120}H_{12}N_{24}F_{72}Ag_{12}$: C, 32.37; H, 0.27; N, 7.55 Found: C, 32.15; H, 0.19; N, 7.46. ^{1}H NMR ($CS_2/CDCl_3$, 2:1): δ 7.03 (s), ^{19}F NMR ($CS_2/CDCl_3$, 2:1): δ -61.0 (s). $^{13}C\{^{1}H\}$ NMR ($CS_2/CDCl_3$, 2:1): δ 102.9 (s)*C*H), 120.0 (q, $^{1}J(C,F)$ = 270.1 Hz, *C*F_3), 143.0 (s, *C*-C_{60}) 144.7 (q, $^{2}J(C,F)$ = 36.9 Hz, *C*CF_3). Raman, cm^{-1}: 1468.

$C_{60}[Au_3]_4$: C_{60} (18 mg, 0.025 mmol) was dissolved in 4 mL of carbon disulfide, $[(3,5\text{-}CF_3)_2PzAu]_3$ (120 mg, 0.1 mmol) was dissolved in 25 mL of benzene and transferred to the C_{60} solution by means of a cannula. Resulting solution was covered with an aluminum foil to protect from light, stirred for 1 hour, concentrated to *ca.*5 mL. Solvents were removed by means of a cannula and dried under reduced pressure to obtain dark purple crystalline solid of $C_{60}\{[(3,5\text{-}(CF_3)_2Pz)Au]_3\}_4$ (115 mg. 83% yield based on $[(3,5\text{-}(CF_3)_2Pz)Au]_3$). X-ray quality reddish - dark purple crystals (almost black to naked eye) were obtained from 1: 20 carbon disulfide: benzene solution at 5°C. Anal. Calc. for $C_{120}H_{12}N_{24}F_{72}Au_{12}$: C, 26.11; H, 0.22; N, 6.09 Found: C, 26.19; H, 0.39; N, 6.31. ^{1}H NMR (C_6D_6): δ 6.49 (s), ^{19}F NMR (C_6D_6): δ -61.2 (s). $^{13}C\{^{1}H\}$ NMR (C_6D_6): δ 105.8 (s)*C*H), 142.9 (s, *C*-C_{60}) – only traces of signals due to significantly low soluability. Raman, cm^{-1}: 266, 490, 1466.

3.4.1 Thermal analysis data (TGA)

Complex	M_3 weight %	Combined weight loss (1^{st} +2^{nd}) %
$C_{60}[Cu_3]_4$	81.6	80.4
$C_{60}[Ag_3]_4$	83.8	82.0
$C_{60}[Au_3]_4$	87.0	82.8

3.4.1.1 $C_{60}[Cu_3]_4$ complex

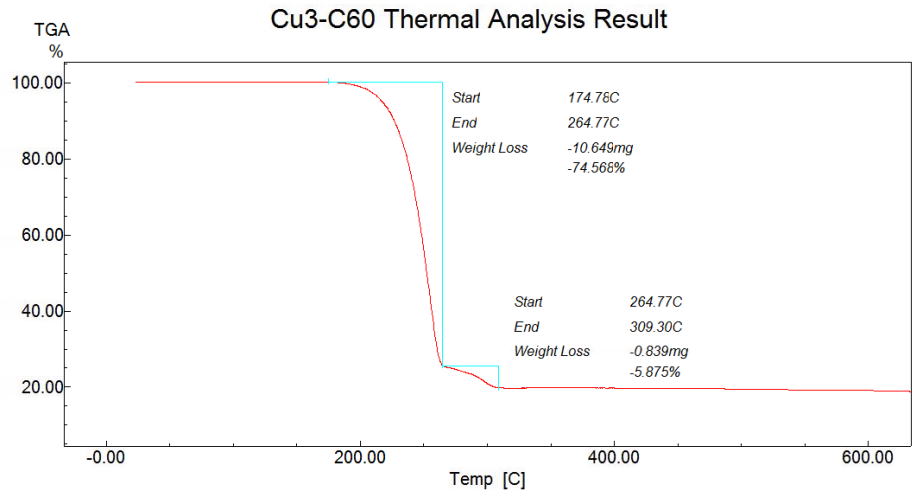

3.4.1.2 $C_{60}[Ag_3]_4$ complex

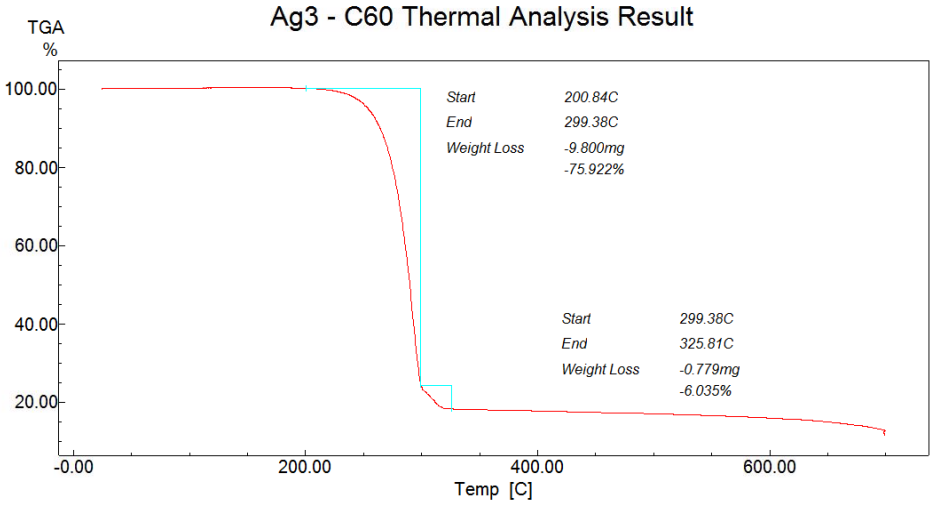

3.4.1.3 $C_{60}[Au_3]_4$ complex

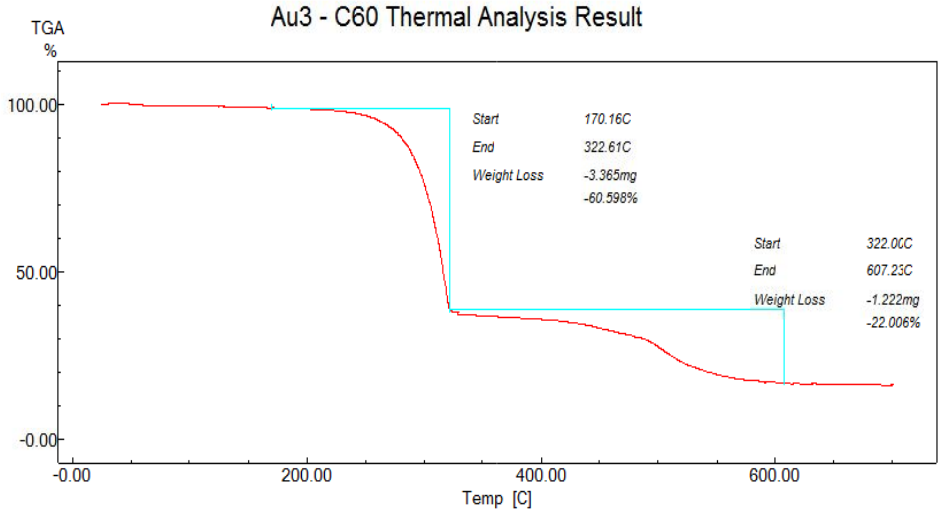

Appendix A

Selected spectroscopy data

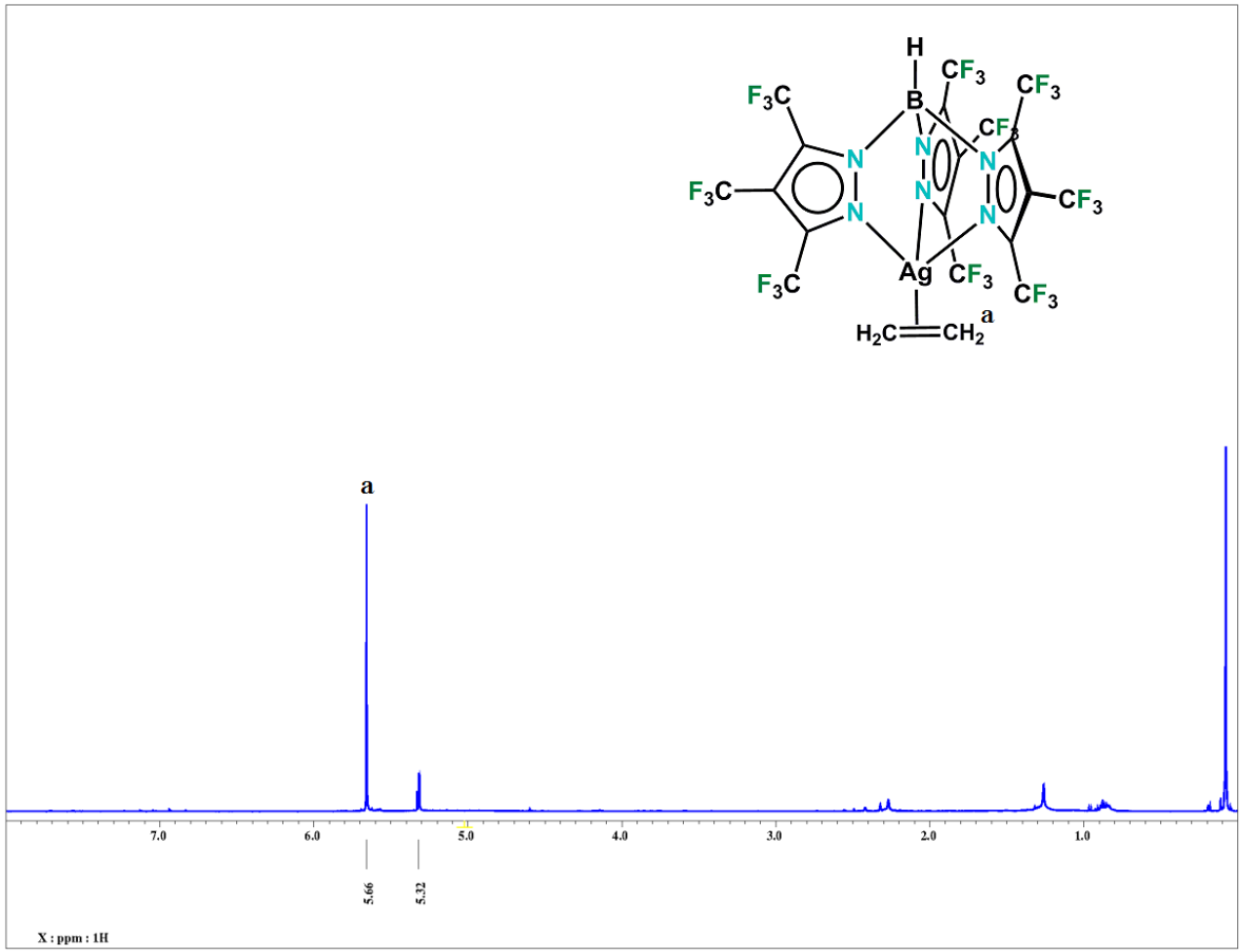

^{1}H NMR of [HB(3,4,5-$(CF_3)_3$Pz)$_3$]Ag(C_2H_4) in CD_2Cl_2

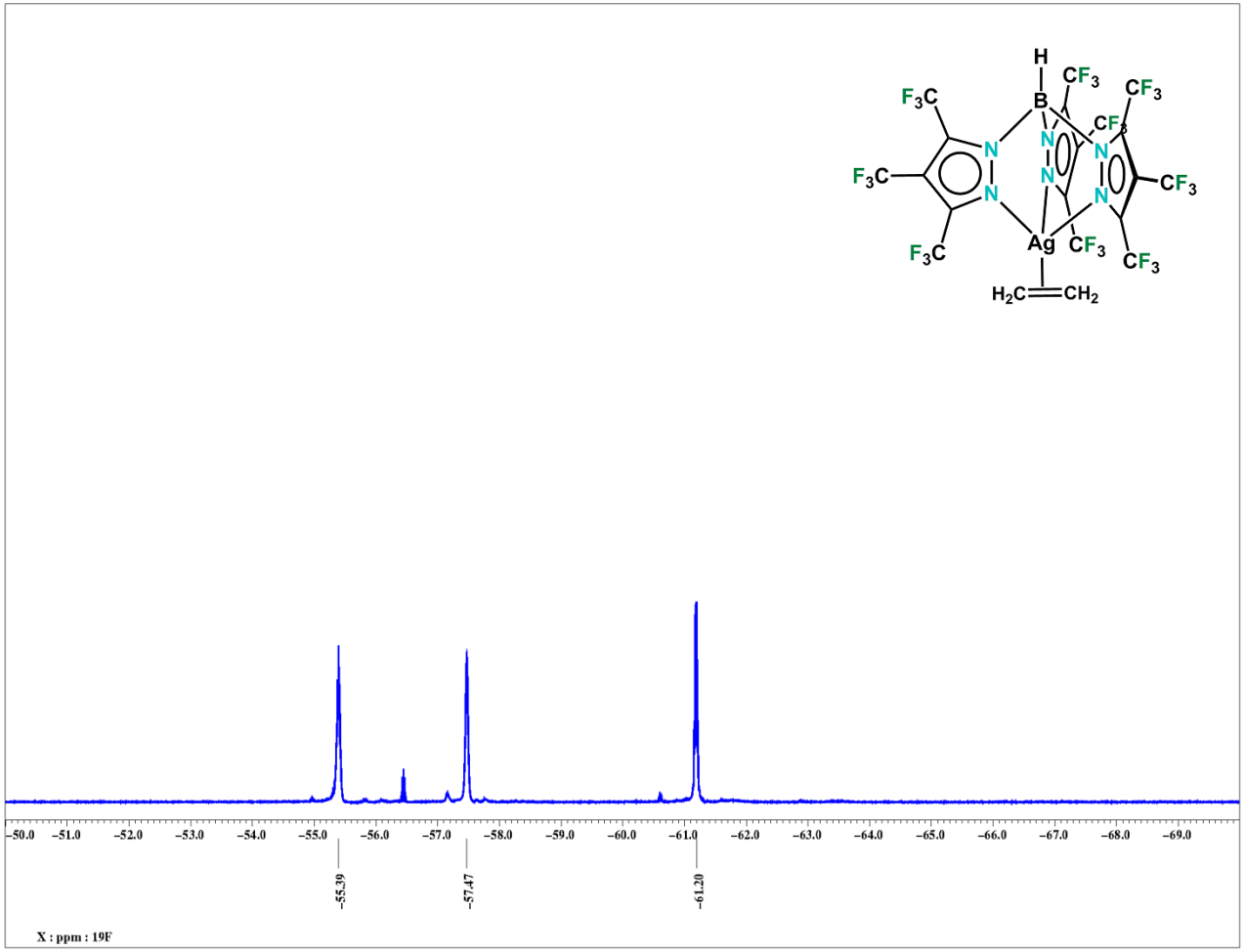

^{19}F NMR of $[HB(3,4,5\text{-}(CF_3)_3Pz)_3]Ag(C_2H_4)$ in CD_2Cl_2

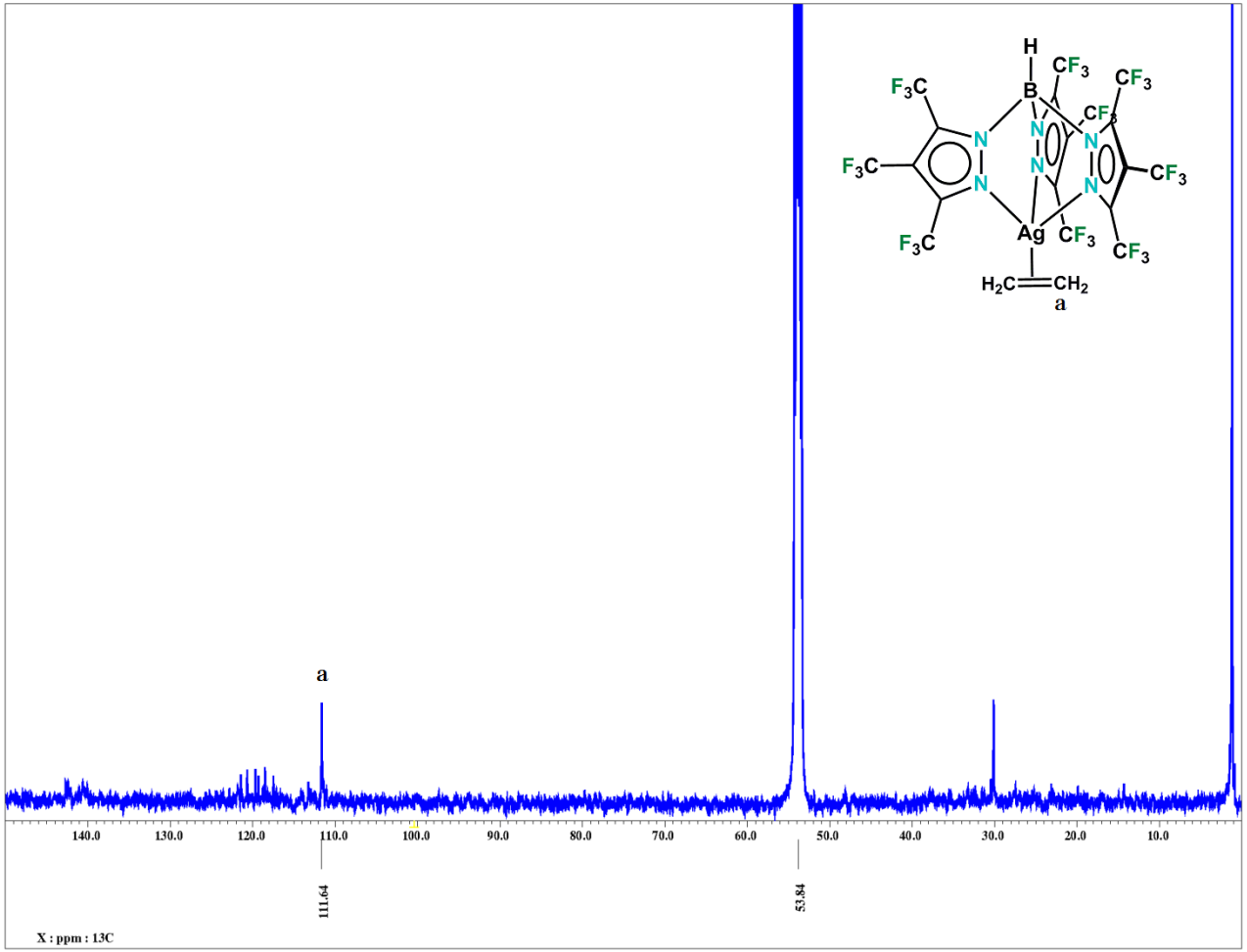

^{13}C NMR of $[HB(3,4,5\text{-}(CF_3)_3Pz)_3]Ag(C_2H_4)$ in CD_2Cl_2

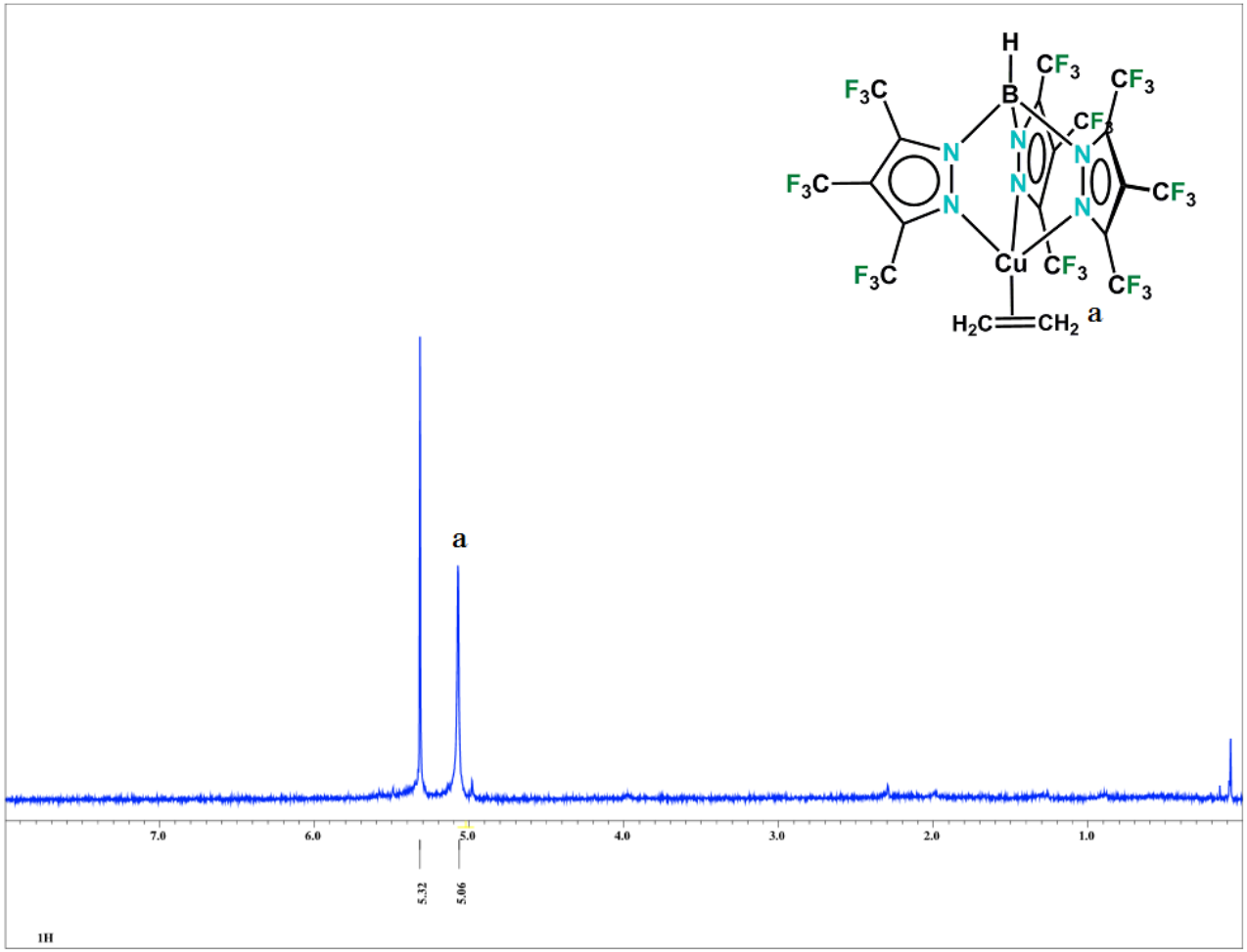

^{1}H NMR of [HB(3,4,5-$(CF_3)_3$Pz)$_3$]Cu(C_2H_4) in CD_2Cl_2

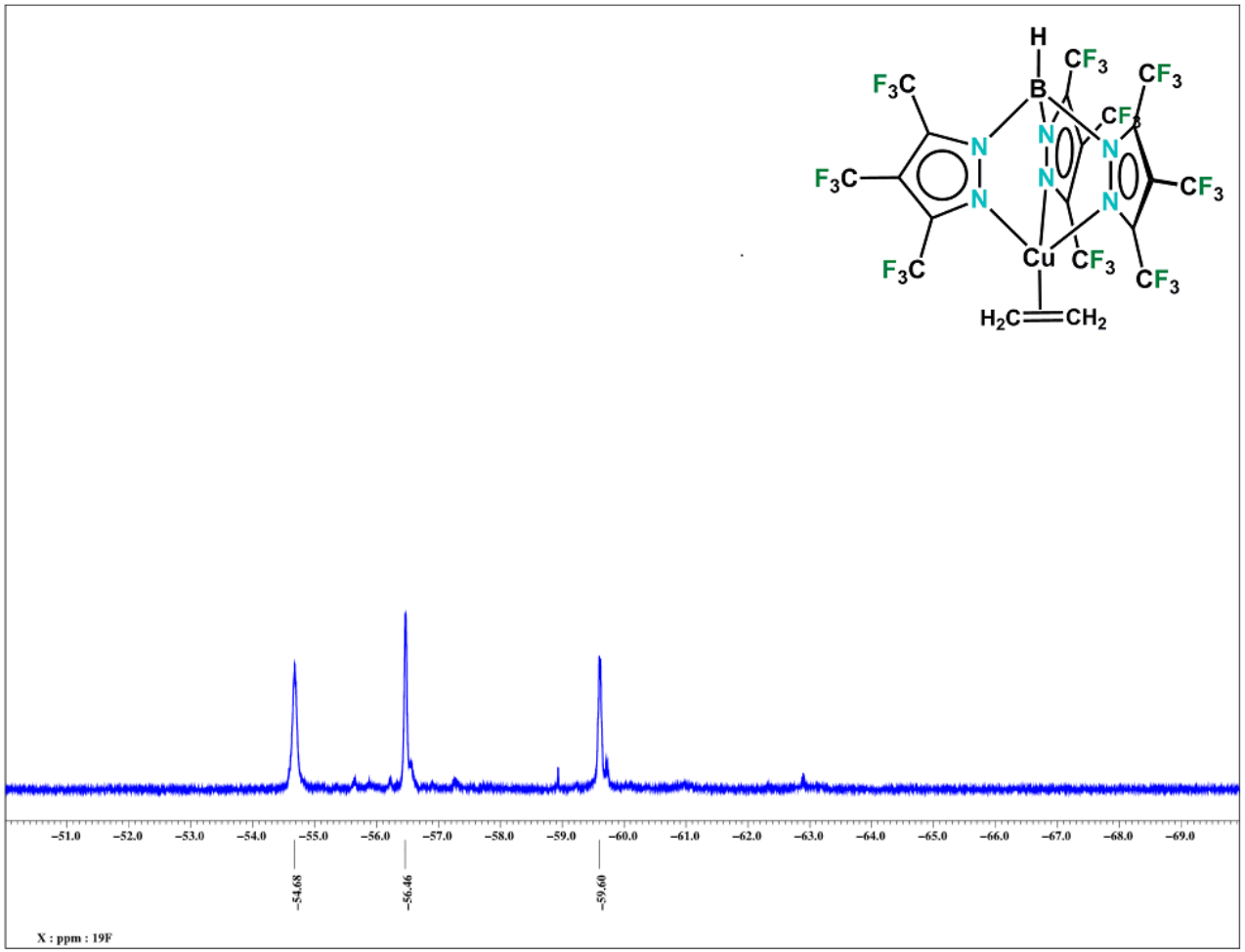

^{19}F NMR of [HB(3,4,5-$(CF_3)_3$Pz)$_3$]Cu(C_2H_4) in CD_2Cl_2

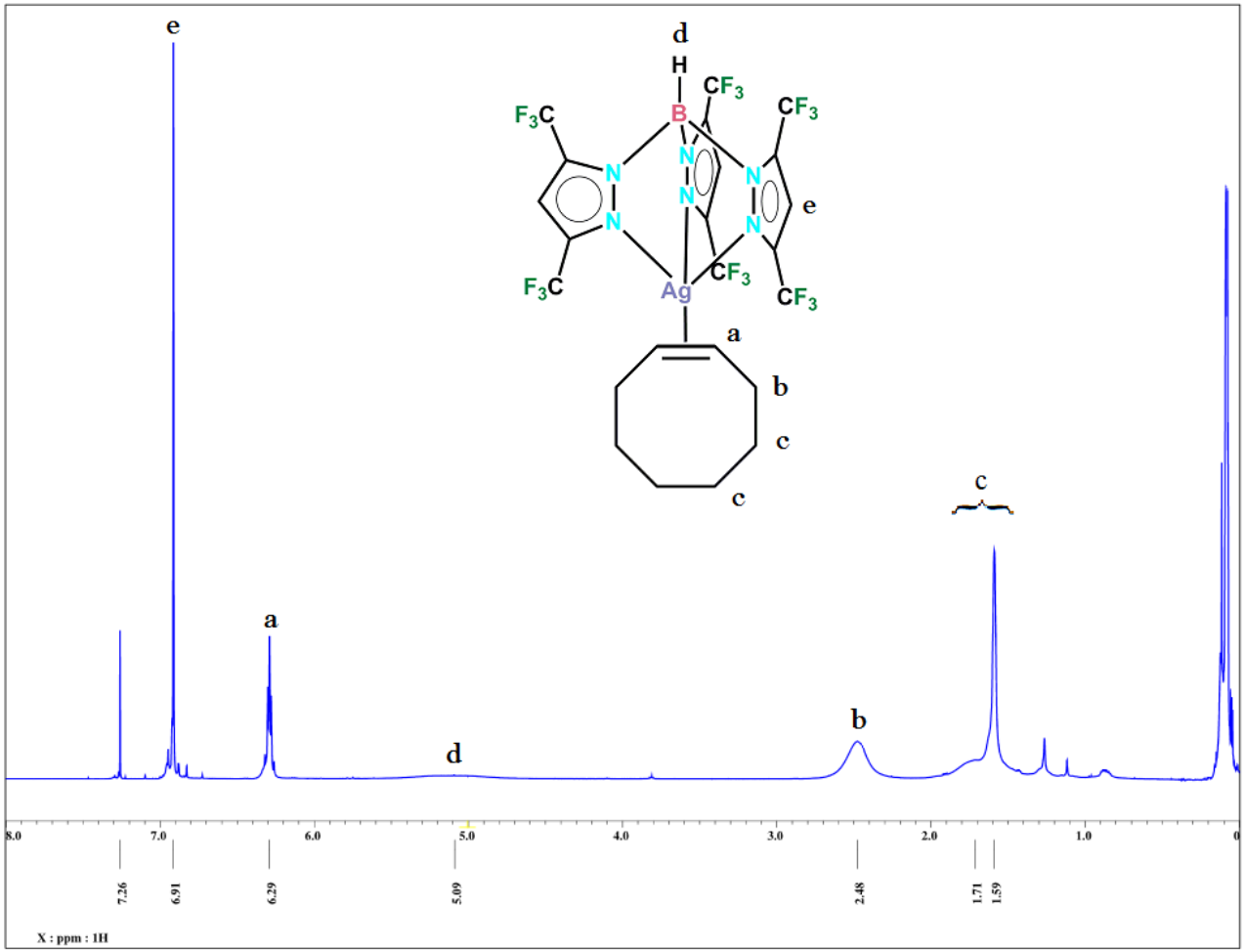

^{1}H NMR of [HB(3,5-(CF$_3$)$_2$Pz)$_3$]Ag(*c*-COE) in CDCl$_3$

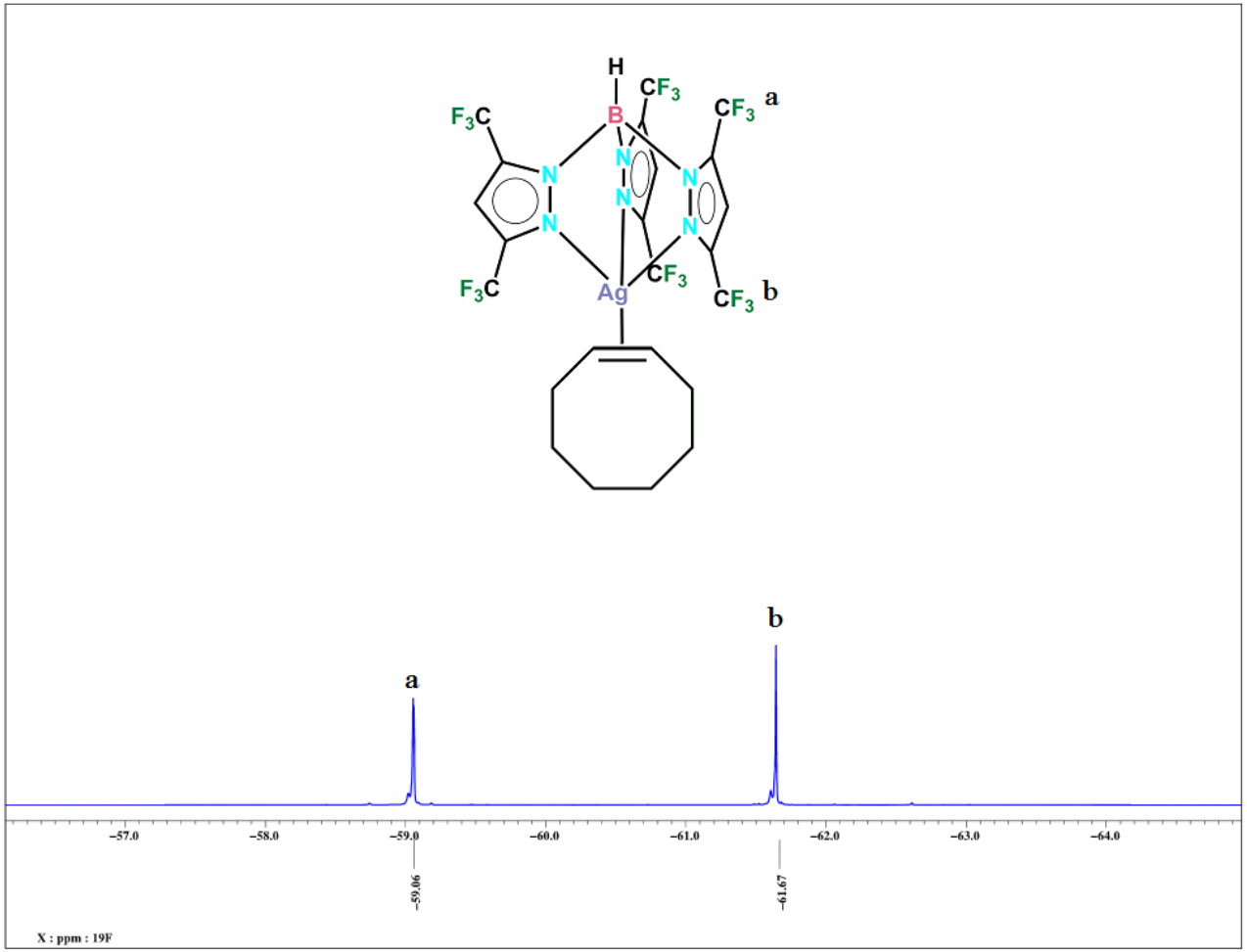

^{19}F NMR of [HB(3,5-$(CF_3)_2$Pz)$_3$]Ag(*c*-COE) in $CDCl_3$

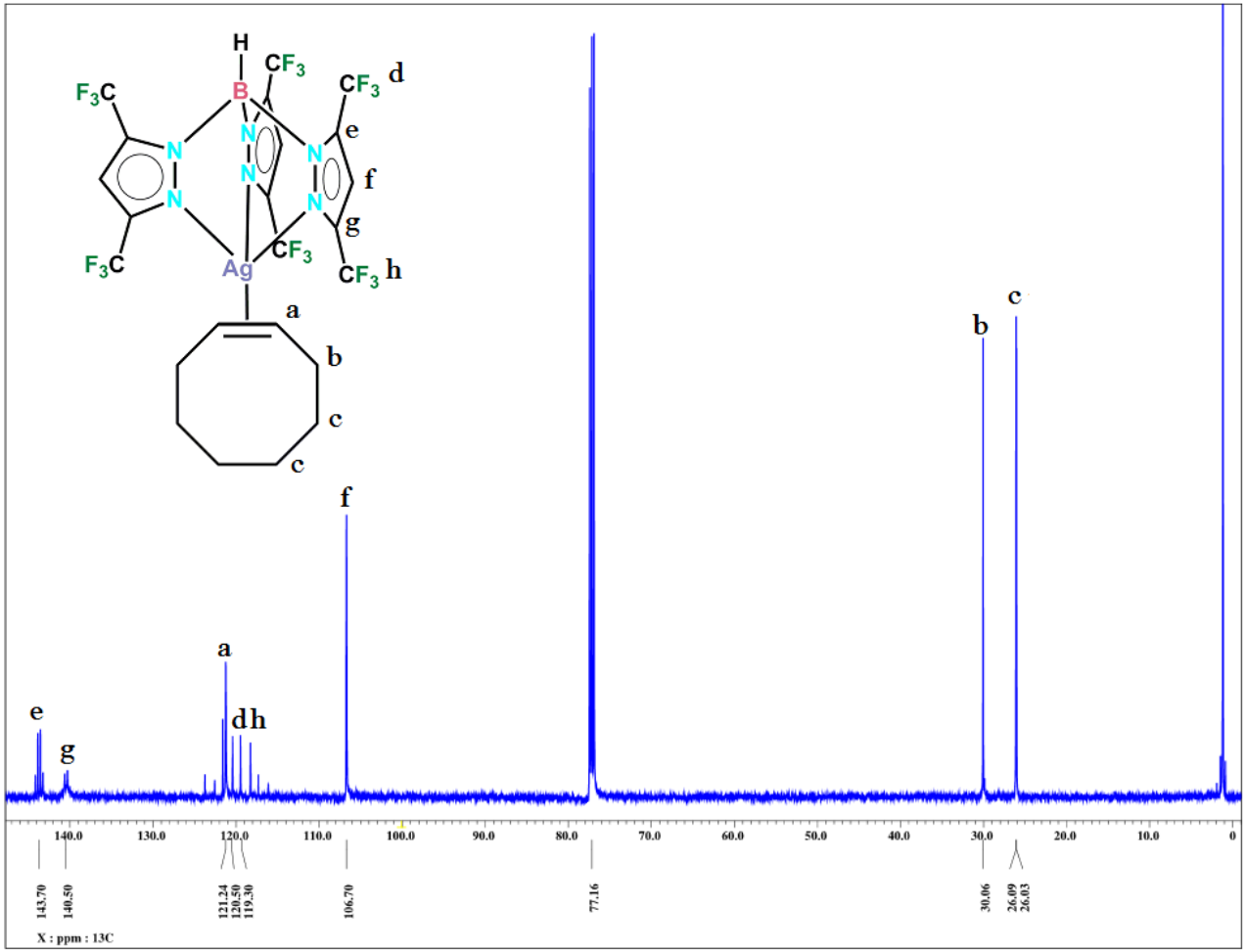

^{13}C NMR of [HB(3,5-(CF$_3$)$_2$Pz)$_3$]Ag(*c*-COE) in CDCl$_3$

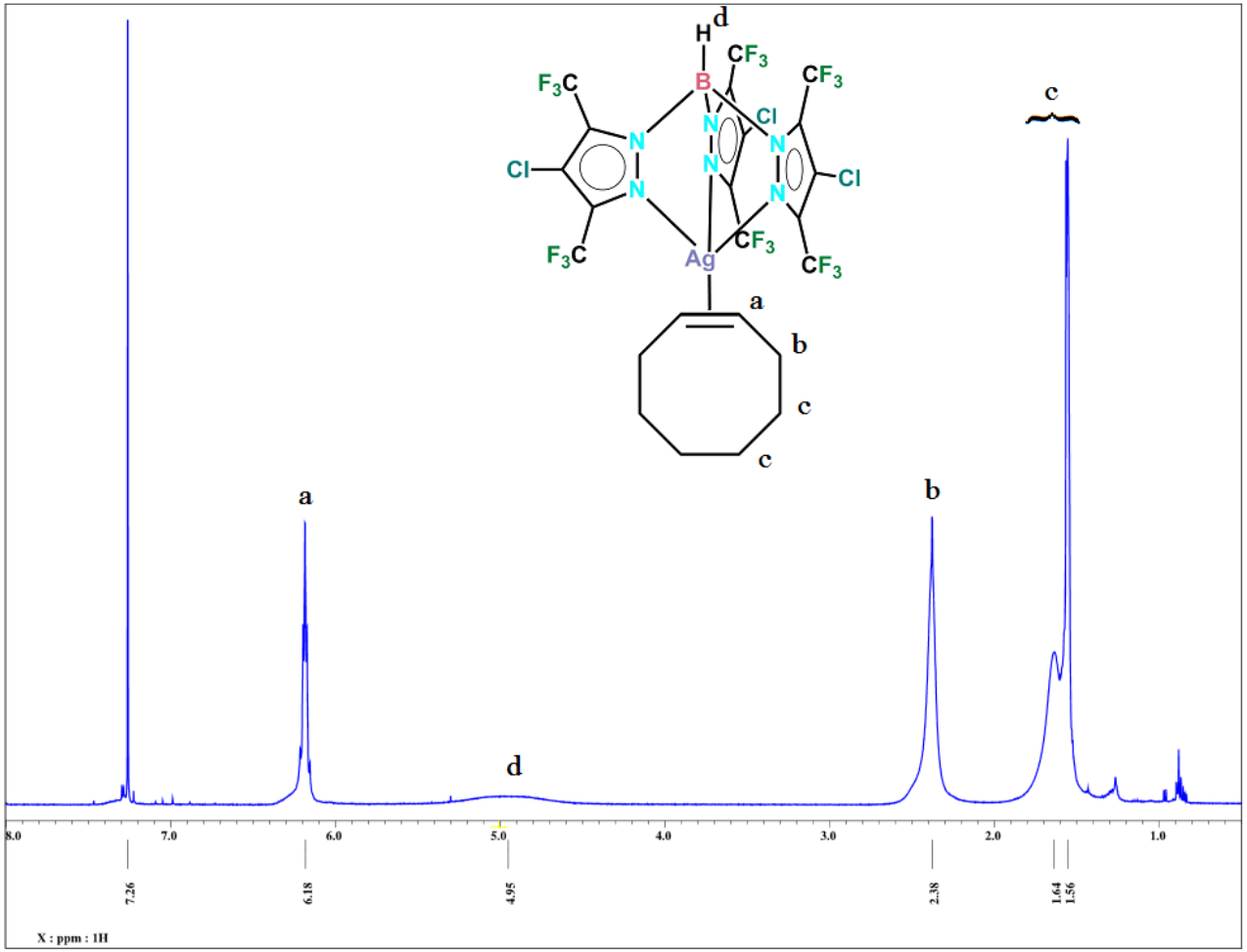

^{1}H NMR of [HB(4-Cl-3,5-$(CF_3)_2$Pz)$_3$]Ag(*c*-COE) in $CDCl_3$

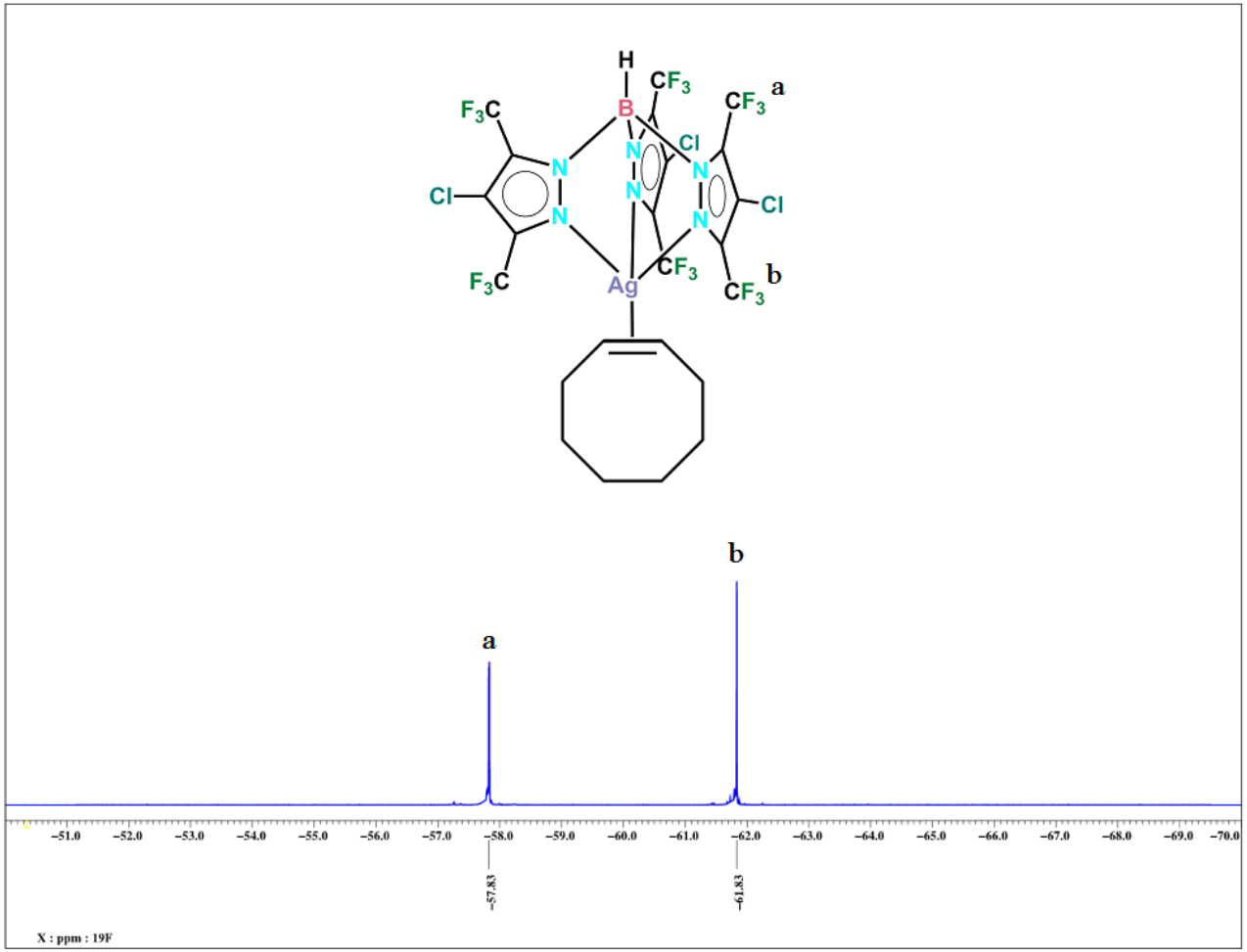

^{19}F NMR of [HB(4-Cl-3,5-$(CF_3)_2$Pz)$_3$]Ag(*c*-COE) in $CDCl_3$

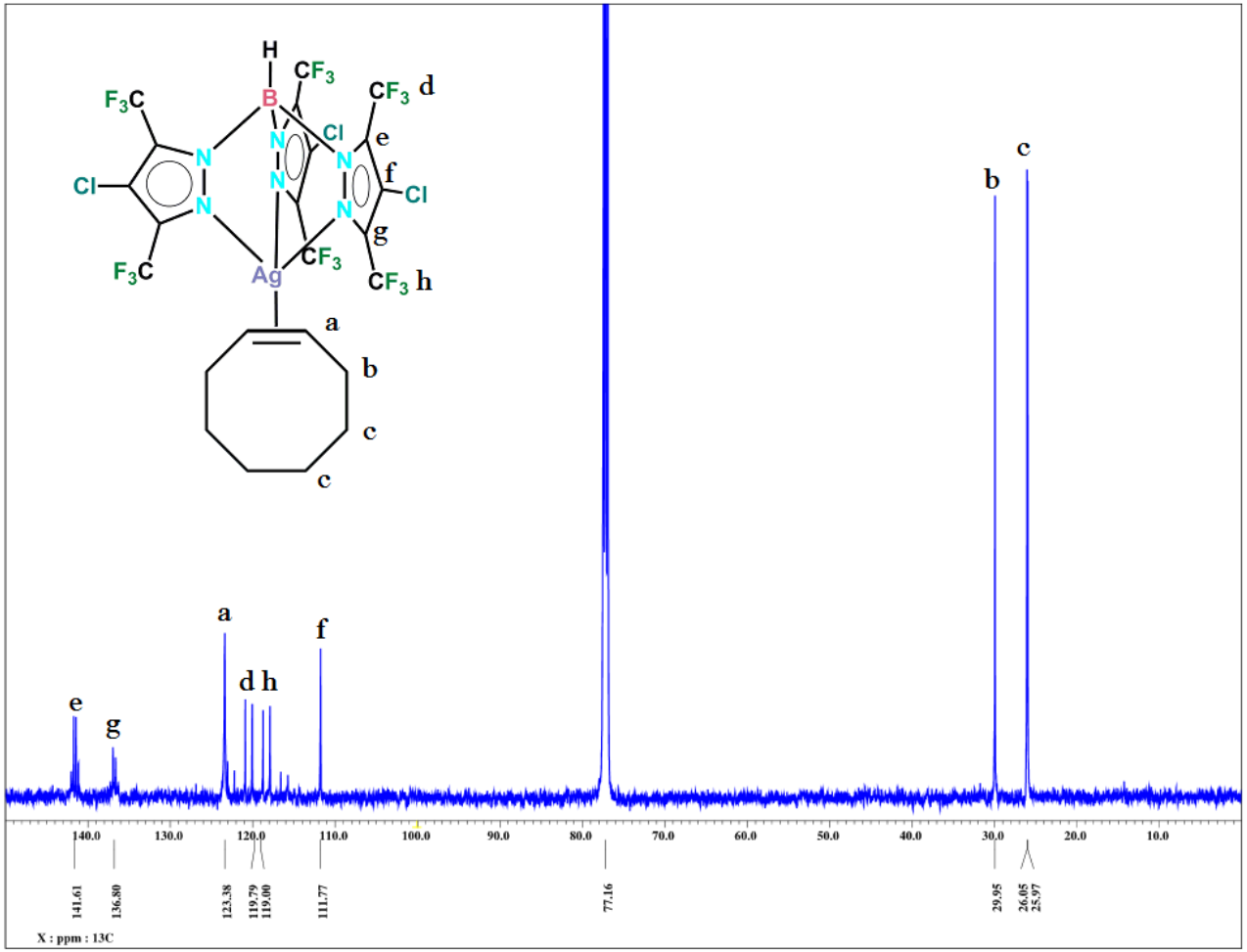

^{13}C NMR of [HB(4-Cl-3,5-(CF$_3$)$_2$Pz)$_3$]Ag(*c*-COE) in CDCl$_3$

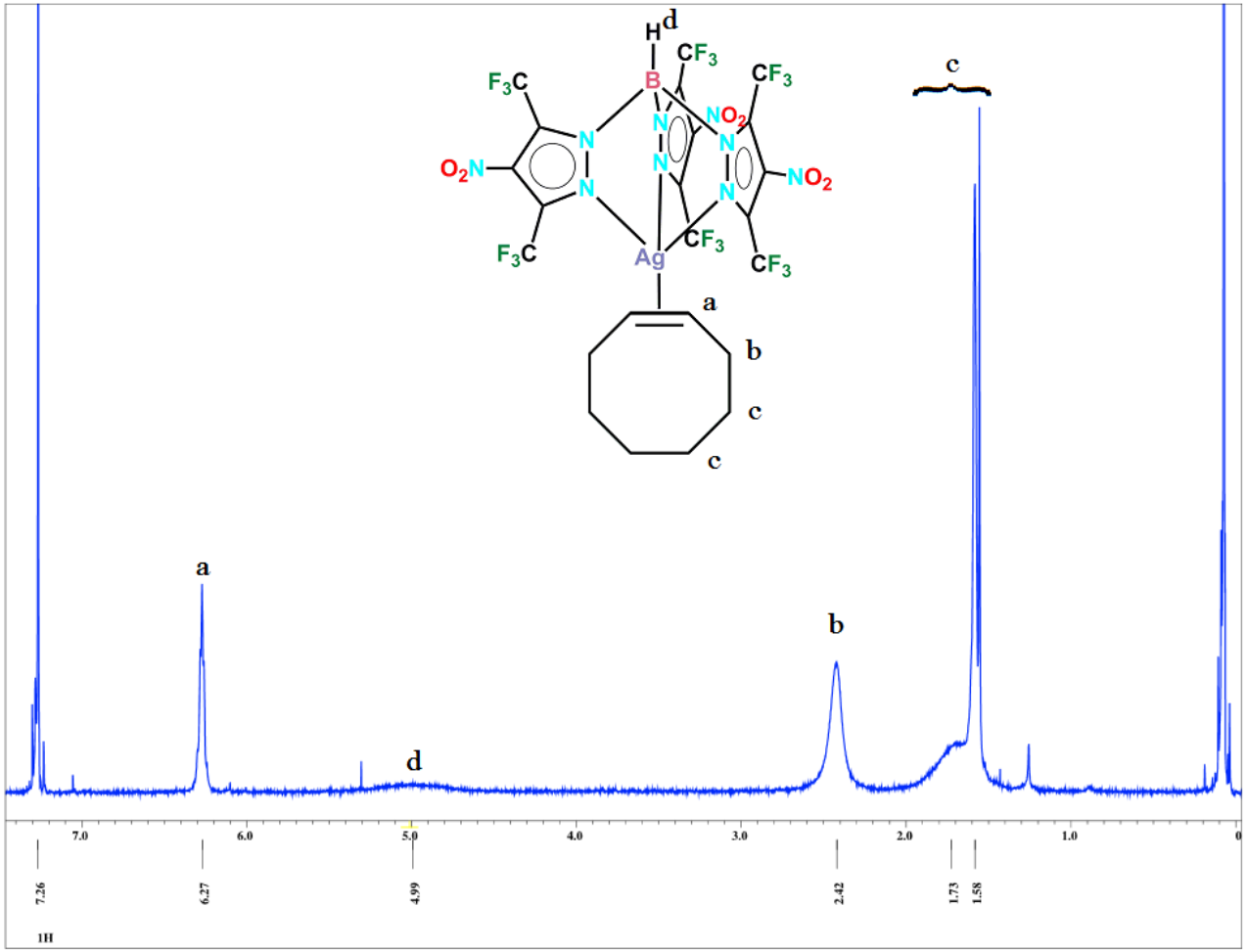

^{1}H NMR of [HB(4-NO_2-3,5-$(CF_3)_2$Pz)$_3$]Ag(*c*-COE) in $CDCl_3$

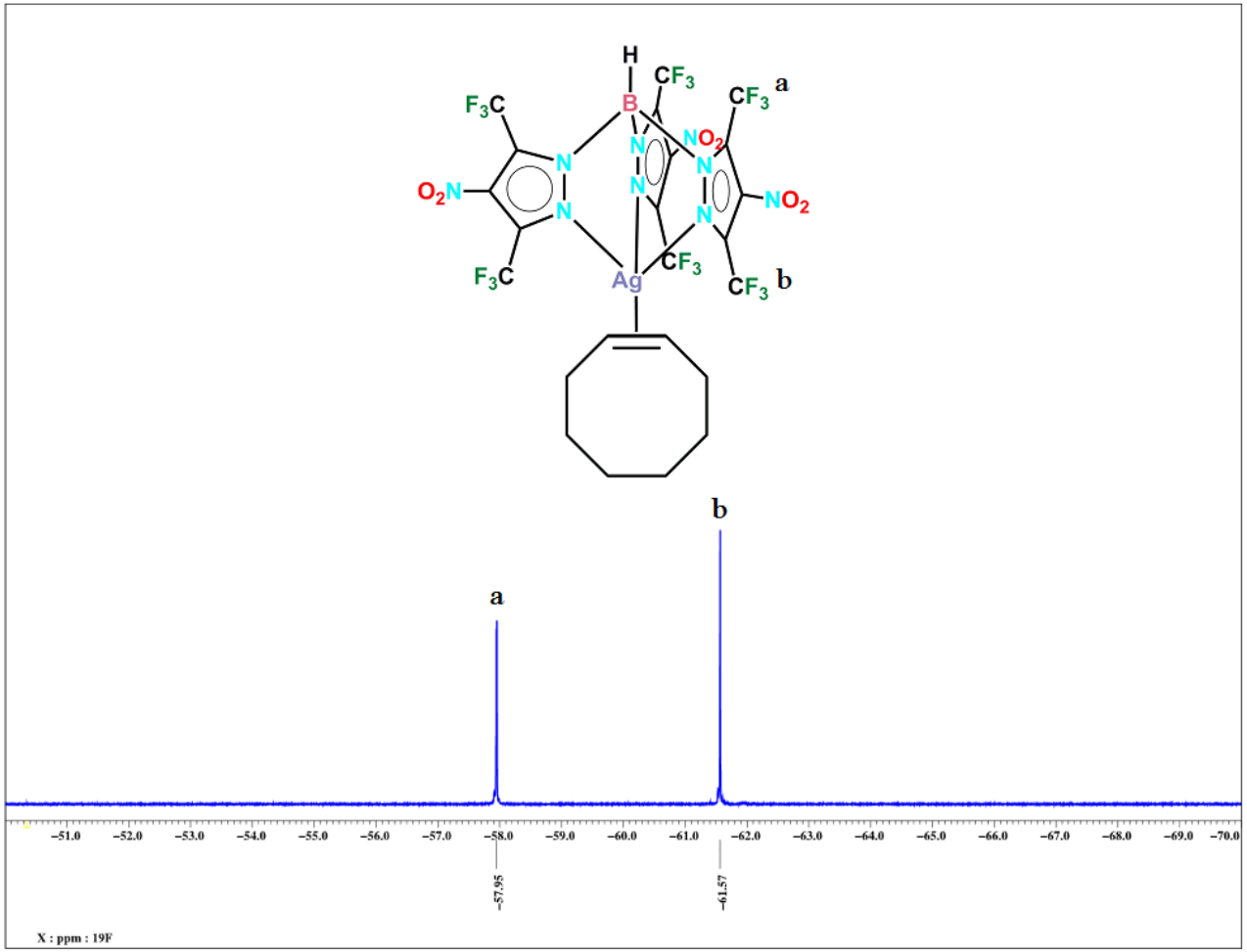

^{19}F NMR of [HB(4-NO_2-3,5-$(CF_3)_2$Pz)$_3$]Ag(*c*-COE) in $CDCl_3$

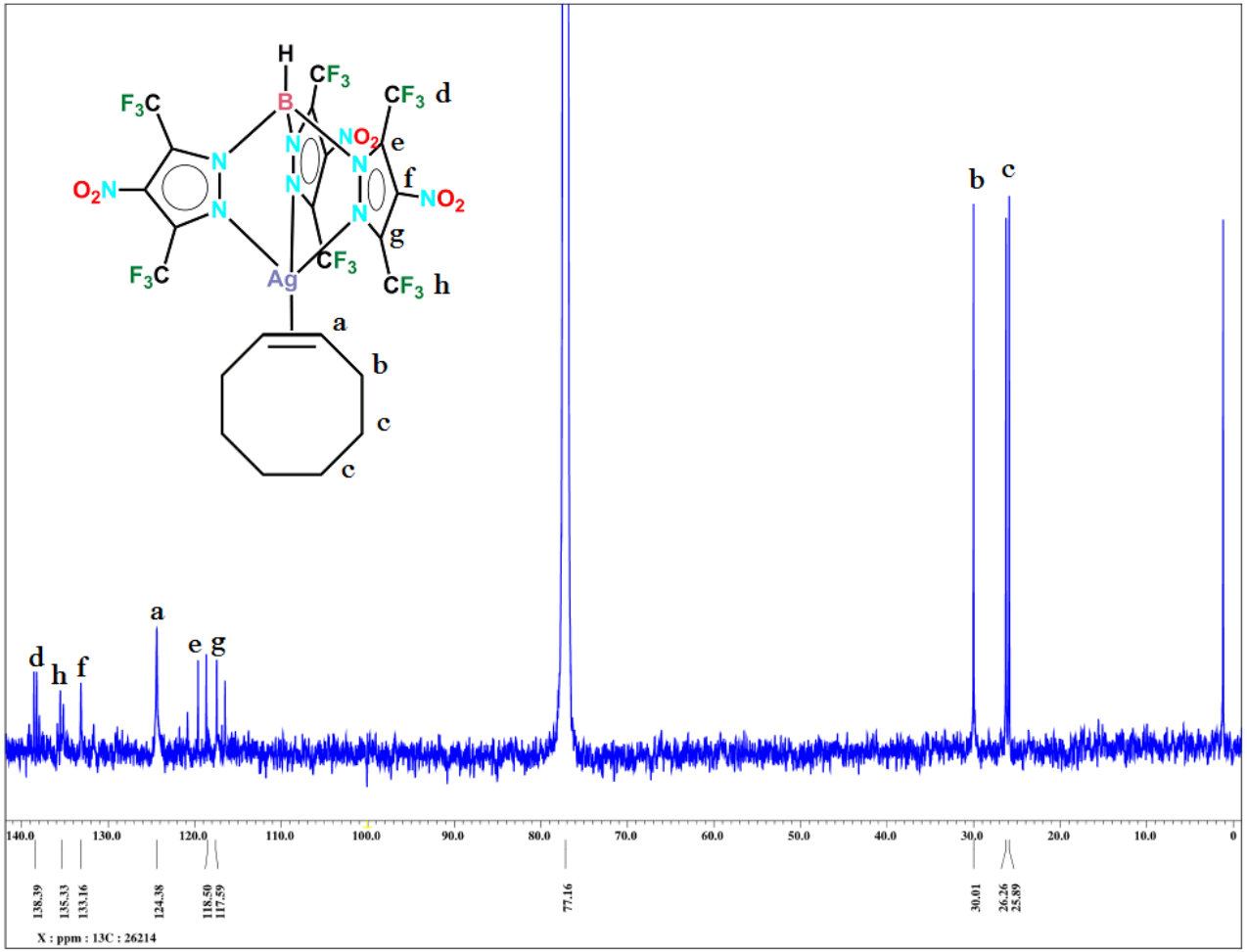

^{13}C NMR of [HB(4-NO_2-3,5-$(CF_3)_2$Pz)$_3$]Ag(*c*-COE) in $CDCl_3$

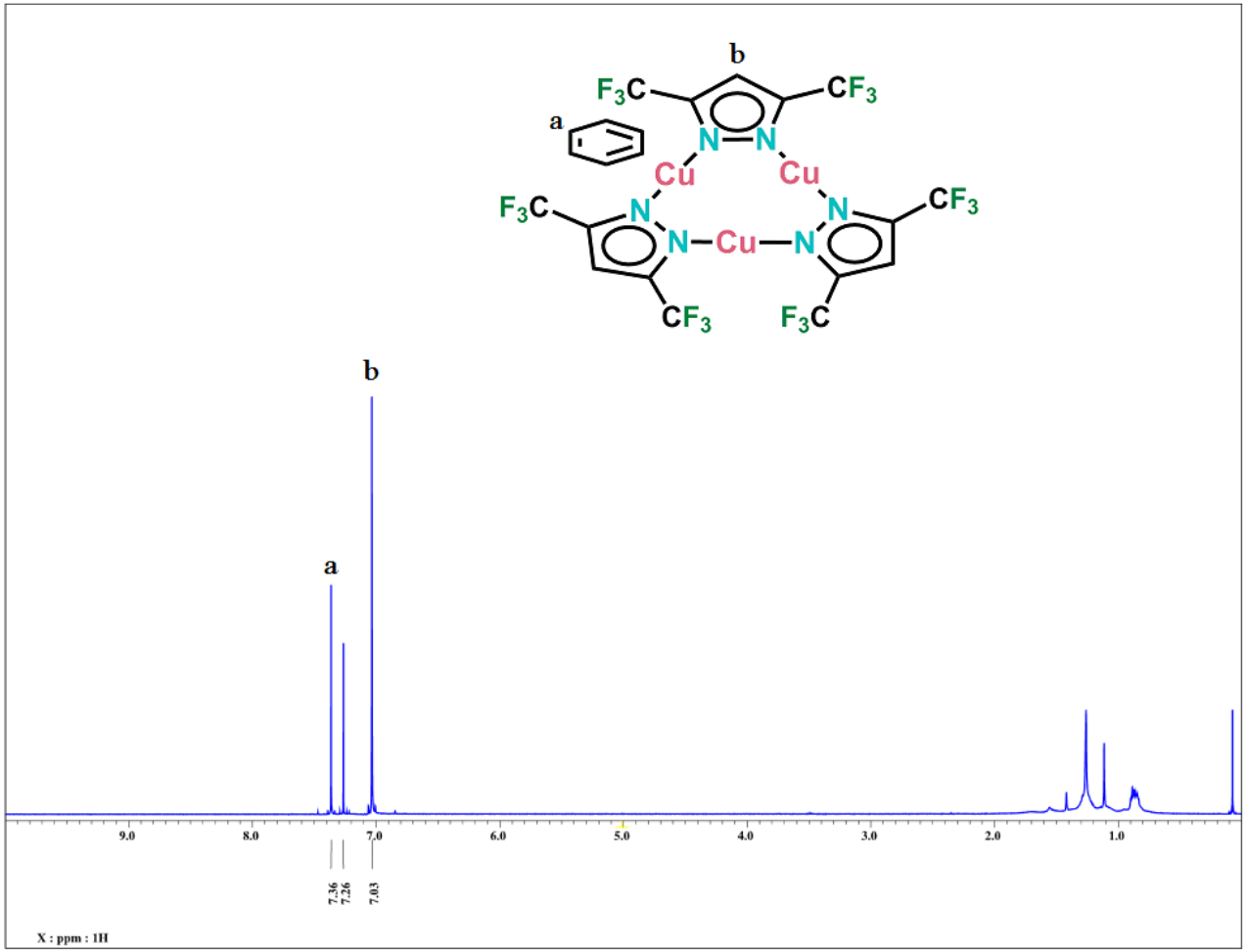

^{1}H NMR of **{[Bz][Cu$_3$]$_2$}$_\infty$** in $CDCl_3$

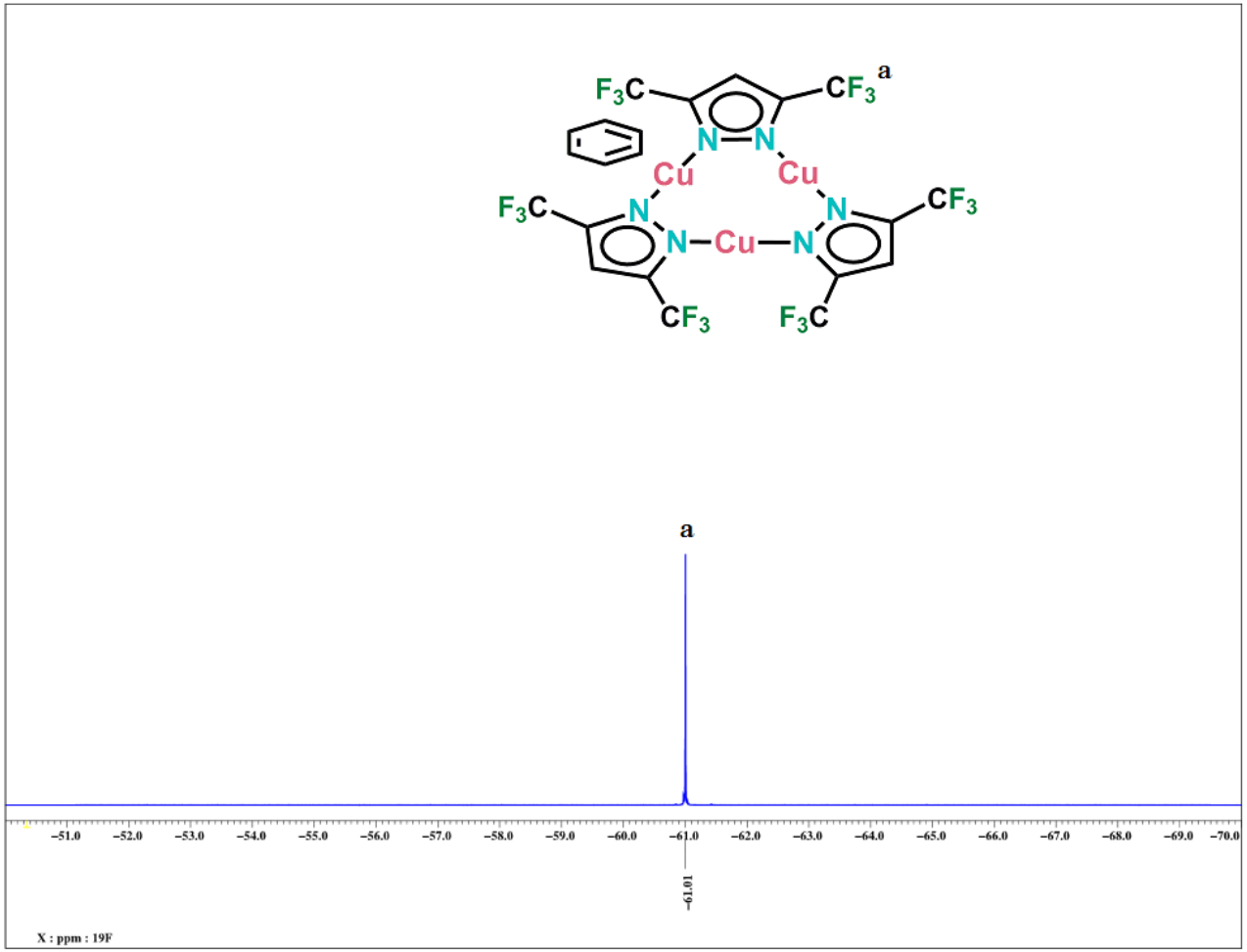

^{19}F NMR of **{[Bz][Cu$_3$]$_2$}$_\infty$** in $CDCl_3$

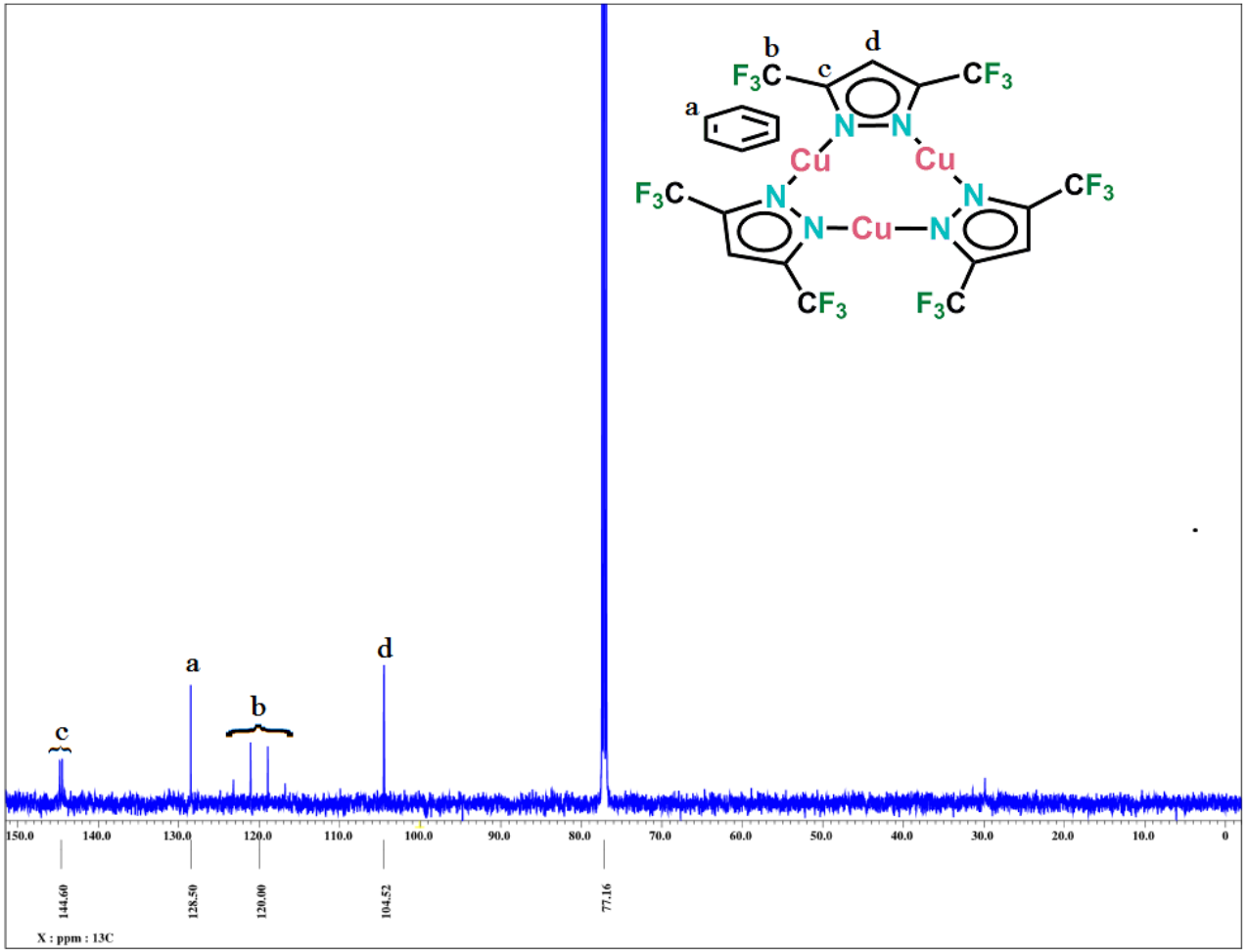

^{13}C NMR of **{[Bz][Cu$_3$]$_2$}$_\infty$** in $CDCl_3$

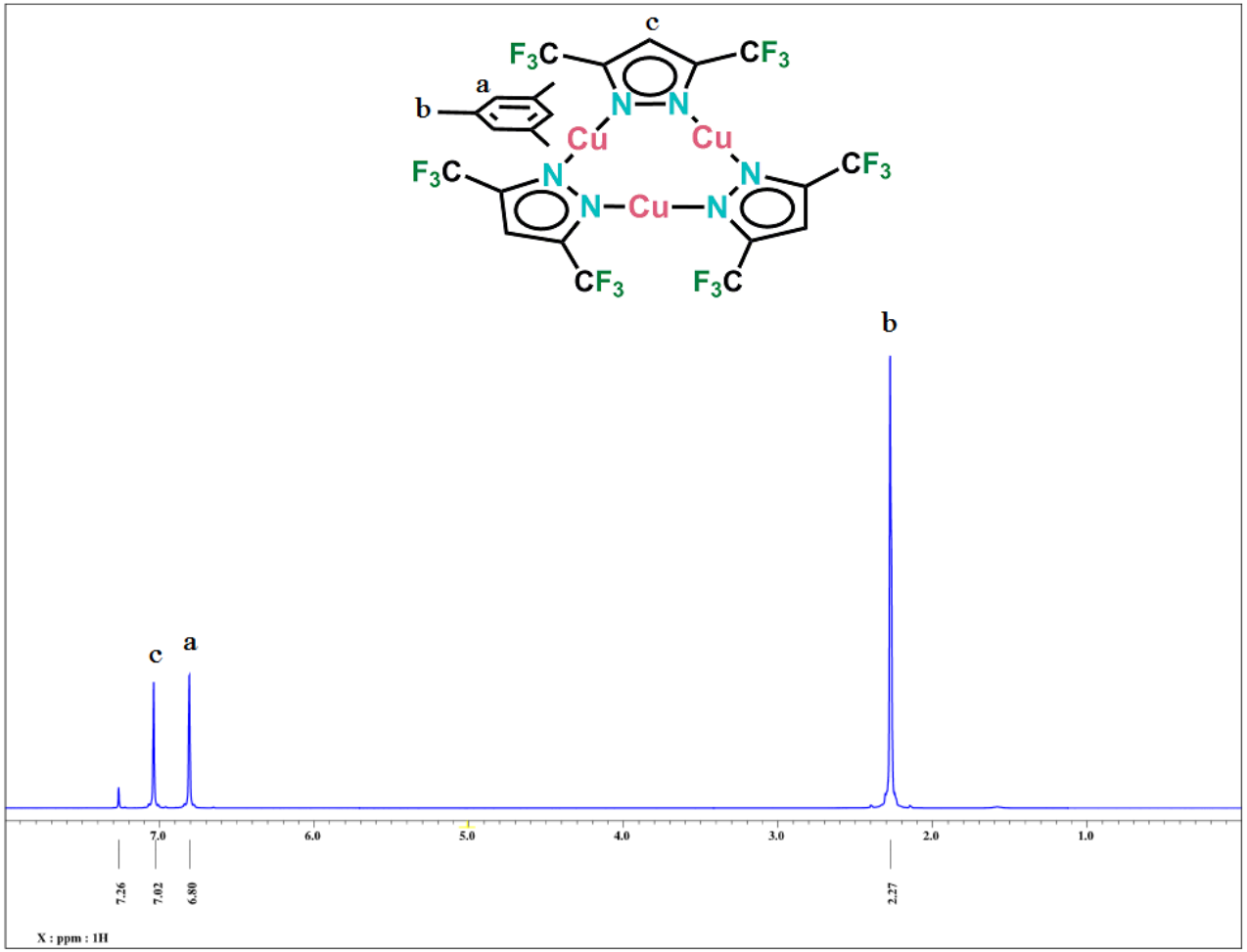

^{1}H NMR of **{[Mes][Cu$_3$]}$_\infty$** in $CDCl_3$

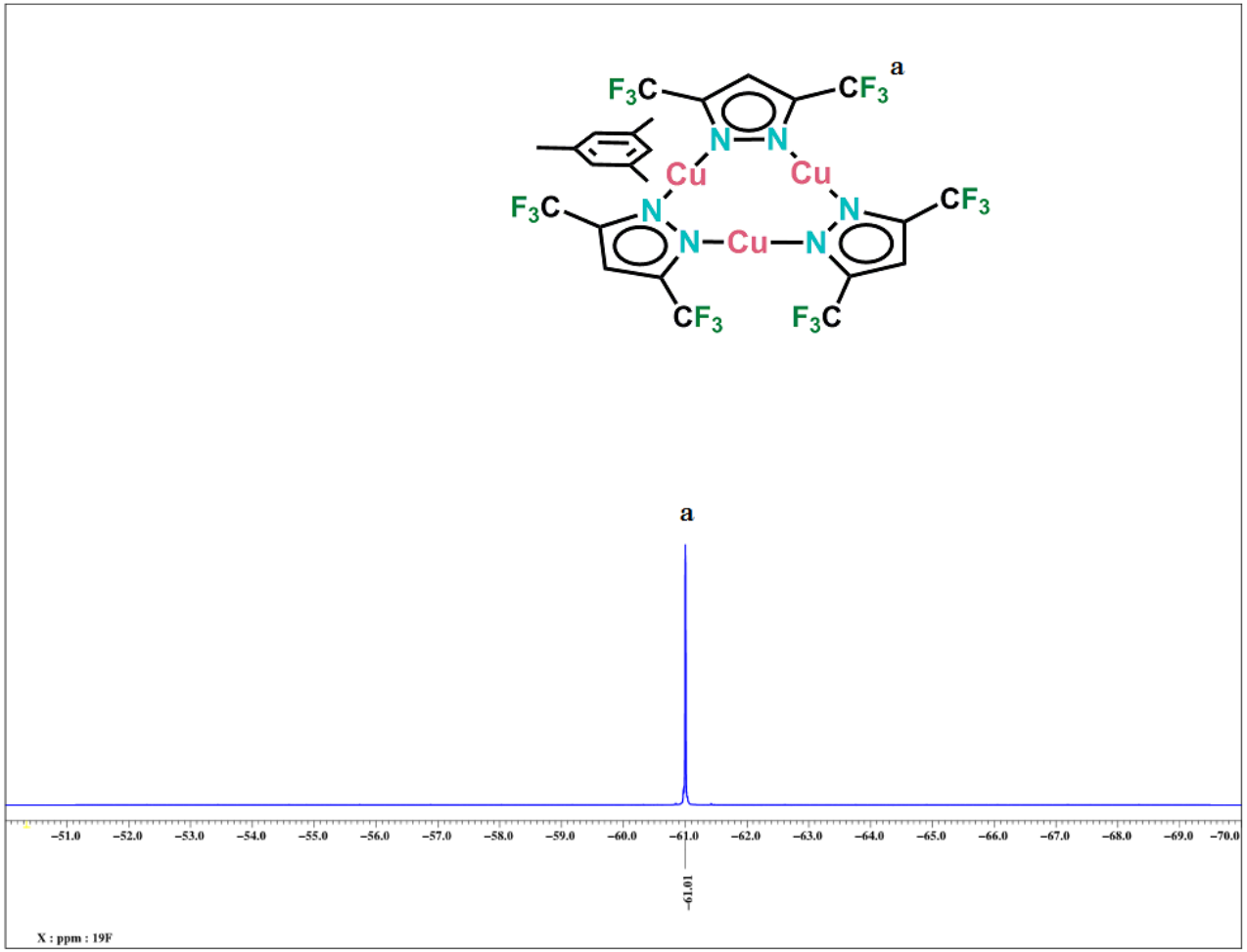

^{19}F NMR of **{[Mes][Cu$_3$]}$_\infty$** in $CDCl_3$

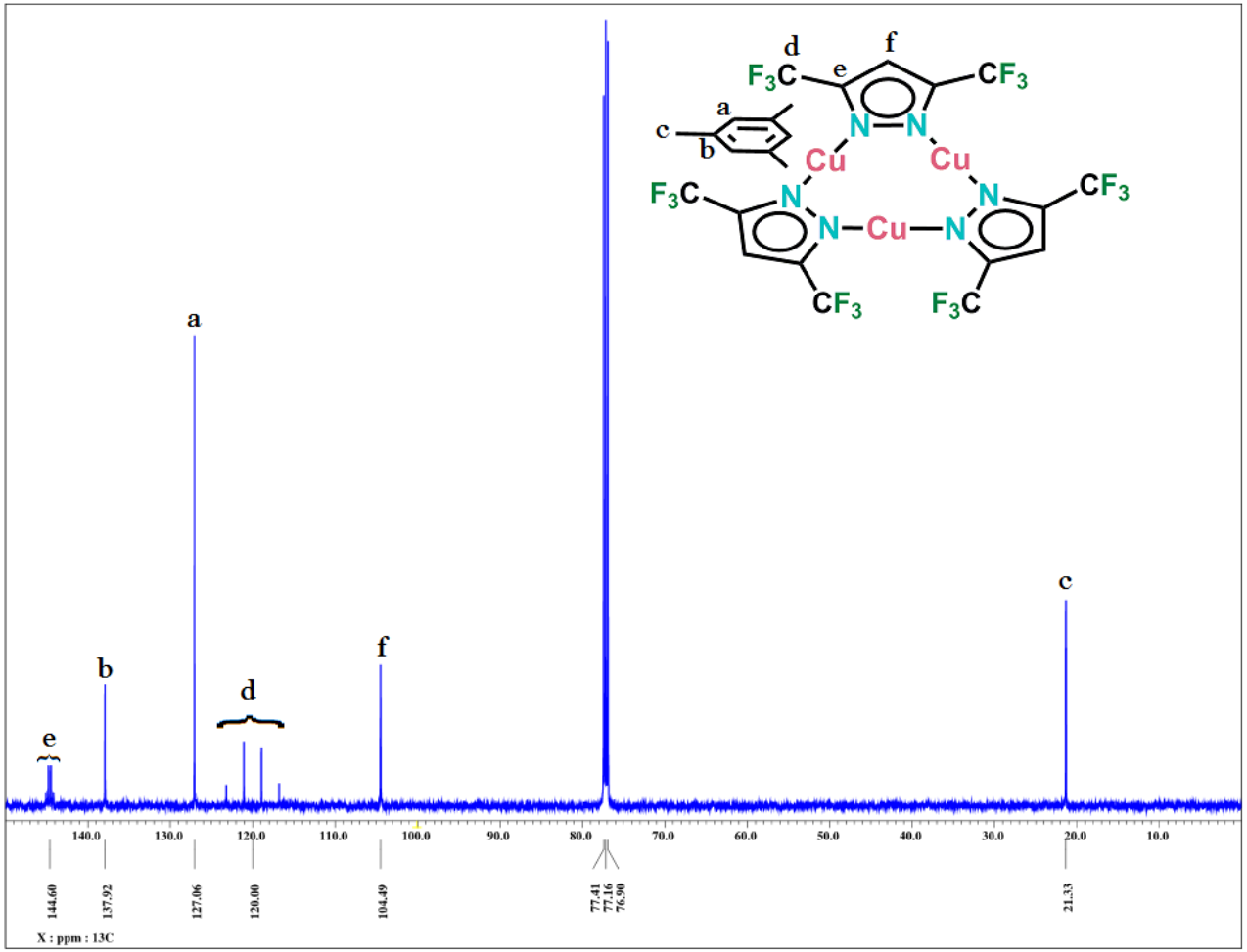

^{13}C NMR of **{[Mes][Cu$_3$]}$_\infty$** in $CDCl_3$

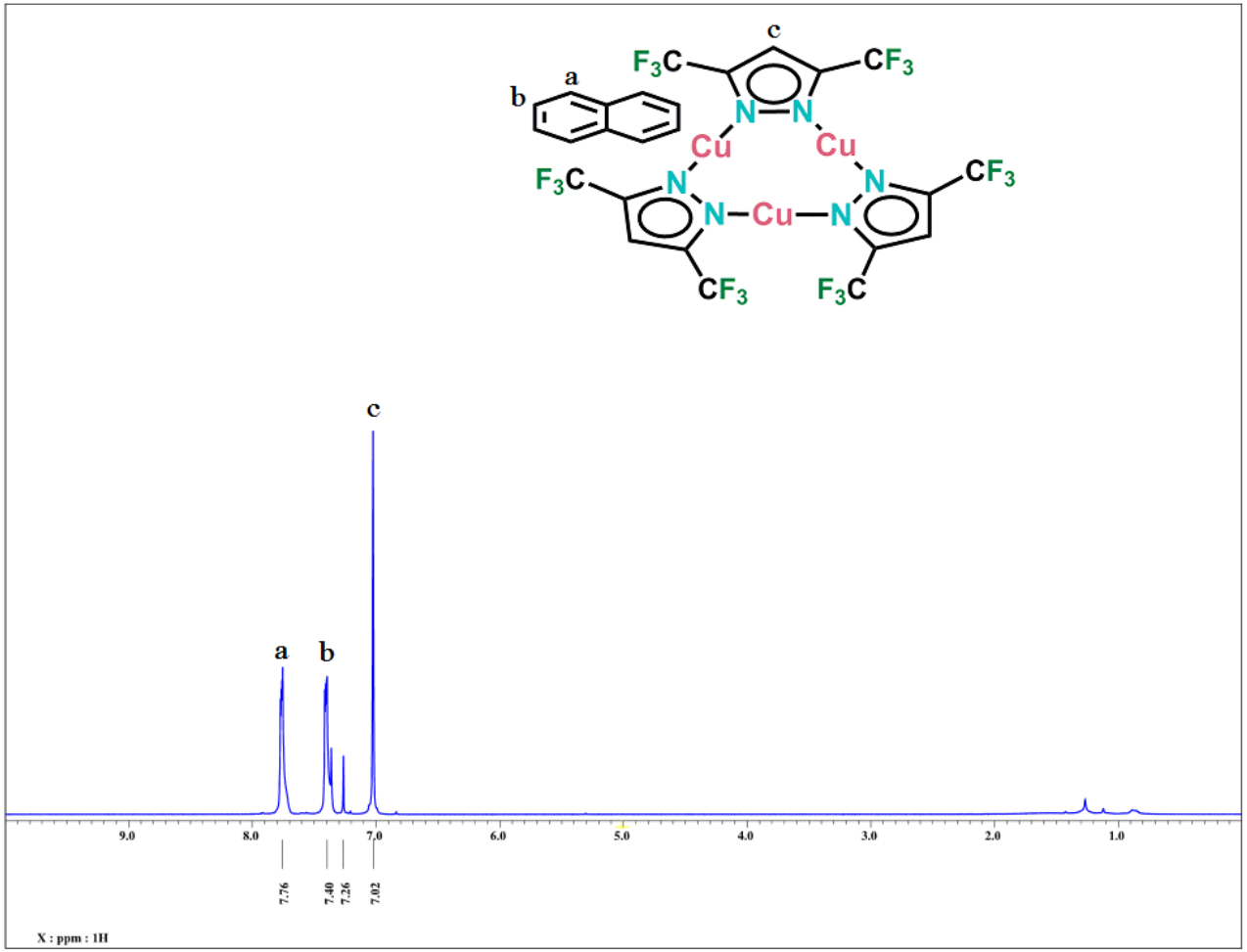

^{1}H NMR of **{[Nap][Cu$_3$]}$_\infty$** in $CDCl_3$

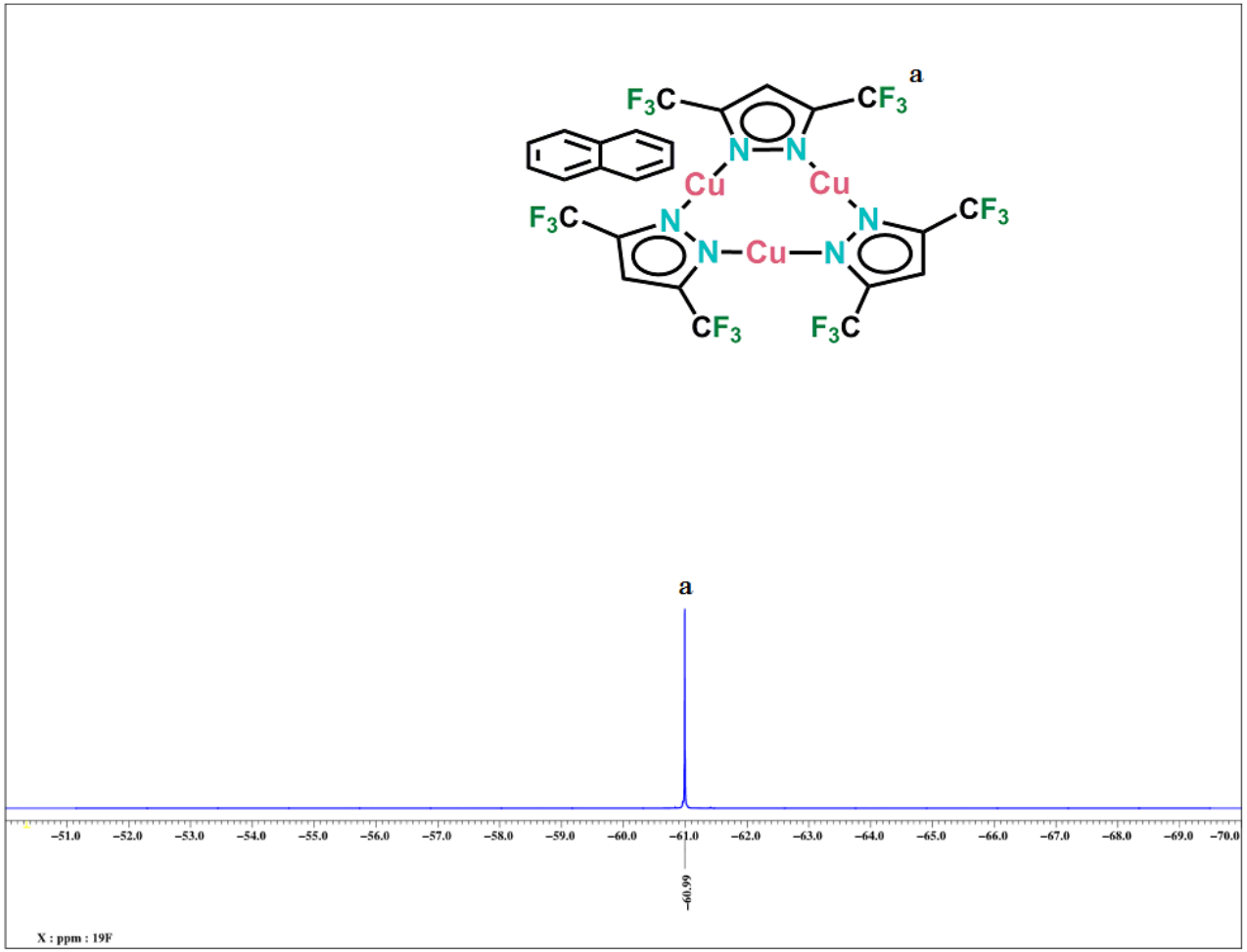

^{19}F NMR of **{[Nap][Cu$_3$]}$_\infty$** in $CDCl_3$

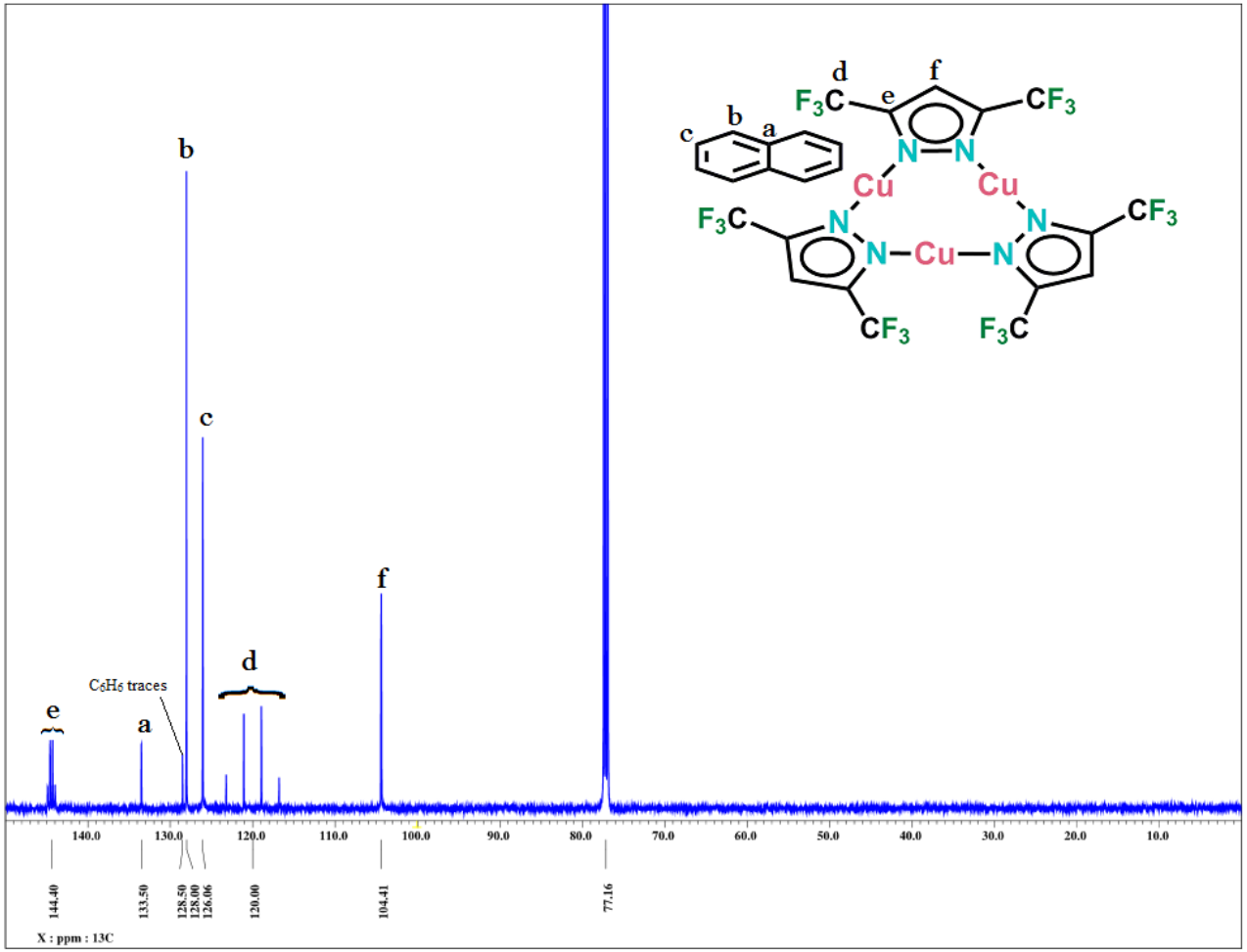

^{13}C NMR of **{[Nap][Cu$_3$]}$_\infty$** in $CDCl_3$

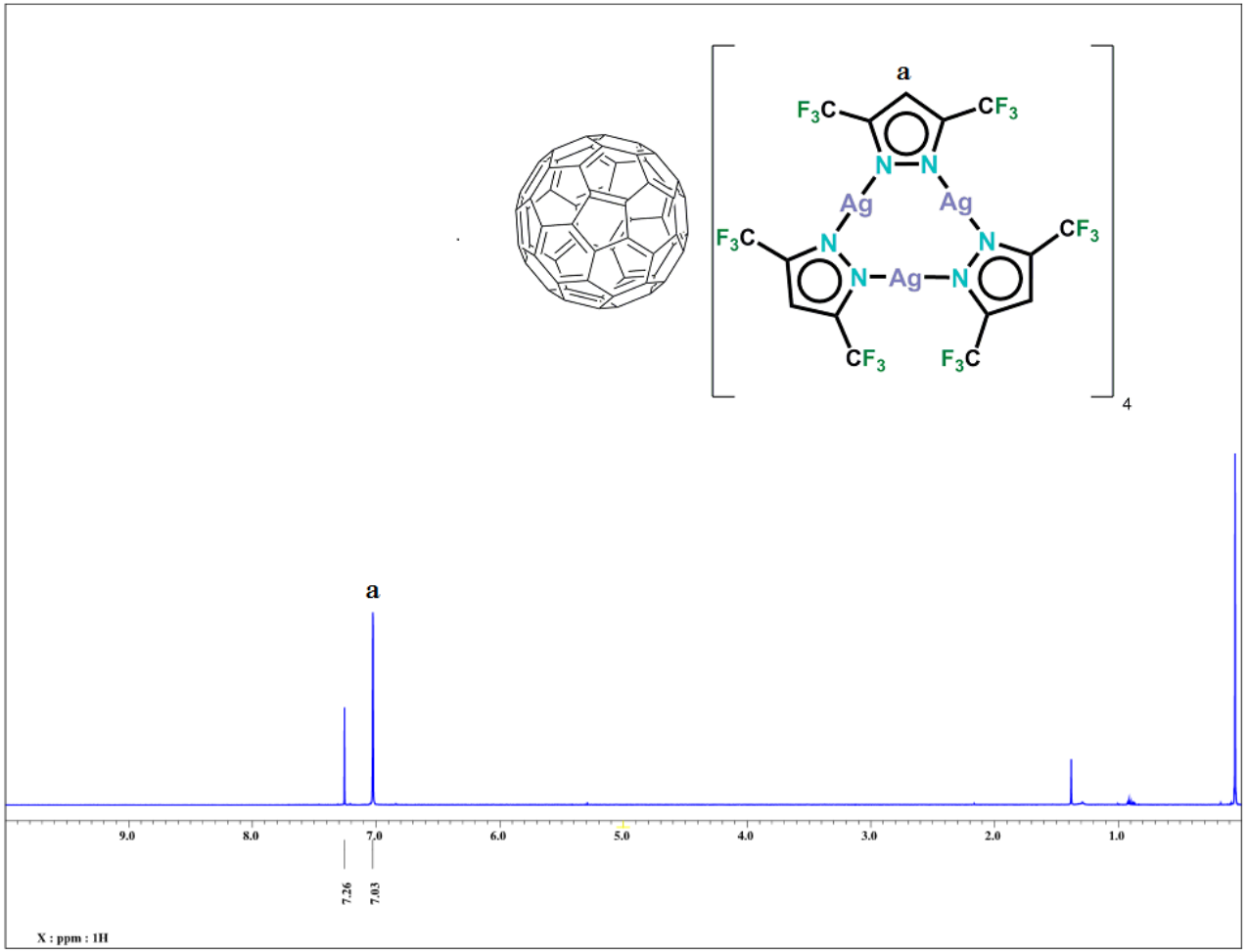

^{1}H NMR of **$C_{60}[Ag_3]_4$** in 2:1 mixture of CS_2:$CDCl_3$

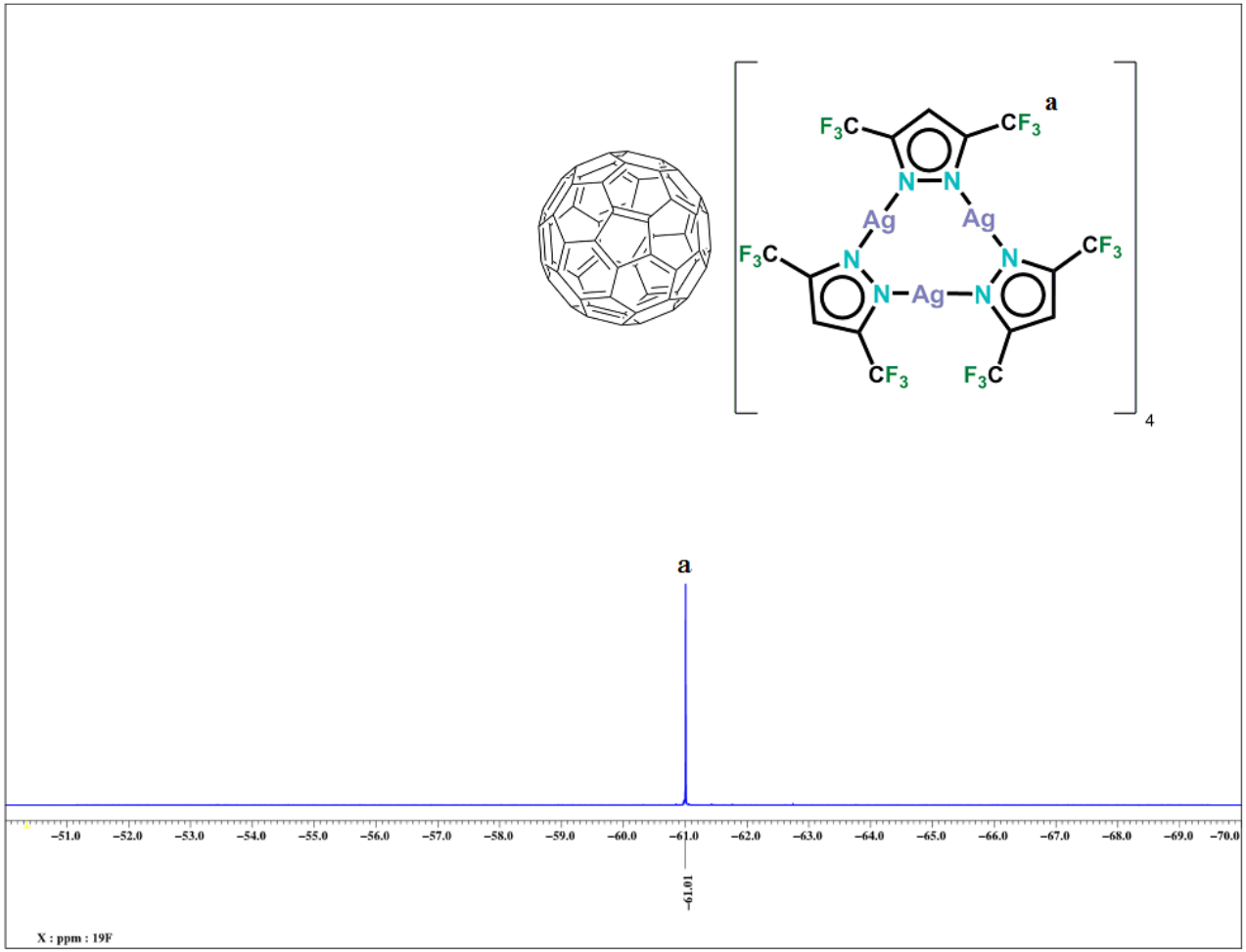

^{19}F NMR of **$C_{60}[Ag_3]_4$** in 2:1 mixture of CS_2:$CDCl_3$

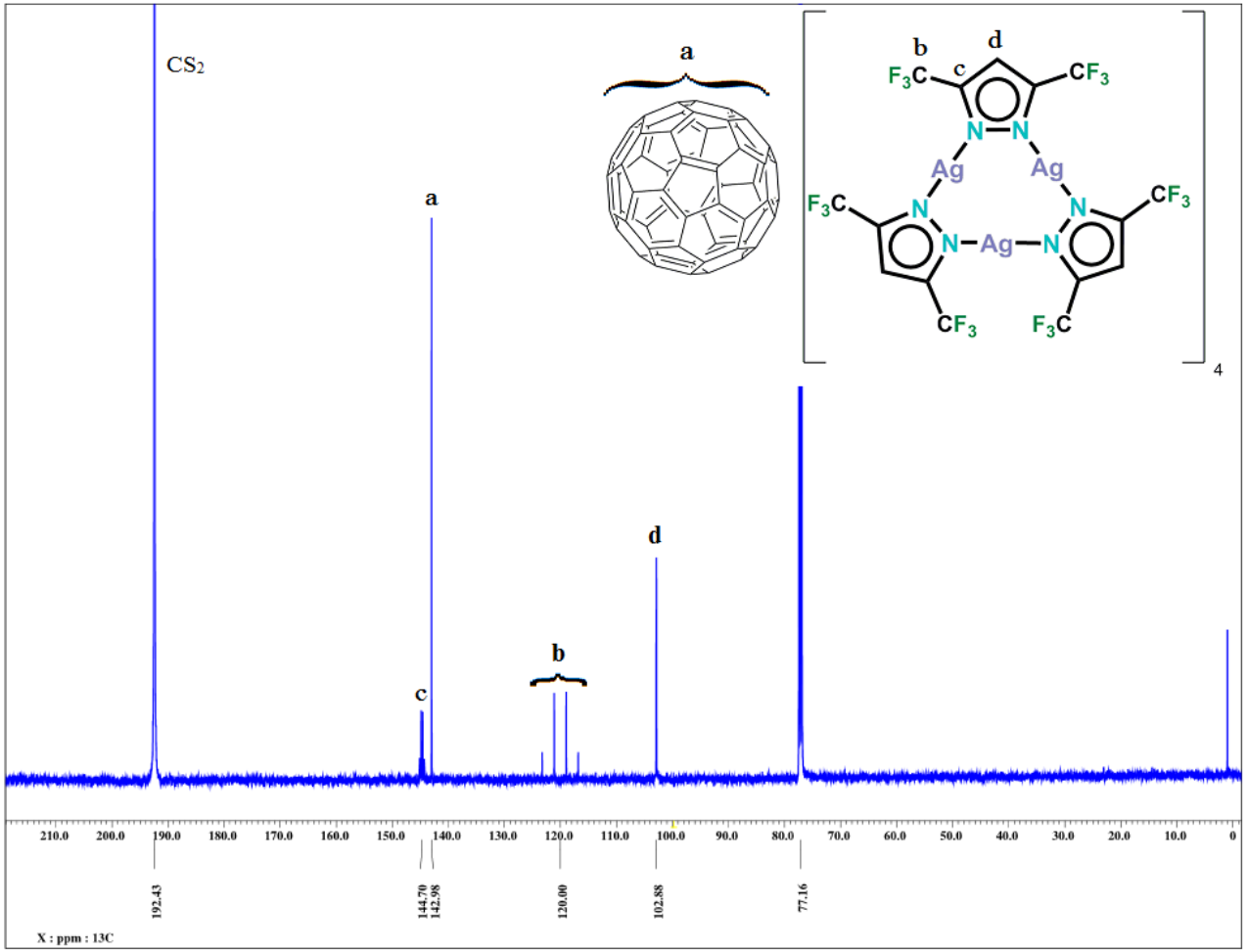

^{13}C NMR of **$C_{60}[Ag_3]_4$** in 2:1 mixture of CS_2:$CDCl_3$

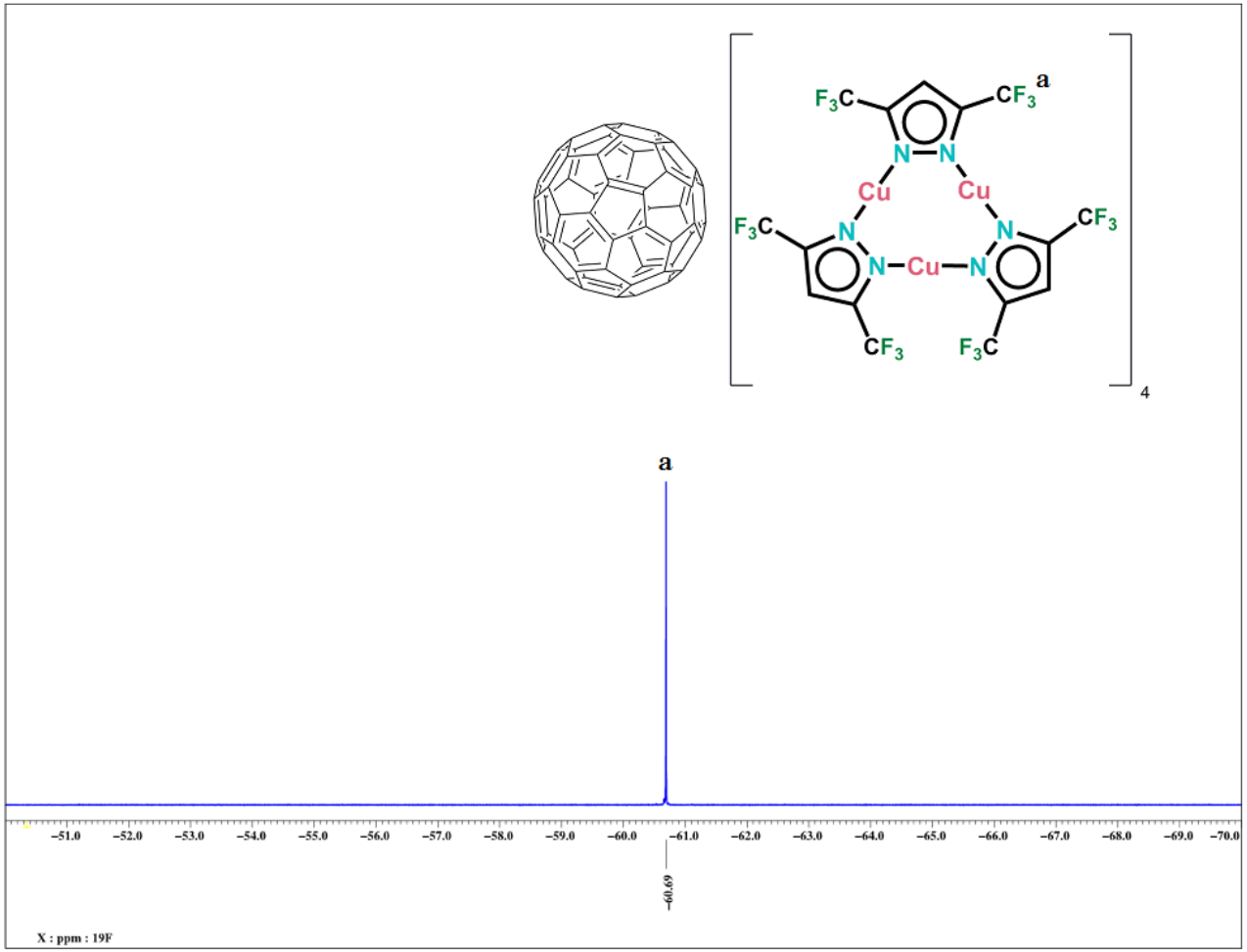

^{19}F NMR of **$C_{60}[Cu_3]_4$** in 2:1 mixture of CS_2:$CDCl_3$

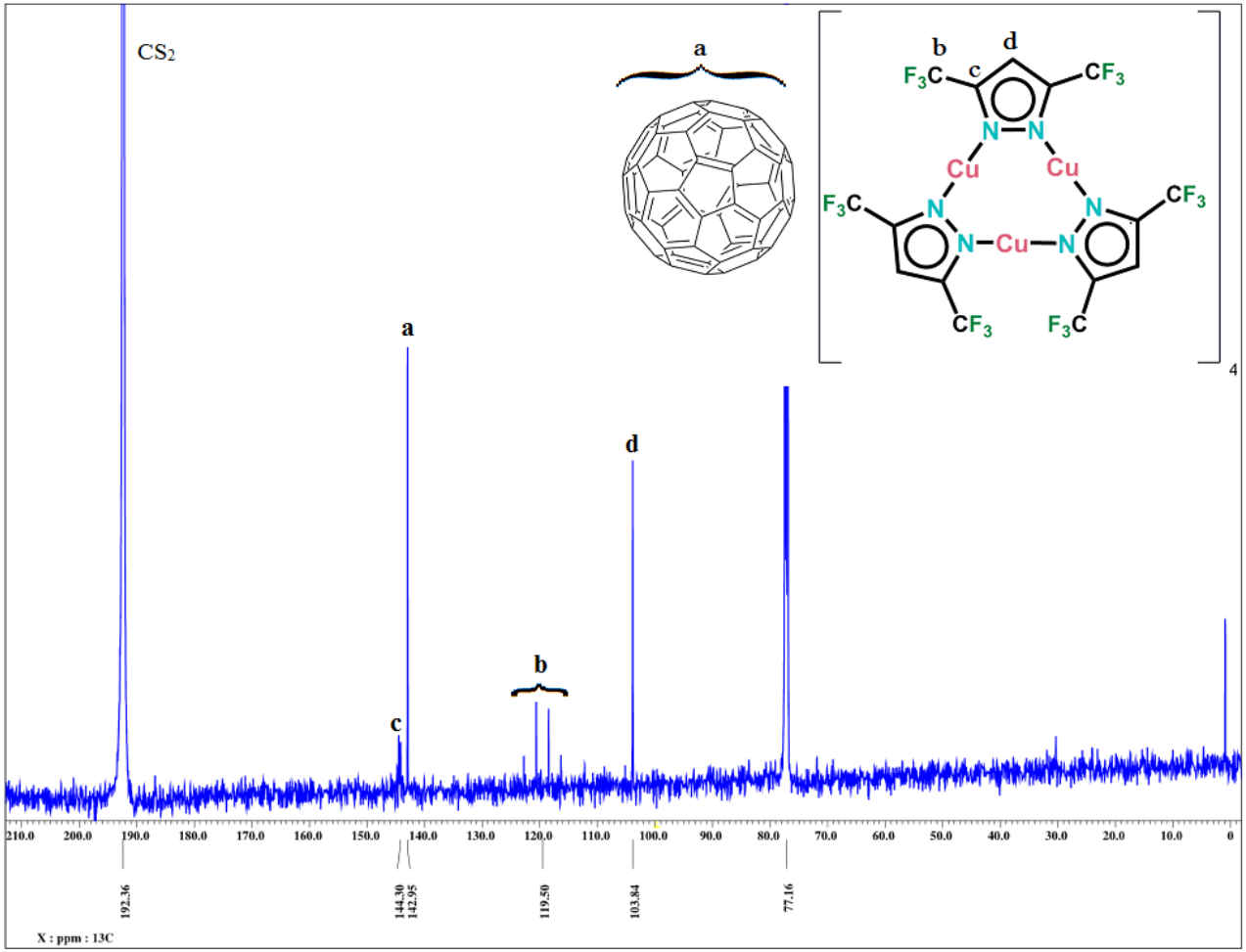

^{13}C NMR of **$C_{60}[Cu_3]_4$** in 2:1 mixture of CS_2:$CDCl_3$

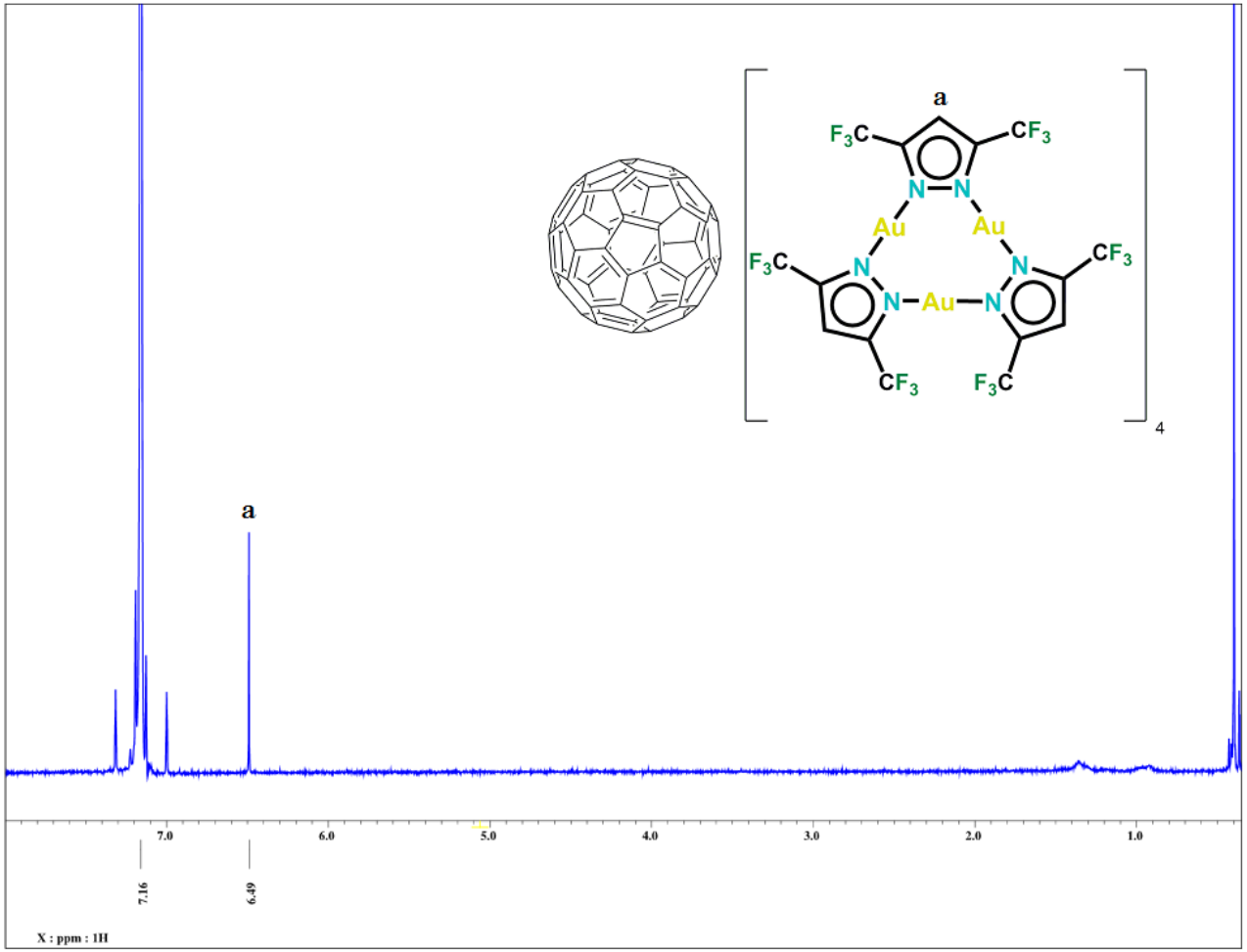

^{1}H NMR of **$C_{60}[Au_3]_4$** in C_6D_6

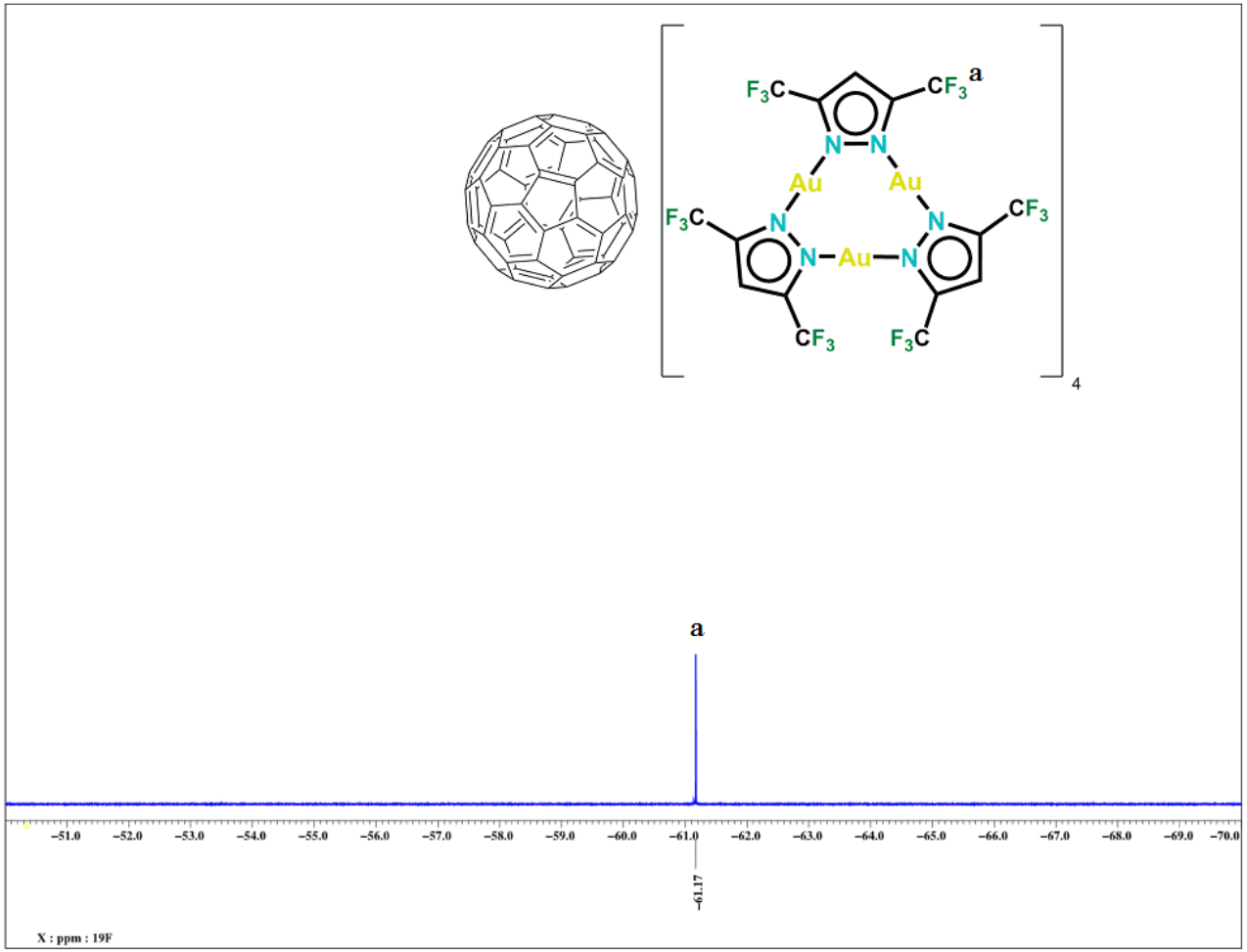

^{19}F NMR of **$C_{60}[Au_3]_4$** in C_6D_6

References

(1) Pettinari, C. *Scorpionates II: Chelating Borate Ligands*; Imperial College Press: London, **2008**.

(2) Trofimenko, S. *J. Am. Chem. Soc.* **1967**, *89*, 3904.

(3) Trofimenko, S. *Chem. Rev.* **1993**, *93*, 943.

(4) Dias, H. V. R.; Jin, W. *J. Am. Chem. Soc.* **1995**, *117*, 11381.

(5) Dias, H. V. R.; Goh, T. K. H. H. *Polyhedron* **2004**, *23*, 273.

(6) Dias, H. V. R.; Wang, X.; Diyabalanage, H. V. K. *Inorg. Chem.* **2005**, *44*, 7322.

(7) Dias, H. V. R.; Kim, H.-J. *Organometallics* **1996**, *15*, 5374.

(8) Dias, H. V. R.; Wang, X. *Dalton Trans.* **2005**, 2985.

(9) Dias, H. V. R.; Jin, W.; Kim, H.-J.; Lu, H.-L. *Inorg. Chem.* **1996**, *35*, 2317.

(10) Dias, H. V. R.; Jin, W. *Inorg. Chem.* **1996**, *35*, 3687.

(11) Dias, H. V. R.; Wang, Z.; Jin, W. *Inorg. Chem.* **1997**, *36*, 6205.

(12) Dias, H. V. R.; Polach, S. A.; Goh, S.-K.; Archibong, E. F.; Marynick, D. S. *Inorg. Chem.* **2000**, *39*, 3894.

(13) Dias, H. V. R; Polach, S. A. *Inorg. Chem.* **2000**, *39*, 4676.

(14) Dias, H. V. R.; Polach, S. A.; Wang, Z. *J. Fluorine Chem.* **2000**, *103*, 163.

(15) Dias, H. V. R.; Browning, R. G.; Polach, S. A.; Diyabalanage, H. V. K.; Lovely, C. J. *J. Am. Chem. Soc.* **2003**, *125*, 9270.

(16) Dias, H. V. R.; Browning, R. G.; Richey, S. A.; Lovely, C. J. *Organometallics* **2004**, *23*, 1200.

(17) Dias, H. V. R.; Browning, R. G.; Richey, S. A.; Lovely, C. J. *Organometallics* **2005**, *24*, 5784.

(18) Lovely, C. J.; Browning, R. G.; Badarinarayana, V.; Dias, H. V. R. *Tetrahedron Lett.* **2005**, *46*, 2453.

(19) Dias, H. V. R.; Lovely, C. J. *Chem. Rev.* **2008**, *108*, 3223.

(20) Dias, H. V. R.; Wu, J. *Eur. J. Inorg. Chem.* **2008**, *2008*, 509.

(21) Kazi, A. B.; Dias, H. V. R.; Tekarli, S. M.; Morello, G. R.; Cundari, T. R. *Organometallics* **2009**, *28*, 1826.

(22) Dias, H. V. R.; Lu, H.-L. *Inorg. Chem.* **1995**, *34*, 5380.

(23) Dias, H. V. R.; Lu, H.-L.; Kim, H.-J.; Polach, S. A.; Goh, T. K. H. H.; Browning, R. G.; Lovely, C. J. *Organometallics* **2002**, *21*, 1466.

(24) Dias, H. V. R.; Wu, J. *Angew. Chem. Int. Ed.* **2007**, *46*, 7814.

(25) Fujisawa, K.; Ono, T.; Ishikawa, Y.; Amir, N.; Miyashita, Y.; Okamoto, K.-i.; Lehnert, N. *Inorg. Chem.* **2006**, *45*, 1698.

(26) Grimm, D. T.; Bartmess, J. E. *J. Am. Chem. Soc.* **1992**, *114*, 1227.

(27) Dias, H. V. R.; Kim, H.-J.; Lu, H.-L.; Rajeshwar, K.; de Tacconi, N. R.; Derecskei-Kovacs, A.; Marynick, D. S. *Organometallics* **1996**, *15*, 2994.

(28) Schneider, J. L.; Carrier, S. M.; Ruggiero, C. E.; Young, V. G.; Tolman, W. B. *J. Am. Chem. Soc.* **1998**, *120*, 11408.

(29) Wu, J., Ph.D. The University of Texas at Arlington, 2010.

(30) Huber, K. P. H., G. *Molecular Spectra and Molecular Structure IV: Constants of Diatomic Molecules* Van Nostrand Reinhold Co: New York **1979**.

(31) Rangan, K.; Fianchini, M.; Singh, S.; Rasika Dias, H. V. *Inorg. Chim. Acta* **2009**, *362*, 4347.

(32) Braga, A. A. C.; Maseras, F.; Urbano, J.; Caballero, A.; Díaz-Requejo, M. M.; Pérez, P. J. *Organometallics* **2006**, *25*, 5292.

(33) Jayaratna, N. B.; Gerus, I. I.; Mironets, R. V.; Mykhailiuk, P. K.; Yousufuddin, M.; Dias, H. V. R. *Inorg. Chem.* **2013**, *52*, 1691.

(34) Pettinari, C. *Scorpionates II: Chelating Borate Ligands*; Imperial College Press: London, 2008.

(35) Dias, H. V. R.; Lovely, C. J. *Chem. Rev.* **2008**, *108*, 3223.

(36) Santini, C.; Pellei, M.; Lobbia, G. G.; Papini, G. *Mini-Rev. Org. Chem.* **2010**, *7*, 84.

(37) Rangan, K.; Fianchini, M.; Singh, S.; Dias, H. V. R. *Inorg. Chim. Acta* **2009**, *362*, 4347.

(38) Dias, H. V. R.; Browning, R. G.; Richey, S. A.; Lovely, C. J. *Organometallics* **2004**, *23*, 1200.

(39) Dias, H. V. R.; Browning, R. G.; Polach, S. A.; Diyabalanage, H. V. K.; Lovely, C. J. *J. Am. Chem. Soc.* **2003**, *125*, 9270.

(40) Gerus, I. I.; Mironetz, R. X.; Kondratov, I. S.; Bezdudny, A. V.; Dmytriv, Y. V.; Shishkin, O. V.; Starova, V. S.; Zaporozhets, O. A.; Tolmachev, A. A.; Mykhailiuk, P. K. *J. Org. Chem.* **2012**, *77*, 47.

(41) Maspero, A.; Giovenzana, G. B.; Monticelli, D.; Tagliapietra, S.; Palmisano, G.; Penoni, A. *J. Fluorine Chem.* **2012**, *139*, 53.

(42) Dias, H. V. R.; Wu, J. *Euro. J. Inorg. Chem.* **2008**, 509.

(43) Dias, H. V. R.; Wang, Z.; Jin, W. *Inorg. Chem.* **1997**, *36*, 6205.

(44) Lindeman, S. V.; Rathore, R.; Kochi, J. K. *Inorg. Chem.* **2000**, *39*, 5707.

(45) Dias, H. V. R.; Wu, J. *Angew. Chem., Int. Ed.* **2007**, *46*, 7814

(46) Kazi, A. B.; Dias, H. V. R.; Tekarli, S. M.; Morello, G. R.; Cundari, T. R. *Organometallics* **2009**, *28*, 1826.

(47) Reisinger, A.; Trapp, N.; Knapp, C.; Himmel, D.; Breher, F.; Ruegger, H.; Krossing, I. *Chem.--Eur. J.* **2009**, *15*, 9505.

(48) Schaub, T.; Radius, U. *Chem.--Eur. J.* **2005**, *11*, 5024.

(49) Kou, X.; Dias, H. V. R. *Dalton Trans.* **2009**, 7529.

(50) Thompson, J. S.; Harlow, R. L.; Whitney, J. F. *J. Am. Chem. Soc.* **1983**, *105*, 3522.

(51) Dias, H. V. R.; Fianchini, M. *Angew. Chem., Int. Ed.* **2007**, *46*, 2188.

(52) Lupinetti, A. J.; Strauss, S. H.; Frenking, G. *Prog. Inorg. Chem.* **2001**, *49*, 1.

(53) Lupinetti, A.; Fau, S.; Frenking, G.; Strauss, S. H. *J. Phys. Chem. A* **1997**, *101*, 9551.

(54) Kou, X.; Wu, J.; Cundari, T. R.; Dias, H. V. R. *Dalton Trans.* **2009**, 915.

(55) Jayaratna, N. B.; Pardue, D. B.; Ray, S.; Yousufuddin, M.; Thakur, K. G.; Cundari, T. R.; Dias, H. V. *Dalton Trans. (Cambridge, England : 2003)* **2013**, *42*, 15399.

(56) Kou, X.; Dias, H. V. R. *Dalton Trans.* **2009**, 7529.

(57) Dias, H. V. R.; Wu, J. *Organometallics* **2012**, *31*, 1511.

(58) Diaconu, D.; Hu, Z.; Gorun, S. M. *J. Am. Chem. Soc.* **2002**, *124*, 1564.

(59) Aullón, G.; Gorun, S. M.; Alvarez, S. *Inorg. Chem.* **2006**, *45*, 3594.

(60) Nakazawa, J.; Terada, S.; Yamada, M.; Hikichi, S. *J. Am. Chem. Soc.* **2013**, *135*, 6010.

(61) Ghosh, C. K.; Hoyano, J. K.; Krentz, R.; Graham, W. A. G. *J. Am. Chem. Soc.* **1989**, *111*, 5480.

(62) Krishnamoorthy, P.; Browning, R. G.; Singh, S.; Sivappa, R.; Lovely, C. J.; Dias, H. V. R. *Chem. Commun.* **2007**, 731.

(63) Reed, C. A. *Acc. Chem. Res.* **1998**, *31*, 133.

(64) Strauss, S. H. *Chem. Rev.* **1993**, *93*, 927.

(65) Beck, W.; Suenkel, K. *Chem. Rev.* **1988**, *88*, 1405.

(66) Krossing, I.; Raabe, I. *Angew. Chem. Int. Ed.* **2004**, *43*, 2066.

(67) Allen, F. *Acta Crystallogr. Sect. B* **2002**, *58*, 380.

(68) Maspero, A.; Giovenzana, G. B.; Monticelli, D.; Tagliapietra, S.; Palmisano, G.; Penoni, A. *J. Fluorine Chem.* **2012**, *139*, 53.

(69) Jurca, T.; Ouanounou, S.; Gorelsky, S. I.; Korobkov, I.; Richeson, D. S. *Dalton Trans.* **2012**, *41*, 4765.

(70) Fulmer, G. R.; Miller, A. J. M.; Sherden, N. H.; Gottlieb, H. E.; Nudelman, A.; Stoltz, B. M.; Bercaw, J. E.; Goldberg, K. I. *Organometallics* **2010**, *29*, 2176.

(71) Hansch, C.; Leo, A.; Taft, R. W. *Chem. Rev.* **1991**, *91*, 165.

(72) Kou, X.; Wu, J.; Cundari, T. R.; Dias, H. V. R. *Dalton Trans.* **2009**, 915.

(73) Cinellu, M. A.; Minghetti, G.; Cocco, F.; Stoccoro, S.; Zucca, A.; Manassero, M.; Arca, M. *Dalton Trans.* **2006**, 5703.

(74) Hahn, C. *Chem. Eur. J.* **2004**, *10*, 5888.

(75) Cavallo, L.; Macchioni, A.; Zuccaccia, C.; Zuccaccia, D.; Orabona, I.; Ruffo, F. *Organometallics* **2004**, *23*, 2137.

(76) Burgess, J.; Steel, P. J. *Coord. Chem. Rev.* **2011**, *255*, 2094.

(77) Cope, A. C.; Pike, R. A.; Spencer, C. F. *J. Am. Chem. Soc.* **1953**, *75*, 3212.

(78) Vardhan, H. B.; Bach, R. D. *J. Org. Chem.* **1992**, *57*, 4948.

(79) Royzen, M.; Taylor, M. T.; DeAngelis, A.; Fox, J. M. *Chem. Sci.* **2011**, *2*, 2162.

(80) Rencken, I.; Boeyens, J. A.; Orchard, S. W. *J. Ctystryst. Spectros* **1988**, *18*, 293.

(81) Cope, A.; Bach, R. D. *Inorg. Synth.* **1969**, *49*, 39.

(82) Pampaloni, G.; Peloso, R.; Belletti, D.; Graiff, C.; Tiripicchio, A. *Organometallics* **2007**, *26*, 4278.

(83) Dias, H. V. R.; Fianchini, M. *Angew. Chem. Int. Ed.* **2007**, *46*, 2188.

(84) Pampaloni, G.; Peloso, R.; Graiff, C.; Tiripicchio, A. *Dalton Trans.* **2006**, 3576.

(85) Huang, H. Y.; Padin, J.; Yang, R. T. *J. Phys. Chem. B* **1999**, *103*, 3206.

(86) Pampaloni, G.; Peloso, R.; Belletti, D.; Graiff, C.; Tiripicchio, A. *Organometallics* **2007**, *26*, 4278.

(87) Dewar, M. J. S. *Bull. Soc. Chim. Fr.,* **1951**, C71.

(88) Chatt, J.; Duncanson, L. A. *J. Chem. Soc.***1953**, 2939.

(89) Urbano, J.; Belderraín, T. R.; Nicasio, M. C.; Trofimenko, S.; Díaz-Requejo, M. M.; Pérez, P. J. *Organometallics* **2005**, *24*, 1528.

(90) Flores, J. A.; Komine, N.; Pal, K.; Pinter, B.; Pink, M.; Chen, C.-H.; Caulton, K. G.; Mindiola, D. J. *ACS Catalysis* **2012**, *2*, 2066.

(91) Rodríguez, P.; Álvarez, E.; Nicasio, M. C.; Pérez, P. J. *Organometallics* **2007**, *26*, 6661.

(92) Omary, M. A.; Rawashdeh-Omary, M. A.; Diyabalanage, H. V. K.; Dias, H. V. R. *Inorg. Chem.* **2003**, *42*, 8612.

(93) Gunnlaugsson, T.; Leonard, J. P.; Senechal, K.; Harte, A. J. *J. Am. Chem. Soc.* **2003**, *125*, 12062.

(94) Omary, M. A.; Rawashdeh-Omary, M. A.; Gonser, M. W. A.; Elbjeirami, O.; Grimes, T.; Cundari, T. R.; Diyabalanage, H. V. K.; Gamage, C. S. P.; Dias, H. V. R. *Inorg. Chem.* **2005**, *44*, 8200.

(95) Dias, H. V. R.; Diyabalanage, H. V. K.; Eldabaja, M. G.; Elbjeirami, O.; Rawashdeh-Omary, M. A.; Omary, M. A. *J. Am. Chem. Soc.* **2005**, *127*, 7489.

(96) Dias, H. V. R.; Palehepitiya Gamage, C. S. *Angew. Chem. Int. Ed.* **2007**, *46*, 2192.

(97) Halcrow, M. A. *Dalton Trans.* **2009**, 2059.

(98) Dias, H. V. R.; Diyabalanage, H. V. K.; Rawashdeh-Omary, M. A.; Franzman, M. A.; Omary, M. A. *J. Am. Chem. Soc.* **2003**, *125*, 12072.

(99) Chi, Y.; Lay, E.; Chou, T. Y.; Song, Y. H.; Carty, A. J. *Chem. Vap. Deposition* **2005**, *11*, 206.

(100) Dias, H. V. R.; Gamage, C. S. P.; Keltner, J.; Diyabalanage, H. V. K.; Omari, I.; Eyobo, Y.; Dias, N. R.; Roehr, N.; McKinney, L.; Poth, T. *Inorg. Chem.* **2007**, *46*, 2979.

(101) Krishantha, D. M. M.; Gamage, C. S. P.; Schelly, Z. A.; Dias, H. V. R. *Inorg. Chem.* **2008**, *47*, 7065.

(102) Kishimura, A.; Yamashita, T.; Aida, T. *J. Am. Chem. Soc.* **2005**, *127*, 179.

(103) Lintang, H. O.; Kinbara, K.; Tanaka, K.; Yamashita, T.; Aida, T. *Angew. Chem. Int. Ed.* **2010**, *49*, 4241.

(104) Mohamed, A. A.; Burini, A.; Fackler, J. P. *J. Am. Chem. Soc.* **2005**, *127*, 5012.

(105) Jahnke, A. C.; Pröpper, K.; Bronner, C.; Teichgräber, J.; Dechert, S.; John, M.; Wenger, O. S.; Meyer, F. *J. Am. Chem. Soc.* **2012**, *134*, 2938.

(106) Hou, L.; Shi, W.-J.; Wang, Y.-Y.; Wang, H.-H.; Cui, L.; Chen, P.-X.; Shi, Q.-Z. *Inorg. Chem.* **2011**, *50*, 261.

(107) Tsupreva, V. N.; Titov, A. A.; Filippov, O. A.; Bilyachenko, A. N.; Smol'yakov, A. F.; Dolgushin, F. M.; Agapkin, D. V.; Godovikov, I. A.; Epstein, L. M.; Shubina, E. S. *Inorg. Chem.* **2011**, *50*, 3325.

(108) Scheele, U. J.; Georgiou, M.; John, M.; Dechert, S.; Meyer, F. *Organometallics* **2008**, *27*, 5146.

(109) den Boer, D.; Krikorian, M.; Esser, B.; Swager, T. M. *The J. Phys. Chem. C* **2013**, *117*, 8290.

(110) Kishimura, A.; Yamashita, T.; Yamaguchi, K.; Aida, T. *Nat. Mater.* **2005**, *4*, 546.

(111) Jozak, T.; Sun, Y.; Schmitt, Y.; Lebedkin, S.; Kappes, M.; Gerhards, M.; Thiel, W. R. *Chem. Eur. J.* **2011**, *17*, 3384.

(112) Barberá, J.; Lantero, I.; Moyano, S.; Serrano , J. L.; Elduque, A.; Giménez, R. *Chem. Eur. J.* **2010**, *16*, 14545.

(113) Rawashdeh-Omary, M. A. *Comments on Inorg. Chem.* **2012**, *33*, 88.

(114) Murray, H. H.; Raptis, R. G.; Fackler, J. P. *Inorg. Chem.* **1988**, *27*, 26.

(115) Omary, M. A.; Kassab, R. M.; Haneline, M. R.; Elbjeirami, O.; Gabbaï, F. P. *Inorg. Chem.* **2003**, *42*, 2176.

(116) Grushin, V. V.; Herron, N.; LeCloux, D. D.; Marshall, W. J.; Petrov, V. A.; Wang, Y. *Chem. Commun.* **2001**, 1494.

(117) Grimes, T.; Omary, M. A.; Dias, H. V. R.; Cundari, T. R. *The J. Phys. Chem. A* **2006**, *110*, 5823.

(118) Omary, M. A.; Elbjeirami, O.; Gamage, C. S. P.; Sherman, K. M.; Dias, H. V. R. *Inorg. Chem.* **2009**, *48*, 1784.

(119) Rawashdeh-Omary, M. A.; Rashdan, M. D.; Dharanipathi, S.; Elbjeirami, O.; Ramesh, P.; Dias, H. V. R. *Chem. Commun.* **2011**, *47*, 1160.

(120) Omary, M. A.; Mohamed, A. A.; Rawashdeh-Omary, M. A.; Fackler Jr, J. P. *Coord. Chem. Rev.* **2005**, *249*, 1372.

(121) Olmstead, M. M.; Jiang, F.; Attar, S.; Balch, A. L. *J. Am. Chem. Soc.* **2001**, *123*, 3260.

(122) Mohamed, A. A.; Rawashdeh-Omary, M. A.; Omary, M. A.; Fackler, J. J. P. *Dalton Trans.* **2005**, 2597.

(123) Jayaratna, N. B.; Hettiarachchi, C. V.; Yousufuddin, M.; Rasika Dias, H. V. *New J. Chem.* **2015**, *39*, 5092.

(124) Zhang, J.-P.; Zhang, Y.-B.; Lin, J.-B.; Chen, X.-M. *Chem. Rev.* **2012**, *112*, 1001.

(125) Hettiarachchi, C. V.; Rawashdeh-Omary, M. A.; Korir, D.; Kohistani, J.; Yousufuddin, M.; Dias, H. V. R. *Inorg. Chem.* **2013**, *52*, 13576.

(126) Raptis, R. G.; Fackler, J. P. *Inorg. Chem.* **1988**, *27*, 4179.

(127) Gong, F.; Wang, Q.; Chen, J.; Yang, Z.; Liu, M.; Li, S.; Yang, G.; Bai, L.; Liu, J.; Dong, Y. *Inorg. Chem.* **2010**, *49*, 1658.

(128) Veronelli, M.; Kindermann, N.; Dechert, S.; Meyer, S.; Meyer, F. *Inorg. Chem.* **2014**, *53*, 2333.

(129) Xiao, Q.; Zheng, J.; Li, M.; Zhan, S.-Z.; Wang, J.-H.; Li, D. *Inorg. Chem.* **2014**, *53*, 11604.

(130) Zhang, J.-P.; Kitagawa, S. *J. Am. Chem. Soc.* **2008**, *130*, 907.

(131) Zhan, S.-Z.; Li, M.; Zhou, X.-P.; Wang, J.-H.; Yang, J.-R.; Li, D. *Chem. Commun.* **2011**, *47*, 12441.

(132) He, J.; Yin, Y.-G.; Wu, T.; Li, D.; Huang, X.-C. *Chem. Commun.* **2006**, 2845.

(133) Masciocchi, N.; Moret, M.; Cairati, P.; Sironi, A.; Ardizzoia, G. A.; La Monica, G. *J. Am. Chem. Soc.* **1994**, *116*, 7668.

(134) Fujisawa, K.; Ishikawa, Y.; Miyashita, Y.; Okamoto, K.-i. *Chem. Lett.* **2004**, *33*, 66.

(135) Omary, M. A.; Rawashdeh-Omary, M. A.; Gonser, M. W. A.; Elbjeirami, O.; Grimes, T.; Cundari, T. R.; Diyabalanage, H. V. K.; Gamage, C. S. P.; Dias, H. V. R. *Inorg. Chem.* **2005**, *44*, 8200.

(136) Alvarez, S. *Dalton Trans.* **2013**, *42*, 8617.

(137) Wright, A. M.; Irving, B. J.; Wu, G.; Meijer, A. J. H. M.; Hayton, T. W. *Angew. Chem. Int. Ed.* **2015**, *54*, 3088.

(138) Tsunoda, M.; Gabbaï, F. P. *J J. Am. Chem. Soc.* **2000**, *122*, 8335.

(139) Haneline, M. R.; King, J. B.; Gabbai, F. P. *Dalton Trans.* **2003**, 2686.

(140) Kroto, H. W.; Heath, J. R.; O'Brien, S. C.; Curl, R. F.; Smalley, R. E. *Nature* **1985**, *318*, 162.

(141) Liu, S.; Lu, Y.-J.; Kappes, M. M.; Ibers, J. A. *Science* **1991**, *254*, 408.

(142) Dias, H. V. R.; Diyabalanage, H. V. K. *Polyhedron* **2006**, *25*, 1655.

(143) Osawa, E. *Perspectives of Fullerene Nanotechnology*; Springer, 2002.

(144) Sheldrick, G. M. *SHELXTL*, version 6.14; Bruker Analytical X.

(145) Dolomanov, O. V.; Bourhis, L. J.; Gildea, R. J.; Howard, J. A. K.; Puschmann, H. *J. Appl. Crystallogr.* **2009**, *42*, 339.

(146) Frisch, M. J. T., G. W.; Schlegel, H. B.; Scuseria, G. E.; Robb, M. A.; Cheeseman, J. R.; Montgomery, Jr., J. A.; Vreven, T.; Kudin, K. N.; Burant, J. C.; Millam, J. M.; Iyengar, S. S.; Tomasi, J.; Barone, V.; Mennucci, B.; Cossi, M.; Scalmani, G.; Rega, N.; Petersson, G. A.; Nakatsuji, H.; Hada, M.; Ehara, M.; Toyota, K.; Fukuda, R.; Hasegawa, J.; Ishida, M.; Nakajima, T.; Honda, Y.; Kitao, O.; Nakai, H.; Klene, M.; Li, X.; Knox, J. E.; Hratchian, H. P.; Cross, J. B.; Bakken, V.; Adamo, C.; Jaramillo, J.; Gomperts, R.; Stratmann, R. E.; Yazyev, O.; Austin, A. J.; Cammi, R.; Pomelli, C.; Ochterski, J. W.; Ayala, P. Y.; Morokuma, K.; Voth, G. A.; Salvador, P.; Dannenberg, J. J.; Zakrzewski, V. G.; Dapprich, S.; Daniels, A. D.; Strain, M. C.; Farkas, O.; Malick, D. K.; Rabuck, A. D.; Raghavachari, K.; Foresman, J. B.; Ortiz, J. V.; Cui, Q.; Baboul, A. G.; Clifford, S.; Cioslowski, J.; Stefanov, B. B.; Liu, G.; Liashenko, A.; Piskorz, P.; Komaromi, I.; Martin, R. L.; Fox, D. J.; Keith, T.; Al-Laham, M. A.; Peng, C. Y.; Nanayakkara, A.; Challacombe, M.; Gill, P. M. W.; Johnson, B.; Chen, W.; Wong, M. W.; Gonzalez, C.; and Pople, J. A. *Gaussian 03, Revision E.01*, 2004.

(147) Perdew, J. P. *Phys. Rev. B* **1986**, *33*, 8822.

(148) Couty, M.; Hall, M. B. *J. Comput. Chem.* **1996**, *17*, 1359.

(149) Ehlers, A. W.; Boehme, M.; Dapprich, S.; Gobbi, A.; Hoellwarth, A.; Jonas, V.; Koehler, K. F.; Stegmann, R.; Veldkamp, A.; et al. *Chem. Phys. Lett.* **1993**, *208*, 111.

(150) Hehre, W. J.; Radom, L.; Schleyer, P. v. R.; Pople, J. *AB INITIO Molecular Orbital Theory*; Wiley: New York, 1896.

(151) Cheeseman, J. R.; Trucks, G. W.; Keith, T. A.; Frisch, M. J. *J. Chem. Phys.* **1996**, *104*, 5497.

(152) Foster, J. P.; Weinhold, F. *J. Am. Chem. Soc.* **1980**, *102*, 7211.

(153) Reed, A. E.; Weinhold, F. *J. Chem. Phys.* **1983**, *78*, 4066.

(154) Reed, A. E.; Weinstock, R. B.; Weinhold, F. *J. Chem. Phys.* **1985**, *83*, 735.

Biographical Information

Naleen Bandupriya Jayaratna was born in Menikhinna, Kandy, Sri Lanka. He started his primary education at Pathadumbara Maha Vidyalaya, completed high school education at Dharmaraja College, Kandy and joined the Institute of Chemistry Ceylon, College of Chemical Sciences, Sri Lanka. He received his B.S. in Chemistry in 2005. He joined Sam Houston State University, Texas and pursued his M.S. in Chemistry in 2010. He joined the Ph.D. graduate program in Chemistry at The University of Texas at Arlington in Fall 2010.